ATTITUDE CONTROL OF AN EARTH ORBITING SOLAR SAIL SATELLITE TO PROGRESSIVELY CHANGE THE SELECTED ORBITAL ELEMENT

A THESIS SUBMITTED TO
THE GRADUATE SCHOOL OF NATURAL AND APPLIED SCIENCES
OF
MIDDLE EAST TECHNICAL UNIVERSITY

BY

ÖMER ATAŞ

IN PARTIAL FULFILLMENT OF THE REQUIREMENTS
FOR
THE DEGREE OF MASTER OF SCIENCE
IN
AEROSPACE ENGINEERING

FEBRUARY 2014

Approval of the thesis:

ATTITUDE CONTROL OF AN EARTH ORBITING SOLAR SAIL SATELLITE TO PROGRESSIVELY CHANGE THE SELECTED ORBITAL ELEMENT

Submitted by **ÖMER ATAŞ** in partial fulfillment of the requirements for the degree of **Master of Science in Aerospace Engineering Department, Middle East Technical University** by,

Prof. Dr. Canan Özgen
Dean, Graduate School of **Natural and Applied Sciences** _____

Prof. Dr. Ozan Tekinalp
Head of Department, **Aerospace Engineering** _____

Prof. Prof. Dr. Ozan Tekinalp
Supervisor, **Aerospace Engineering Dept., METU** _____

Examining Committee Members:

Assoc.Prof. Dr. İlkay Yavrucuk
Aerospace Engineering Dept, METU _____

Prof. Dr. Ozan Tekinalp
Aerospace Engineering Dept, METU _____

Assoc. Prof. Dr. Melin Şahin
Aerospace Engineering Dept, METU _____

Asst. Prof. Dr. Ali Türker Kutay
Aerospace Engineering Dept, METU _____

Dr. Egemen İmre
TÜBİTAK UZAY _____

Date: 06.02.2014

I hereby declare that all information in this document has been obtained and presented in accordance with academic rules and ethical conduct. I also declare that, as required by these rules and conduct, I have fully cited and referenced all material and results that are not original to this work.

Name, Last Name: **ÖMER ATAŞ**

Signature:

ABSTRACT

ATTITUDE CONTROL OF AN EARTH ORBITING SOLAR SAIL SATELLITE TO PROGRESSIVELY CHANGE THE SELECTED ORBITAL ELEMENT

Ataş, Ömer

M.S., Department of Aerospace Engineering

Supervisor : Prof. Dr. Ozan Tekinalp

February 2014, 79 pages

Solar sailing is currently under investigation for space propulsion. Radiation pressure from the Sun is utilized to propel the spacecraft. This thesis examines locally optimal steering law to progressively change the selected orbital elements, without considering others, of an Earth centered Keplerian orbit of a cube satellite with solar sail. The proper attitude maneuver mechanization is proposed to harvest highest solar radiation force in the desired direction for such Earth orbiting satellites. The satellite attitude control is realized by developing quaternion feedback controller. The changes of the orbital elements are observed.

Keywords: Solar Sail, Orbital Elements, Locally Optimal Steering Law, Attitude Control, Quaternion Feedback Control.

ÖZ

DÜNYA YÖRÜNGESİNDE DOLAŞAN GÜNEŞ YELKENLİ UYDUNUN YÖRÜNGE PARAMETRESİNİN YAVAŞ YAVAŞ DEĞİŞTİRİLMESİ AMACIYLA YÖNELİM KONTORLÜ

Ataş, Ömer
Yüksek Lisans, Havacılık ve Uzay Mühendisliği Bölümü
Tez Yöneticisi : Prof. Dr. Ozan Tekinalp

Şubat 2014, 79 sayfa

Son dönemlerde güneş yelkenlerinin uzayda itki kaynağı olarak kullanılmasıyla ilgili çalışmalar artmıştır. Bu tezde local optimal yönelim ile Dünya merkezli bir yörüngede dolanan Güneş yelkenli uydunun seçilmiş yörünge parametresinin tedrici olarak değiştirilmesi amacıyla gerekli yönelimin bulunması için bir algoritma önerilmiştir. Dünya merkezli Kepler orbitalindeki yelkenli bir küp uydu, Güneşe göre uygun yönelim belirlenilerek quaternion geri beslemeli kontrol ile yönlendirilimiş ve orbital elemanlarındaki değişim diğerlerinden bağımsız olarak maksimize edilmiştir. Yörünge parametrelerindeki değişim izlenmiştir.

Anahtar Kelimeler: Güneş Yelkeni, Yörünge Parametreleri, Yerel Optimal Yönlendirme Kanunu, Quaternion Geri Beslemeli Kontrol, Yönelim Kontrolü.

To my family…

ACKNOWLEDGMENTS

I would like to express my profound gratitude and deep regards to my supervisor Prof. Dr. Ozan Tekinalp for his patience, exemplary guidance and constant encouragement throughout this thesis. I would like to thank his valuable and constructive suggestions during the planning and development of this thesis. I have been amazingly fortunate to have an advisor who gave me the freedom to explore on my own and at the same time the guidance to recover when my steps faltered. I owe a very important debt to him.

Lastly, my deepest appreciation goes to my family for their moral support and unceasing encouragement in every stage of this process. Without their thrust and understanding this thesis would not have been possible.

TABLE OF CONTENTS

LIST OF TABLES

TABLES

LIST OF FIGURES

FIGURES

LIST OF SYMBOLS

$\mathbf{J}$	Inertia matrix of the solar sail
$\tilde{\boldsymbol{\omega}}$	Skew symmetric matrix of angular velocity
$\mathbf{K}$, $\mathbf{C}$	Controller gain matrixes
$\mathbf{j}$	Induced current
$\mathbf{B}$	Magnetic field
$\mathbf{E}$	Electric field
$\mathbf{L}_{\mathrm{l}}$	Lorentz force
$\mathbf{u}_{\mathrm{i}}$	Incident light
$\mathbf{u}_{\mathrm{r}}$	Reflected light
$\mathbf{f_i}$	Force exerted on the sail due to incident light
$\mathbf{f_r}$	Force exerted on the sail due to reflected light
$\mathbf{f_a}$	Force due to absorption of light
$\mathbf{f_e}$	Force due to emission of light
$\mathbf{f_n}$	Solar force in normal direction of sail
$\mathbf{f_l}$	Solar force in direction of $\mathbf{l}$
$\mathbf{f}$	Total radiation force on the sail
$\mathbf{n}$	Solar sail unit normal
$\mathbf{l}$	Unit normal vector to sail normal vector $\mathbf{n}$
$\mathbf{m}$	Direction of the resultant solar force vector
$\mathbf{a}$	Solar sail acceleration due to radiation force
$\mathbf{f_X}$, $\mathbf{f_Y}$, $\mathbf{f_Z}$	Inertial frame components of the acceleration due to solar radiation force acting on the spacecraft
$\mathbf{R}$, $\mathbf{T}$, $\mathbf{N}$	Radial, transverse and normal components of accelerations of the spacecraft with respect to orbital plane
$\boldsymbol{\lambda}(Z)$	Vector function of any orbital element Z
$\mathbf{f}_{\boldsymbol{\lambda}}$	Solar force component along the vector function $\boldsymbol{\lambda}$
$\mathbf{s}$	Sunline vector
$\boldsymbol{\gamma}$	Rotation axis of $\mathbf{s}$
$\mathbf{q}_r$	Rotation quaternion
$\mathbf{q}_r{}^*$	Conjugate of $\mathbf{q}_r$

$\mathbf{n}_d$	Desired solar sail normal direction
e	Rotation axis of solar sail
t	Vector part of to-go quaternion *t*
ω	Angular velocity of the spacecraft
u	Control torques on the spacecraft
t	To-go quaternion
E_p	Energy of the photon
v_p	Frequency of photon
h_p	Planck constant
m_0	Rest mass of photon
c	Speed of light
p	Momentum of photon
W_E	Energy flux at Earth's distance from the Sun
W	Energy flux of light at a distance *r* from the sun
L_s	Solar luminosity
j_z	Induced current density in the reflective surface
ε_0	Electric permittivity of the space
μ_0	Permeability of the space
U	Energy density of the electromagnetic wave
$\tilde{r}$	Coefficient for reflection
$\breve{\alpha}$	Coefficient for absorption
τ	Coefficient for emission
B_f	Front surface of the solar sail non-Lambertian
B_b	Back surface of the solar sail non-Lambertian
ε_f	Front emissivity of the sail
ε_b	Back emissivity of the sail
A	Area of the solar sail
P	Radiation pressure on the solar sail
μ	Gravitational constant
h	Orbital angular momentum
a	Semi-major axis
e	Eccentricity
i	Inclination
Ω	Right ascension of the ascending node
w	Argument of periapse
v	True anomaly
$\emptyset$	Argument of latitude
p	semi-latus rectum

σ	Sail loading
m	Mass of sail
ψ	Angle between sunline and vector function of orbital element
α_1	Angle between sunline and sail normal for increasing orbital element
α_2	Angle between sunline and sail normal for decreasing orbital element
β	Angle between sail normal and desired sail normal
V	Lyapunov function
V_w	Angular Lyapunov
V_q	Quaternion Lyapunov
k_c, c_c	Controller gain constants
θ	The rotation angle about the eigenaxis
ω_n	Natural frequency
ξ	Damping ratio

LIST OF ABBREVIATIONS

JAXA	Japan Aerospace Exploration Agency
SRP	Solar Radiation Pressure
DLR	German Aerospace Center
LEO	Low Earth Orbit
NASA	National Aeronautics and Space Administration
OTW	Overlap Thin-Wall
MTW	Multi-element Thin-Wall
CFRP	Carbon-Fiber-Reinforced Polymer
TRAC	Triangular Rollable And Collapsible
AFRL	American Air Force Research Laboratory
GEO	Geosynchronous orbit
Au	Astronomical unit

CHAPTER 1

INTRODUCTION

Including the deep space probe missions, there are thousands of space missions that have been launched since the first space mission. But the extended of our space trip is limited by the internal combustion rocket engines and the amount of the fuel. On board traditional chemical propulsion requires large storage tanks for a spacecraft to carry the propellant for a space mission. Today approximately 95 percent of mass of a space shuttle is fuel [1]. That's why international space agencies, universities and some private space corporations do research on solar sails to decrease the need to the rocket engines and fuels in the space. There are many advancements over chemical propulsion, including nuclear fission, fusion reactors and other novel concepts. But most of them are either not proven or impractical for the next decades compared with solar sails which are proved for propulsion capabilities [2].

1.1 History of Solar Sail Concept

Even so the solar sailing has been considered as a practical means of spacecraft propulsion only recently, the basic ideas are by no means new [3]. The actual solar sailing concept has a long history, which is dating back to the Soviet pioneers of astronautics [4]. The existence of radiation pressure was first demonstrated by Scottish physicist James Clerk Maxwell in 1873. But it was not measured experimentally until Russian physicist Peter Lebedew [4]. He experimentally established the existence of force exerted by light upon gases [5]. Konstantin Tsiolkovsky, and his co-worker, Fridrickh Tsander , Both wrote the 'Using tremendous mirrors of very thin sheets' and 'Using the pressure of light to

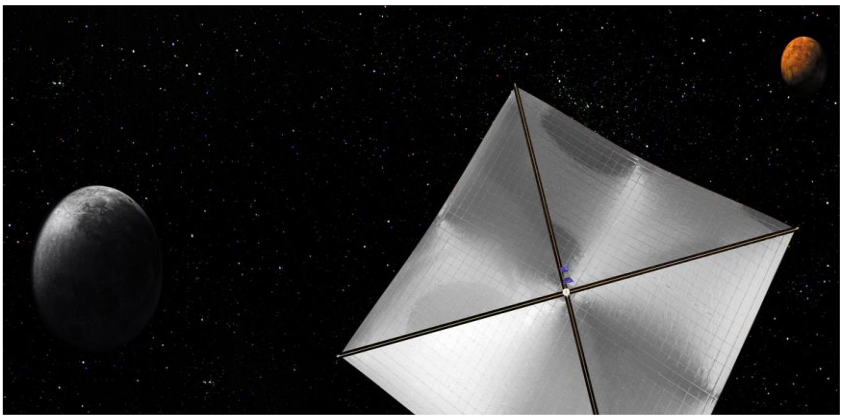

Figure 1.1 Solar Sail [6]

attain cosmic velocities' in 1924 [4]. The term of solar sailing was used in the late 1950's and was popularized by Arthur C. Clarke in the short story Sunjammer (The Wind From the Sun) in May 1964 [7]. NASA used sailing techniques to extend the operational life of the Mariner 10 spacecraft in 1974-1975. A problem in control system was causing Mariner 10 to go off course. By controlling the attitude of Mariner 10 and the angle of the solar power panels relative to the sun, ground controllers were able to correct the problem without using precious fuel [8].

1.2 Literature Survey

Recent, attention has been focused on the utilization of solar sail for orbital elements control, sustaining displaced orbits, halo orbits, interplanetary travel and attitude control. This literature review is based on the studies on these topics.

There are very few books about the solar sail. McInnes's book [4] stands out among them in terms of content and clarity. He introduces solar sail orbits and mission applications, puts emphasis on solar sail orbital dynamics and gives analysis of solar radiation pressure. In the book, orbital analysis are separately conducted for Sun-centered and planet-centered orbits. He explains the locally optimal steering law and the usage of it to change the orbital elements of a Sun centered orbit. Studied displaced orbits for solar sails around Sun.

The study of Wie [9] presents a mathematical formulation of the thrust vector control design problem of solar sail spacecraft. Using Gauss's form of the variational equations and finds the desired orientation of solar sail thrust vector orientation in order to maximize the rate of change of inclination. He also gives examples of solar sail trajectory design and simulations.

In the study of Benjamin [10] , the attitude of the solar sail is controlled by means of displaying the center of mass of the solar sail with respect to center of solar radiation pressure. By using this attitude control he shows the availability of solar sail for interplanetary travels especially for Earth-Mars, Earth-Venus and Earth-Jupiter trajectories.

One of the possible usages is monitoring sun from a closer distance in order to make an accurate prediction on solar upcoming winds. [11]. A solar sail spacecraft with particle detector may be located between Earth and Sun to detect the upcoming solar winds. As it is stated in [11] the *L1* Lagrangian point of Earth-Sun system, at a distance of 1.5 million [km] upstream from the Earth, offers opportunity to detect the storm condition about one hour before the solar wind reaches the Earth.

Halo orbits are also in the possible application field of solar sails. Farres and Jorba [12], describe the dynamics of solar sail around a Halo orbit. They derive a station keeping strategy for solar sails around Halo orbit.

Solar sails may also be used to deorbit satellites at the end of their life time. Lucking and his colleagues [13] derive the required area to mass ratio of a solar sail to deorbit from MEO analytically, and the results are verified numerically, they also analyse inclined and eccentric orbits. The author of this thesis has also worked on such project called DeOrbitSail (European Union 7^{th} framework project).

1.3 Solar Sail Missions

Many solar and drag sail projects have been undertaken as ground studies are proposed but not realized. In recent years, however, demonstration missions have succeeded in deploying large sails in space, as well as confirming deployment and demonstrating

solar sailing capabilities. In this section some important solar sail missions are summarized.

1.3.1 NanoSail-D

NanoSail-D was a NASA sail demonstration mission. After the destruction of the original NanoSail-D satellite in 2008 launch failure [14]. NanoSail-D2 was launched in 2010 and deorbited in approximately 8 months [15]

Figure 1.2 Deployed NanoSail-D [15]

Due to size and a tight schedule, NanoSail-D was not able to carry significant diagnostic instrumentations and relied on ground imaging to confirm deployment [14].

Figure 1.3 Ground imaging of NanoSail-D2 [15]

1.3.2 IKAROS

IKAROS is a JAXA mission which has demonstrated the first deep space solar sail. The mission launched in May 2010 and deployed its 200 m^2 solar sail in June 2010 [16]. Rather than using any rigid booms or frame, the IKAROS sail was deployed and kept stretched using centrifugal force. Several cameras were incorporated in the mission design, so there is ample evidence of the successful deployment of this sail. The effectiveness of the solar sailing mission was evaluated with attitude and trajectory data. IKAROS combined many new technologies for solar sailing and ultra-lightweight deployable structure, as well as a unique steering system. As a deep space mission, it was able to demonstrate the use of solar radiation pressure in an environment where SRP is more significant than atmospheric drag.

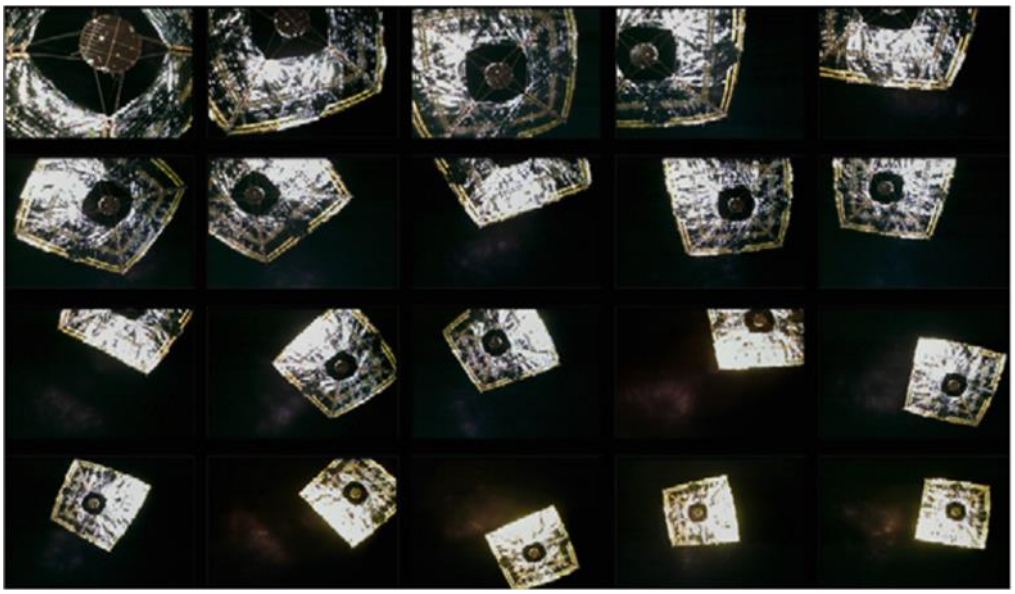

Figure 1.4 Deployed IKAROS from deployable camera [16]

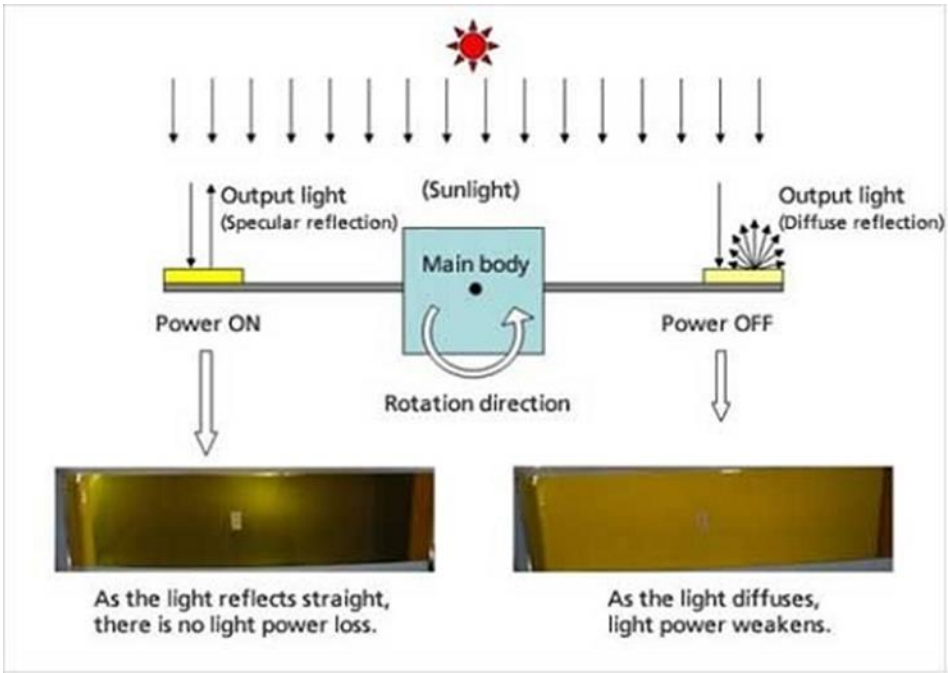

Figure 1.5 IKAROS steering system [16]

1.3.3 DLR Gossamer

DLR's gossamer project will launch three solar sails of increasing size into orbits of increasing altitude, with Gossamer-1 slated for 2013 [17]. Gossamer-1 will be a 5-by-5 m sail flown with the QB50 CubeSat project in a 300-320 km orbit. The Gossamer-1 baseline design is a square sail that will be extended by four tip-deployed booms of DLR's design [18]

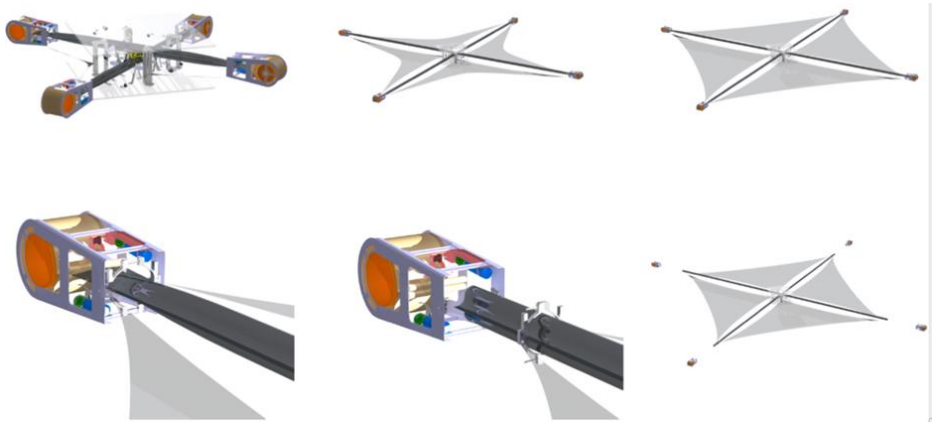

Figure 1.6 Gossamer-1 deployment sequence [18]

1.3.4 LightSail

The Planetary Society's LightSail program will comprise three solar sail projects. The first, LightSail-1, will be a 32 m^2, 4.5 µm thick, mylar sail. The Planetary Society is searching for launch opportunities for LightSail-1. The Planetary Society had previously planned a 2005 solar sail mission, Cosmos-1, which was unable to reach orbit due to a launch vehicle failure [19]

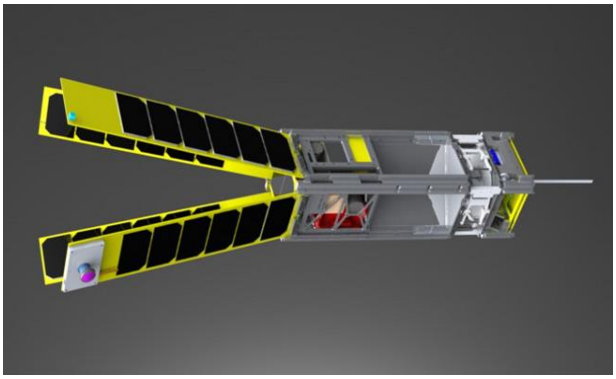

Figure 1.7 The LightSail-1 spacecraft bus with extended solar panels [19]

1.3.5 CU Aerospace's CubeSail

CU Aerospace together with the University of Illinois are designing a mission to demonstrate deployment and measure the thrust on a 0.077-by-260 m membrane (around 20m^2). This membrane will be deployed from two 1.5U cubesats that will separate from each other in orbit. It is intended as a first step towards a larger sail concept called UltraSail. This last consists of multiple structures that extend kilometers long film blades to ultimately form a heliogyro [20].

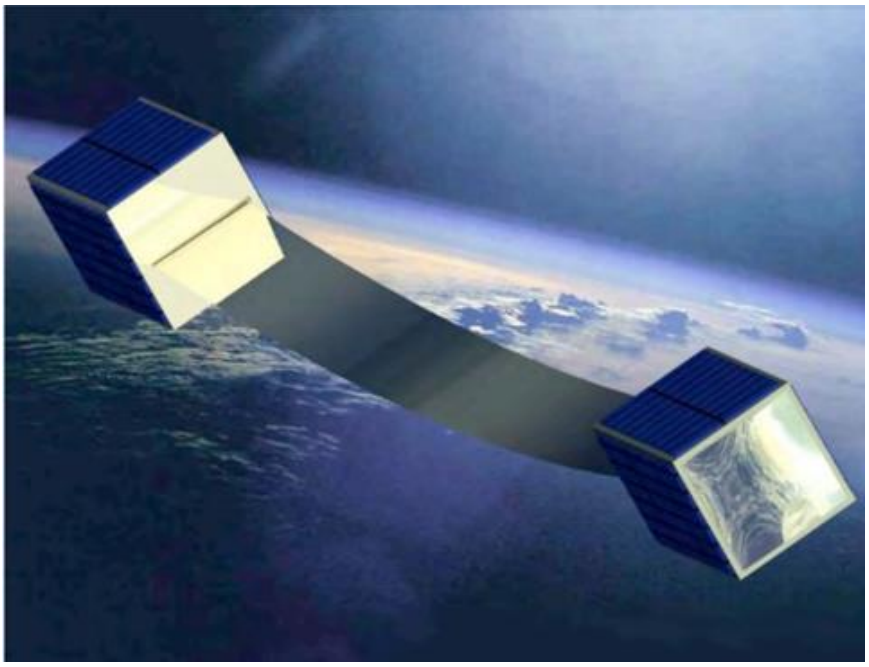

Figure 1.8 Artist's rendition of CubeSail solar sail deployment [21].

1.3.6 Surrey Space Centre's CubeSail

CubeSail is a project to build and deploy in space a 5-by-5 m sail with attitude control in a 3U CubeSat standard package [22]. A significant portion of the research in CubeSail is going into the characterization of two competing boom concepts and a number of sail packing strategies [23].

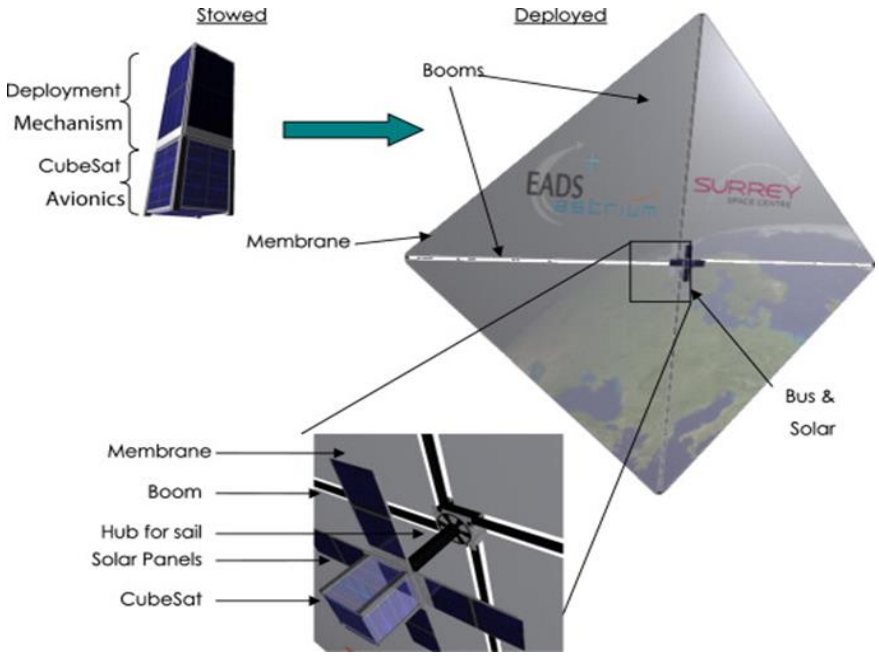

Figure 1.9 Surrey Space Centre CubeSail concept [22]

1.3.7 DeOrbitSail Project

The Deorbitsail project is a European Union 7th Framework program project lead by Surrey Space Centre is the coordinator and Middle East Technical University Aerospace Department is one of partner of the project. The collaboration is aim to build a 3U CubeSat sized satellite with a deployable sail to demonstrate rapid deorbiting.

Thus it will utilize the increased aerodynamic drag from the large surface area. Aerodynamic drag is the force that acts opposite the relative velocity vector of a satellite in low Earth orbit (LEO). It is a result of air molecules interacting with the satellite surface and the general result is a decrease in orbit eccentricity and semi-major axis over time. Eventually a satellite that is influenced by drag will return to the Earth and either burn up in the atmosphere or impact the surface (or have fragments that impact the Earth surface). [24].

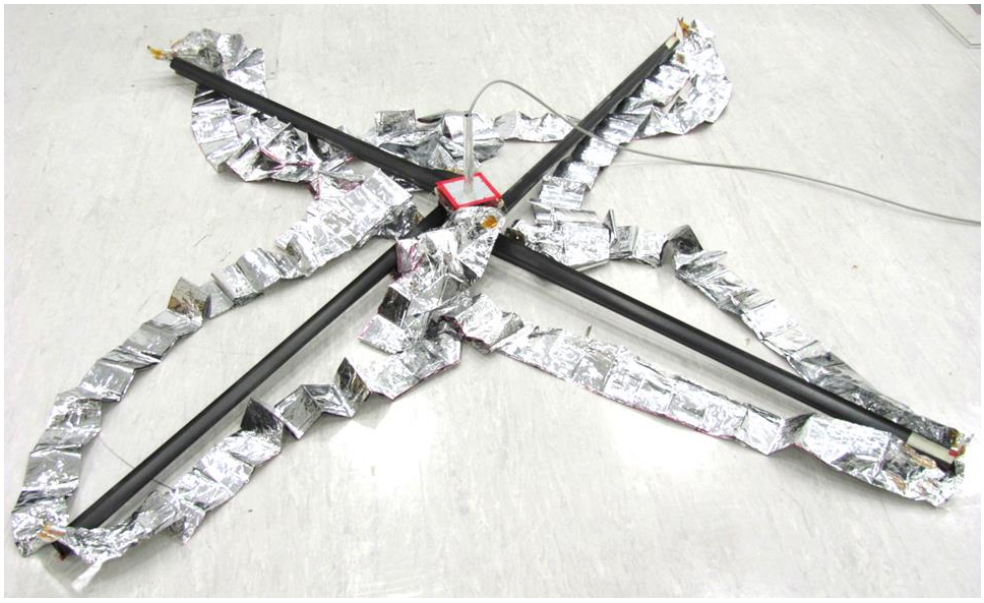

Figure 1.10 DeOrbitSail Deployment [25]

The Deorbitsail project aims to demonstrate that deorbiting can be achieved with a deployable sail, and to provide a proven design for the deployment system that can be re-used as a deorbiting device on future spacecraft. The Satellite will launch in 2014.

1.4 Purpose of the Thesis

The purpose of this study to mechanize the calculation of necessary attitude for solar sails to achieve propulsion goals. In addition to show that, by using solar sail, the orbital elements can be changed progressively for an Earth orbiting satellite. For this purpose proper sail direction is calculated. The desired attitude in terms of to-go quaternion is calculated based on the current sail direction and desired sail direction. Then the Lyapunov function based nonlinear attitude control law is used to steer the spacecraft.

1.5 Contents of the Thesis Report

In chapter 2, the physics of radiation pressure is described with two perspectives of physics. And force model of solar sails is explained.

In chapter 3, the formulation of the problem is given. The orbital dynamics, the method of maximizing orbital element rate of change and the desired to-go attitude mechanization are described in detail.

In chapter 4, simulation results are given and explained for increasing semi-major axis, eccentricity and inclination.
In chapter 5, general conclusion and future work are presented.

Finally in appendix, simulation results are given for decreasing semi-major axis, eccentricity and inclination.

CHAPTER 2

RADIATION PRESSURE

2.1 The Physics of Radiation Pressure

This section follows heavily the chapter of 'Solar radiation pressure' of McInnes book [4].

2.1.1 Quantum physics description

From the quantum physics point of view energy and momentum are carried by packets. The light packets are called photons. The origin of concept of photons is the investigation of the thermal radiation by Planck and others at the beginning of 20th century [4]. In 1905 Einstein successfully showed that incident light on a metal consist of individual quanta that interacted with the electrons in the metal. This study of Einstein is called photoelectric effect and that study brought him the Nobel Prize in 1921.

Denoting, E_p as the energy of a photon of frequency ν_p can be calculated from Planck Law;

$$E_p = h_p \nu_p \tag{2.1}$$

where h_p is Planck constant. In addition to equation (2.1) the mass-energy equivalence of special relativity the total energy of a moving objects to be written as.

$${E_p}^2 = m_0^2 c^4 + p^2 c^2 \tag{2.2}$$

Where m_0 is the rest mass of the object, p is the momentum and c is the speed of light. The first term in equation (2.2) is the rest energy of the object and the second term is the energy of the body due to its motion. Because of the zero rest mass of photon, the energy of it can be written as

$$E_p = pc \tag{2.3}$$

So from equations (2.1) and (2.3) the amount of momentum which is carried by one photon is found as,

$$p = \frac{h_p v_p}{c} \tag{2.4}$$

This result is derived from by combining the quantum physics with relativity. To find the pressure exerted on a surface of a body, the amount of total momentum transported by a flux of light must be found.

The energy flux of light W at a distance r from the sun can be written in terms of the solar luminosity L_s and scaled by the Sun-Earth distance R_E as [4].

$$W = W_E \left(\frac{R_E}{r}\right)^2 \tag{2.5}$$

$$W_E = \frac{L_s}{4\pi R_E^2} \tag{2.6}$$

Where W_E is the energy flux at Earth's distance from the Sun. By using equation (2.5) the total energy reaches a surface area A which is normal to the incident light at a distance 1 astronomical unit (au) in time Δt is given by

$$\Delta E = WA\Delta t \tag{2.7}$$

Then the transported momentum Δp may be written as

$$\Delta p = \frac{\Delta E}{c} \tag{2.8}$$

The pressure P is defined as the momentum transported per unit time on a unit area,

$$P = \frac{1}{A}\left(\frac{\Delta p}{\Delta t}\right) \tag{2.9}$$

Then

$$P = \frac{W}{c} \tag{2.10}$$

For a perfectly reflective surface the amount of pressure P is given by equation (2.10) is doubled, because of the reaction of the reflected light. The orbit of the Earth is elliptic that's why the flux received at the Earth surface varies by approximately 3.5 percent over the year. The flux is generally accepted as a constant W_E of 1368 [$Js^{-1}m^{-}$

^{2}] . And the pressure on a perfectly reflective surface normal to the solar flux at 1 Au is 9.2×10^{-6} [Nm^{-2}].

2.1.2 Electromagnetic description

Electromagnetic wave is composed of electric and magnetic fields. When the electromagnetic wave interacts with the sail material the electric field **E** induces a current **j** in the sail. And magnetic field **B** creates Lorenz force in the direction of propagation of light.

$$\mathbf{L}_{\mathrm{l}} = \mathbf{j} \times \mathbf{B} \tag{2.11}$$

Where $\mathbf{L}_{\mathrm{l}}$ is the Lorenz force. The reflection of incident light is generated by the induced current. As it is shown in the Figure 2.1 for a propagating wave in the direction of the x-axis the force exerted on a current is given by [4].

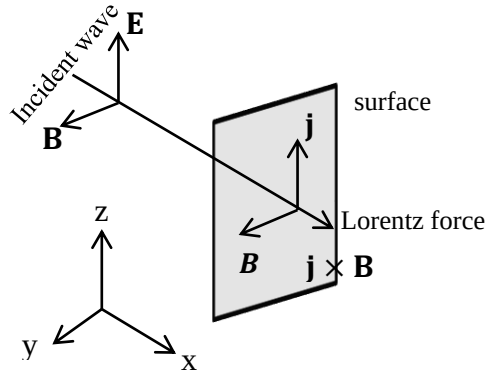

Figure 2.1 Electromagnetic radiation pressure description [4]

$$df = j_z B_y d_x d_y d_z \tag{2.12}$$

Where j_z is the induced current density in the reflective surface. The pressure on the current element is given as

$$dP = j_z B_y d_x \tag{2.13}$$

From Maxwell's equation the current term in equation (2.13) may be replaced as follows

$$dP = -\frac{\partial}{\partial x}\left(\frac{1}{2}\varepsilon_0 E_z^2 + \frac{1}{2\mu_0} B_{yz}^2\right) d_x \tag{2.14}$$

$$U = \frac{1}{2}\varepsilon_0 E_z^2 + \frac{1}{2\mu_0} B_{yz}^2 \tag{2.15}$$

Where U is the energy density of the electromagnetic wave, ε_0 is the electric permittivity of the space and $\mu_0$is the permeability of the space. Then the pressure exerted on a surface of thickness Δl can be found by integrating the equation (2.15) as

$$P = -\int_0^{\Delta l} \frac{\partial U}{\partial x} dx \tag{2.16}$$

As it can be understood the pressure on the perfectly absorbing materials will be

$$P = U \tag{2.17}$$

Equation (2.17) indicates that pressure is equal to the energy density of the radiation. Now consider two waves which are separated with a distance Δx and are incident on a surface area A, as shown in Figure 2.2 the volume of the space between the waves is $A\Delta x$.

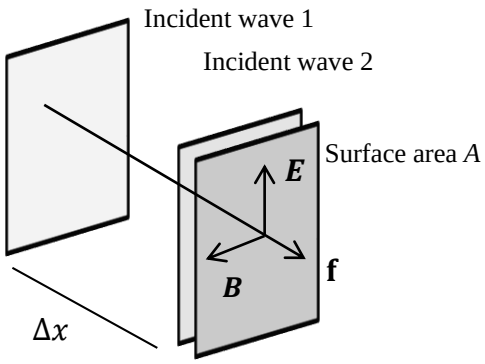

Figure 2.2 Energy density of electromagnetic wave [4]

$$\Delta x = c\Delta t \tag{2.18}$$

Where c is speed of light and Δt is the travel time then energy density may be written as

$$U = \frac{\Delta E}{A(c\Delta t)} \tag{2.19}$$

Where ΔE is the energy contained in the volume element. The energy flux may be written as

$$W = \frac{1}{A}\left(\frac{\Delta E}{\Delta t}\right) \tag{2.20}$$

And finally

$$P = U = \frac{W}{c} \tag{2.21}$$

In conclusion the expression given in equation (2.21) is equivalent to the expression given in equation (2.10). Therefore quantum mechanical and electromagnetic approaches give the same radiation pressure.

2.2 Solar Radiation Force Models

In the previous topics the radiation pressure was given. In this section solar sail force models are presented. The models do not include the effect of sail film wrinkles, thermal deformation and structural vibration.

2.2.1 Force on a perfectly reflective solar sail

The force exerted on a solar sail is the function of solar sail orientation with respect to Sun. In McInnes book [4] the model is explained as follows

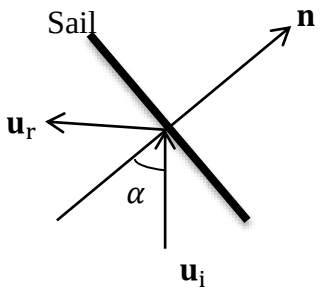

Figure 2.3 Perfectly reflecting solar sail [4]

As shown in Figure 2.3 $\mathbf{u}_i$ is the incident light and $\mathbf{u}_r$ is the reflected light and α is the angle between sail normal and incident light. The force exerted on the sail due to $\mathbf{u}_i$ is given as follows

$$\mathbf{f_i} = PA(\mathbf{u}_i \cdot \mathbf{n})\mathbf{u}_i \tag{2.22}$$

Where $\mathbf{n}$ is the sail normal and $A(\mathbf{u}_i \cdot \mathbf{n})$ is the projected area in the $\mathbf{u}_i$ direction. The reflected light $\mathbf{u}_r$ will exert a force of equal magnitude on the sail, but in the opposite direction.

$$\mathbf{f}_r = -PA(\mathbf{u}_i \cdot \mathbf{n})\mathbf{u}_r \tag{2.23}$$

By using the vector identity

$$\mathbf{u}_i - \mathbf{u}_r = 2(\mathbf{u}_i \cdot \mathbf{n})\mathbf{n} \tag{2.24}$$

The total force on the solar sail is given as

$$\mathbf{f} = 2PA(\mathbf{u}_i \cdot \mathbf{n})^2\mathbf{n} \tag{2.25}$$

From equations (2.5) and (2.10) the total force can be express as

$$\mathbf{f} = \frac{2AW_E}{c}\left(\frac{R_E}{r}\right)^2 (\mathbf{u}_i \cdot \mathbf{n})^2\mathbf{n} \tag{2.26}$$

The performance of the solar sail can be parameterized by using the mass and the area of the solar sail. The mass per unit area of the sail is known as sail loading, which is given as

$$\sigma = \frac{m}{A} \tag{2.27}$$

And by using the angle between solar sail normal and incident light, the specific force on solar sail may be written as

$$\mathbf{a} = \frac{2W_E}{c}\frac{1}{\sigma}\left(\frac{R_E}{r}\right)^2 cos^2(\alpha)\mathbf{n} \tag{2.28}$$

2.2.2 Force on a non-perfect solar sail

Considering the reflectivity, absorption and emissivity of a solar sail an exact solar sail force model can be derived [4].

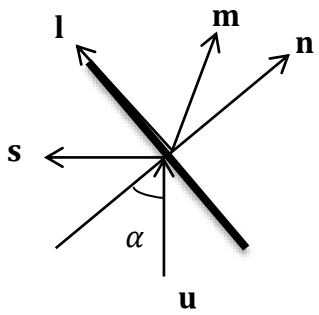

Figure 2.4 Non-perfect solar sail [4]

Solar radiation force may be written as

$$\mathbf{f} = \mathbf{f_r} + \mathbf{f_a} + \mathbf{f_e} \tag{2.29}$$

Where $\mathbf{f_r}, \mathbf{f_a}$ and $\mathbf{f_e}$ are the forces due to reflection, absorption and emission respectively. The coefficient for reflection $\tilde{r}$, absorption $\breve{\alpha}$ and emission τ is [4]

$$\tilde{r} + \breve{\alpha} + \tau = 1 \tag{2.30}$$

On the reflective side $\tau = 0$, so

$$\breve{\alpha} = 1 - \tilde{r} \tag{2.31}$$

As shown in Figure 1.5 solar sail normal is **n** and **l** is the unit normal vector to the solar sail normal **n. u** is the direction of the incident light and **s** is the direction of the reflected light and **m** is the direction of the resultant solar force vector. By considering the non-ideal solar sail the resulting force vector can be written as

$$\begin{aligned}\mathbf{f_n} = PA\Big\{&(1+\tilde{r}s)cos^2(\alpha) + B_f(1-s)\tilde{r}cos(\alpha) \\ &+ (1-\tilde{r})\frac{\varepsilon_f B_f - \varepsilon_b B_b}{\varepsilon_f + \varepsilon_b}cos(\alpha)\Big\}\mathbf{n}\end{aligned} \tag{2.32}$$

$$\mathbf{f_l} = PA(1-\tilde{r}s)cos(\alpha)sin(\alpha)\mathbf{l} \tag{2.33}$$

Where B_f and B_b indicate the front and back surface of the non-Lambertian solar sail.

Lambertian surface appears equally bright when viewed from any aspect [4]. Where ε_f and ε_b are the front and back emissivity of the sail.

Detail derivation of the equation (2.32) and (2.33) may be found in [4].

In this chapter the physics of radiation pressure is explained. And radiation force models are introduced.

CHAPTER 3

FORMULATION OF THE PROBLEM

3.1 Reference Frames

3.1.1 Earth centered inertial frame

Inertial frame of reference is defined to be stationary in space or moving at a constant velocity. The Earth centered inertial frame is used to define the motion of the solar sail. The origin of the frame is at the center of the earth. The Z-axis pointing the Earth's rotation axis, the x-axis is in the equatorial plane and pointing from Sun to Earth and y-axis completes the right handed system.

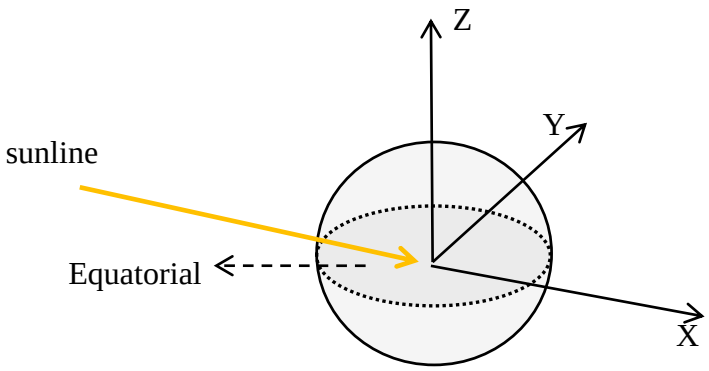

Figure 3.1 Illustration of ECI

As it is seen in the Figure 3.2 the frame is assumed to be stationary in the space and X-axis is aligned with the line of intersection of ecliptic plane and equatorial plane in the direction from Sun to Earth.

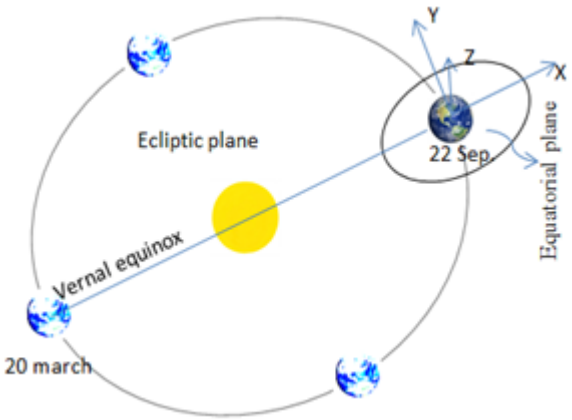

Figure 3.2 Orientation of Earth centered frame

3.1.2 Orbital frame of reference

The origin of the frame is at the center of the satellite. Keplerian orbital elements are used to define the position of a satellite. The fundamental plane is the instantaneous orbital plane of the satellite. Z_o-axis is directed from center of Earth to center of satellite and Y_o-axis is perpendicular to the fundamental plane in the positive direction of instantaneous orbital angular momentum vector. And X_o-axis completes the triad, and is in the velocity vector direction for circular orbits.

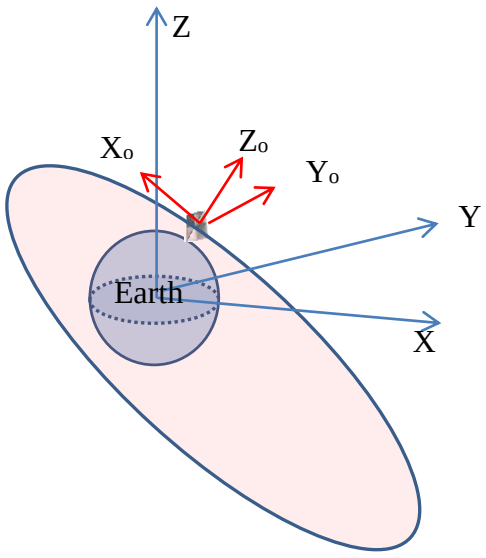

Figure 3.3 Illustration of orbital frame

3.1.3 Body fixed coordinate system

Body fixed coordinate system is used to define the attitude dynamics of the vehicle. In body fixed coordinate system mass moment of inertia of a rigid body is constant. The origin of the frame is at the mass center of the body. As shown in Figure 3.3, x-axis is the roll axis and it is normal to the solar sail and directed from non-reflective side of the solar sail. The y-axis is the pitch axis, it is in the sail plane, and z-axis is the yaw axis and it is in the sail plane

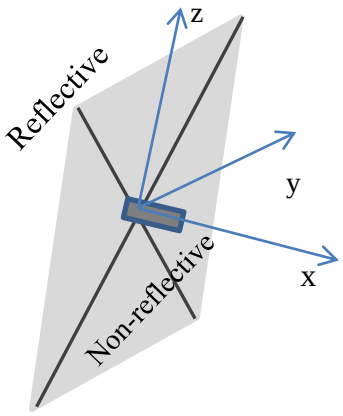

Figure 3.4 Body fixed coordinate system

3.2 Orbital Mechanics of the Solar Sail

The equation of the orbital motion of a satellite with respect to the Earth centered inertial Cartesian coordinates may be expressed as

$$\ddot{\mathbf{X}} = -\mu\frac{\mathbf{X}}{r^3} + \mathbf{f_X}$$
$$\ddot{\mathbf{Y}} = -\mu\frac{\mathbf{Y}}{r^3} + \mathbf{f_Y} \qquad (3.1)$$
$$\ddot{\mathbf{Z}} = -\mu\frac{\mathbf{Z}}{r^3} + \mathbf{f_Z}$$

The double dots on $\mathbf{X}$, $\mathbf{Y}$ and $\mathbf{Z}$ is the second time derivative of them. Where $r = \sqrt{\mathbf{X}^2 + \mathbf{Y}^2 + \mathbf{Z}^2}$, and $\mathbf{f_X}$, $\mathbf{f_Y}$ and $\mathbf{f_Z}$ are the inertial frame components of the acceleration due to solar radiation force acting on the spacecraft. And $\mu = GM$ where G is gravitational constant and M is the mass of the Earth.

3.3 Osculating Orbital Elements

The motion of a satellite can be expressed also in terms of the orbital elements. The variaton of six orbtal elements, a is the semi-major axis, e is the eccentricity, i is the inclination, Ω is the right ascension of the ascending node, w is the argument of periapse, and v is the true anomaly, are expressed in 6 first order differential equations, they are called Gauss's form which may be written as [26] [27].

$$\frac{da}{dt} = \frac{2a^2}{h}\left(esin(v)\mathbf{R} + \frac{p}{r}\mathbf{T}\right) \tag{3.2}$$

$$\frac{de}{dt} = \frac{1}{h}\{psin(v)\mathbf{R} + [(p+r)\cos(v) + re]\mathbf{T}\} \tag{3.3}$$

$$\frac{di}{dt} = \frac{rcos(\emptyset)}{h}\mathbf{N} \tag{3.4}$$

$$\frac{d\Omega}{dt} = \frac{rsin(\emptyset)}{hsin(i)}\mathbf{N} \tag{3.5}$$

$$\frac{dw}{dt} = \frac{1}{he}[-pcos(v)R + (p+r)\sin(v)\mathbf{T}] - \frac{rsin(\emptyset)\cos(i)}{hsin(i)}\mathbf{N} \tag{3.6}$$

$$\frac{dv}{dt} = \frac{h}{r^2} + \frac{1}{eh}[pcos(v)\mathbf{R} - (p+r)\sin(v)\mathbf{T}] \tag{3.7}$$

Where

$\emptyset = v + w$, is argument of latitude

$p = a(1-e^2)$, is the semi-latus rectum

$r = \frac{p}{1+ecos(v)}$, is the instantaneous radius of the satellite

$h = \sqrt{\mu p}$, is the magnitude of the angular momentum

Where $\mathbf{R}$, $\mathbf{T}$ and $\mathbf{N}$ are the specific forces in the radial, transverse, and orbit normal directions.

In the case of circular orbit or zero inclination Gauss's form of planetary equations i.e. equations (3.5),(3.6) and (3.7) are singular. Because in circular orbit, the true anomaly

and the argument of periapsis are undefined. And also for zero inclination some terms in differential equations also go to infinity. To get rid of singularity nonsingular equinoctial elements may be used. Since desired solar sail orientation with respect to orbital element and sunline, is needed, the Gauss's form of planetary equations are used.

3.4 Locally Optimal Orientation of Solar Sail

Locally optimal steering laws are used to maximize the instantaneous rate of change of orbital elements. However, these locally optimal orientation laws do not guarantee global optimality [4].

Before, describing the general mechanization of changing orbital elements, we can begin with a simple and intuitive way of maximization of rate of change of semi-major axis by considering orbital energy.

3.4.1 Energy approach for semi-major axis

For orbital decay the radiation force vector must be oriented in such a way to decrease the orbital energy, or for orbital rise the radiation force vector must be oriented to increase the orbital energy. For this reason the sail must be oriented such that the component of the drag or thrust due to solar radiation is maximized. Consider the orbital equation given below with gravitational attraction, and solar sail characteristic acceleration [4]

$$\frac{d^2\mathbf{r}}{dt^2} + \mu\frac{\mathbf{r}}{r^3} = K(\mathbf{s}\cdot\mathbf{n})^2\mathbf{n} \tag{3.8}$$

K is specific force of solar sail due to solar radiation, μ Earth's gravitational parameter, and **n** is the sail normal, and **s** sun-line direction vector. An energy equation may be obtained by multiplying equation (3.8) by the velocity vector, **v**.

$$\frac{d^2\mathbf{r}}{dt^2}\cdot\mathbf{v} + \mu\frac{\mathbf{r}\cdot\mathbf{v}}{r^3} = K(\mathbf{s}\cdot\mathbf{n})^2\mathbf{n}\cdot\mathbf{v} \tag{3.9}$$

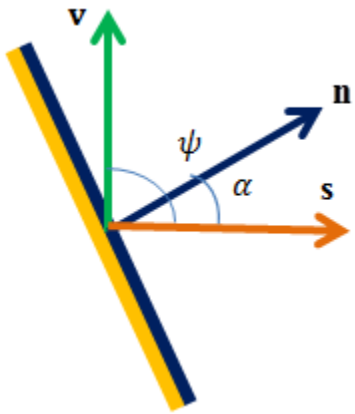

Figure 3.5 Solar sail orientation

Since the left hand side of the above equation (3.9) represents the rate of change of total energy

$$\frac{dE}{dt} = K(\mathbf{s}\cdot\mathbf{n})^2\mathbf{n}\cdot\mathbf{v} \tag{3.10}$$

The right hand side of the equation (3.10) may be written as:

$$(\mathbf{s}\cdot\mathbf{n})^2\mathbf{n}\cdot\mathbf{v} = cos^2(\alpha)\, cos(\psi-\alpha) \tag{3.11}$$

Where ψ is the angle between sunline and the velocity vector and α is the angle between sunline and the solar sail normal as shown in Figure 3.5. To find the angles that will result on maximum solar drag or solar thrust. We take the derivative of equation (3.10) with respect to angle α,

$$\frac{d}{d\alpha}\left(\frac{dE}{dt}\right) = \frac{d}{d\alpha}K(\boldsymbol{s}\cdot\boldsymbol{n})^2\boldsymbol{n}\cdot\boldsymbol{v} = 0 \tag{3.12}$$

$$\frac{d}{d\alpha}\left(\frac{dE}{dt}\right) = \frac{d}{d\alpha}(2PAcos^2(\alpha)\cos(\psi-\alpha)) \tag{3.13}$$

$$\frac{d}{d\alpha}(cos^2(\alpha)\cos(\psi-\alpha)) = \frac{1}{2}[\sin(\psi) - 3\sin(\psi-2\alpha)]\cos(\alpha) \tag{3.14}$$

The root of the right hand side of the equation (3.14) will give us the values of α which maximize the rate of change.

$$\sin(\psi) - 3\sin(\psi-2\alpha) = 0 \tag{3.15}$$

$$\sin(\psi-2\alpha) = \frac{1}{3}\sin(\psi) \tag{3.16}$$

Now by taking the inverse of both sides we have

$$\psi - 2\alpha = \sin^{-1}\left(\frac{\sin(\psi)}{3}\right) \tag{3.17}$$

Or we have

$$\psi - 2\alpha = \pi - \sin^{-1}\left(\frac{\sin(\psi)}{3}\right) \tag{3.18}$$

After some arrangements

$$\alpha_1 = \frac{1}{2}\left[\psi - \sin^{-1}\left(\frac{\sin(\psi)}{3}\right)\right] \tag{3.19}$$

$$\alpha_2 = \frac{1}{2}[\psi + \sin^{-1}\left(\frac{\sin(\psi)}{3}\right) - \pi] \tag{3.20}$$

These values of α's are give the orientation of solar sail normal with respect to sunline to maximize the rate of change of orbital energy and semi-major axis of the solar sail.

3.4.2 Best direction approach to change orbital elements

The Gauss's planetary equations defined in the previous section may be written in the following form for arbitrary orbital elements [4].

$$\frac{dZ}{dt} = \boldsymbol{\lambda}(Z) \cdot \mathbf{f} \tag{3.21}$$

Where $\boldsymbol{\lambda} = (\lambda_{\mathbf{R}}, \lambda_{\mathbf{T}}, \lambda_{\mathbf{N}})$ is the vector function of the orbital element, and $\mathbf{f} = (\mathbf{R}, \mathbf{T}, \mathbf{N})$ is the solar sail force. To maximize the rate of change of element i, the radiation pressure force component in the direction of $\boldsymbol{\lambda}$ must be maximized. The radiation force on the perfectly reflective solar sail is given in equation (2.25). When dot product with $\boldsymbol{\lambda}(Z)$ is carried out.

$$\mathrm{f}_{\boldsymbol{\lambda}} = 2PA(\mathbf{n} \cdot \mathbf{s})^2 \mathbf{n} \cdot \boldsymbol{\lambda}(Z) \tag{3.22}$$

From the Figure 3.6 the equation (3.22) may be written as

$$\mathrm{f}_{\boldsymbol{\lambda}} = 2PAcos^2(\alpha)\cos(\psi - \alpha) \tag{3.23}$$

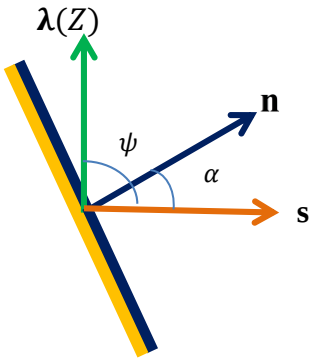

Figure 3.6 Solar sail orientation to maximize the increase in $\boldsymbol{\lambda}(Z)$

In order to maximize the change we need to take the derivative with respect to α

$$\frac{df_{\lambda}}{d\alpha} = \frac{d}{d\alpha}(2PAcos^2(\alpha)\cos(\psi - \alpha)) \tag{3.24}$$

As it can be seen equation (3.13) and (3.24) have the same form. So following procedures will be the same to find solar sail desired orientation with respect to sunline.

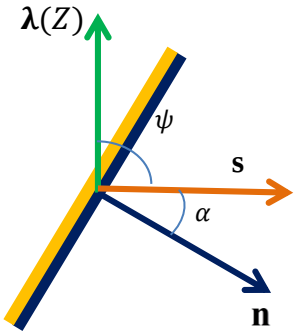

Figure 3.7 Solar sail orientation to maximize the decrease in $\boldsymbol{\lambda}(Z)$

The root α_1 represents the orientation of the solar sail shown in Figure 3.6. And when the solar sail normal is oriented in that fashion it will maximize the increase in $\boldsymbol{\lambda}(Z)$**.** And the root α_2 represents the orientation of the solar sail shown in Figure 3.7, which maximize the decrease in the orbital element $\boldsymbol{\lambda}(Z)$.

3.5 Quaternions to describe Satellite Attitude

It is desirable to use quaternion for attitude parameterization. If the current attitude with respect to a reference frame is given in terms of a quaternion such as: $q = q_1\mathbf{i} + q_2\mathbf{j} + q_3\mathbf{k} + q_4 = \mathbf{q} + q_4$, $q = \boldsymbol{\delta}\sin(\frac{\varphi}{2}) + \cos(\frac{\varphi}{2})$ where $\boldsymbol{\delta}$ represents the unite vector where the rotation take place and φ is the angle of rotation, the desired attitude is $d = (\mathbf{d} + d_4)$, and attitude change to reach the desired attitude from the current attitude expressed by quaternion is $t = (\mathbf{t} + t_4)$. And t is named as the to-go quaternion.

Between these quaternions the following relations may be written.

$$\begin{aligned} d &= qt \\ &= (\mathbf{q} + q_4)(\mathbf{t} + t_4) \\ &= \mathbf{q} \times \mathbf{t} + q_4\mathbf{t} + t_4\mathbf{q} - \mathbf{q} \cdot \mathbf{t} + q_4 t_4 \end{aligned} \tag{3.25}$$

Then the to-go quaternion may be calculated from:

$$t = q^{-1}d \tag{3.26}$$

Where q^{-1} is the inverse quaternion or the conjugate quaternion.

Quaternion derivative may be written as:

$$\begin{aligned} \dot{\mathbf{q}} &= -\frac{1}{2}\tilde{\boldsymbol{\omega}}\mathbf{q} + \frac{1}{2}q_4\boldsymbol{\omega} \\ \dot{q}_4 &= -\frac{1}{2}\boldsymbol{\omega}^T\mathbf{q} \end{aligned} \tag{3.27}$$

Or in matrix vector form,

$$\begin{aligned} \begin{Bmatrix} \dot{\mathbf{q}} \\ \dot{q}_4 \end{Bmatrix} &= \frac{1}{2}\begin{bmatrix} -\tilde{\boldsymbol{\omega}} & \boldsymbol{\omega} \\ -\boldsymbol{\omega}^T & 0 \end{bmatrix}\begin{Bmatrix} \mathbf{q} \\ q_4 \end{Bmatrix} \\ &= \frac{1}{2}\begin{bmatrix} 0 & \omega_3 & -\omega_2 & \omega_1 \\ -\omega_3 & 0 & \omega_1 & \omega_2 \\ \omega_2 & -\omega_1 & 0 & \omega_3 \\ -\omega_1 & -\omega_2 & -\omega_3 & 0 \end{bmatrix}\begin{Bmatrix} q_1 \\ q_2 \\ q_3 \\ q_4 \end{Bmatrix} \end{aligned} \tag{3.28}$$

Where, $$\tilde{\boldsymbol{\omega}} = \begin{bmatrix} 0 & \omega_3 & -\omega_2 \\ -\omega_3 & 0 & \omega_1 \\ \omega_2 & -\omega_1 & 0 \end{bmatrix}$$

Similarlly for the to-go quaternion the following may be written

$$\dot{\mathbf{t}} = -\frac{1}{2}\tilde{\boldsymbol{\omega}}\mathbf{t} - \frac{1}{2}t_4\boldsymbol{\omega} \tag{3.29}$$

$$\dot{t}_4 = \frac{1}{2}\boldsymbol{\omega}^T \mathbf{t}$$

$$\begin{Bmatrix} \dot{\mathbf{t}} \\ \dot{t}_4 \end{Bmatrix} = \frac{1}{2}\begin{bmatrix} -\tilde{\boldsymbol{\omega}} & -\boldsymbol{\omega} \\ \boldsymbol{\omega}^T & 0 \end{bmatrix}\begin{Bmatrix} \mathbf{t} \\ t_4 \end{Bmatrix}$$

$$= \frac{1}{2}\begin{bmatrix} 0 & \omega_3 & -\omega_2 & -\omega_1 \\ -\omega_3 & 0 & \omega_1 & -\omega_2 \\ \omega_2 & -\omega_1 & 0 & -\omega_3 \\ \omega_1 & \omega_2 & \omega_3 & 0 \end{bmatrix}\begin{Bmatrix} q_1 \\ q_2 \\ q_3 \\ q_4 \end{Bmatrix} \tag{3.30}$$

3.6 Determination of Desired Attitude of the Solar Sail

Since the locally optimal angular orientation of solar sail normal with respect to sunline is found as a function of angle between function vector $\boldsymbol{\lambda}(Z)$ and sunline **s** the following relations can be used to go to desired attitude. In this case we follow the development given in the McInnes Book [4]. Here the main difference is that in the Book of McInnes, the sun vector lies in the orbital plane. However, there will be out of plane forces, which will cause the change in inclination as well as the motion of the right ascension of the ascending node. In this case, it is meaningful to use satellite measured attitudes. First assume that the satellite x-axis, is in the normal direction of the solar sail Thus, the solar sail normal direction is originally $\mathbf{n} = [1\ 0\ 0]$ in body fixed coordinate system.Both the direction of the sun as well as the direction of the $\boldsymbol{\lambda}(Z)$ vector is measured in the body fixed frame.

In order to find a way to orient the solar sail in order to increase the change, let

$$\boldsymbol{\gamma} = \frac{\mathbf{s} \times \boldsymbol{\lambda}}{\|\mathbf{s} \times \boldsymbol{\lambda}\|} \tag{3.31}$$

Then rotate **s** by α according to

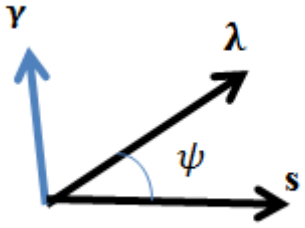

Figure 3.8 Cross product of sunline and vector function

$$\mathbf{q}_r = [\cos\left(\frac{\alpha}{2}\right)\ \boldsymbol{\gamma}\sin(\frac{\alpha}{2})] \tag{3.32}$$

Then the desired normal direction can be calculated by rotating sunline **s** about vector $\boldsymbol{\gamma}$ through the angle α

$$\mathbf{n_d} = \mathbf{q}_r \mathbf{s} \mathbf{q}_r{}^* \tag{3.33}$$

Where $\mathbf{q}_r{}^*$ is the conjugate of $\mathbf{q}_r$. Once the desired normal direction $\mathbf{n_d}$ is found, the to-go quaternion to carry out the attitude control may be found from current sail normal direction and desired sail normal direction. Since two vectors are known the angle between them may be found as,

$$\beta = \cos^{-1}\left(\frac{\mathbf{n}\cdot\mathbf{n_d}}{\|\mathbf{n}\|\|\mathbf{n_d}\|}\right) \tag{3.34}$$

The direction of the to-go quaternion may be found from

$$\mathbf{e} = \frac{\mathbf{n}\times\mathbf{n_d}}{\|\mathbf{n}\times\mathbf{n_d}\|} \tag{3.35}$$

$$\mathbf{t} = [\mathbf{e}sin(\frac{\beta}{2})\ \ \cos\left(\frac{\beta}{2}\right)] \tag{3.36}$$

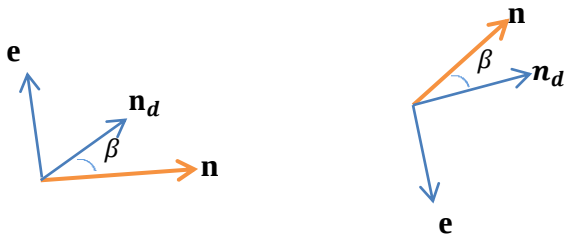

(a) (b)

Figure 3.9 Illustration of to-go from **n** to $\boldsymbol{n_d}$

As it is seen in Figure 3.9, no matter what the orientation of the normal and desired, normal positive rotation about **e** through the angle β will bring the normal to the desired normal orientation.

Therefore the way of reorientation of sail normal is described.

3.7 Attitude Dynamics and Control

The attitude of the rigid solar sail may be define as

$$\mathbf{J}\dot{\boldsymbol{\omega}} + \boldsymbol{\omega} \times \mathbf{J}\boldsymbol{\omega} = \mathbf{u} \tag{3.37}$$

Where **J** is the inertia matrix, $\boldsymbol{\omega}$ is angular velocity vector and **u** is the control torque.

$$\boldsymbol{\omega} = \begin{bmatrix} \omega_x \\ \omega_y \\ \omega_z \end{bmatrix} \qquad \mathbf{u} = \begin{bmatrix} u_x \\ u_y \\ u_z \end{bmatrix}$$

Quaternion is the most convenient and numerically efficient way of representing the attitude of spacecraft. As given in equation (3.38) a quaternion is formed by four parameters

$$\begin{aligned} \mathrm{q} &= [q_1 \;\; q_2 \;\; q_3 \;\; q_4] \\ &= [\mathbf{q} \;\; q_4] \end{aligned} \tag{3.38}$$

And the attitude kinematics equations in quaternion form is given as follows,

$$\begin{Bmatrix} \dot{\mathbf{q}} \\ \dot{q}_4 \end{Bmatrix} = \frac{1}{2} \begin{bmatrix} 0 & \omega_z & -\omega_y & \omega_x \\ -\omega_z & 0 & \omega_x & \omega_y \\ \omega_y & -\omega_x & 0 & \omega_z \\ -\omega_x & -\omega_y & -\omega_z & 0 \end{bmatrix} \begin{Bmatrix} \mathbf{q} \\ q_4 \end{Bmatrix} \tag{3.39}$$

And derivative of to-go quaternion may be written as

$$\begin{Bmatrix} \dot{\mathbf{t}} \\ \dot{t}_4 \end{Bmatrix} = \frac{1}{2} \begin{bmatrix} 0 & \omega_z & -\omega_y & -\omega_x \\ -\omega_z & 0 & \omega_x & -\omega_y \\ \omega_y & -\omega_x & 0 & -\omega_z \\ \omega_x & \omega_y & \omega_z & 0 \end{bmatrix} \begin{Bmatrix} \mathbf{t} \\ t_4 \end{Bmatrix} \tag{3.40}$$

Once we found the to-go quaternion in section 3.6, nonlinear attitude control of the spacecraft may be carried out using the following positive definite Lyapunov function [27]:

$$V = \frac{1}{2}\boldsymbol{\omega}^T \mathbf{K}^{-1} \mathbf{J}\boldsymbol{\omega} + 2(1 \pm \mathrm{t}_4) \tag{3.41}$$

Provided that $\mathbf{K}^{-1}$ is positive definite, this expression is always positive definite. Its time rate change may be written as:

$$\dot{V} = \boldsymbol{\omega}^T \mathbf{K}^{-1} \mathbf{J}\dot{\boldsymbol{\omega}} \pm 2\dot{\mathrm{t}}_4 \tag{3.42}$$

$$\dot{V} = \boldsymbol{\omega}^T \mathbf{K}^{-1}(-\boldsymbol{\omega} \times \mathbf{J}\boldsymbol{\omega} + \mathbf{u}) \mp \boldsymbol{\omega}^T \mathbf{t} \tag{3.43}$$

Setting the decay rate to

$$\dot{V} = -\boldsymbol{\omega}^T \mathbf{K}^{-1} \mathbf{C} \boldsymbol{\omega} \tag{3.44}$$

where $\mathbf{C}$ is also positive definete. And control law takes the following form

$$\mathbf{u} = \boldsymbol{\omega} \times \mathbf{J}\boldsymbol{\omega} + \mathbf{K}\mathbf{t} - \mathbf{C}\boldsymbol{\omega} \tag{3.45}$$

The closed-loop system with controller given in equation (3.45) is globally asymptotically stable if $\mathbf{K}^{-1}\mathbf{C}$ if a positive definite matrix. By selecting $\mathbf{K}$ and $\mathbf{C}$ such that,

$$\mathbf{K} = k_c \mathbf{J} \tag{3.46}$$

$$\mathbf{C} = c_c \mathbf{J} \tag{3.47}$$

Will guarantee the stability. Where k_c and c_c are positive scalar constants.
And finally we have

$$\mathbf{u} = \boldsymbol{\omega} \times \mathbf{J}\boldsymbol{\omega} + k_c \mathbf{J}\mathbf{t} - c_c \mathbf{J}\boldsymbol{\omega} \tag{3.48}$$

Controller gain constants k_c and c_c can be chosen for a specified maneuver time $(4/\xi\omega_n)$ from the following relationship [27].

$$\ddot{\theta} + c_c\dot{\theta} + \frac{k_c}{2}\theta = \ddot{\theta} + 2\xi\omega_n\dot{\theta} + {\omega_n}^2\dot{\theta} \tag{3.49}$$

Where θ is the rotation angle about the eigenaxis.

$$k_c = 2{\omega_n}^2 \tag{3.50}$$

$$c_c = 2\xi\omega_n \tag{3.51}$$

Where ω_n is natural frequency and ξ is damping ratio. In this way proper agility may be achieved.

CHAPTER 4

SIMULATION RESULTS

In this chapter simulations will be given for increasing orbital elements, particularly for semi-major axis, eccentricity and inclination.

The flowchart is shown in Figure 4.1. The simulation code is developed in MATLAB/Simulink environment to simulate the satellite orbital motion as well as attitude dynamics.

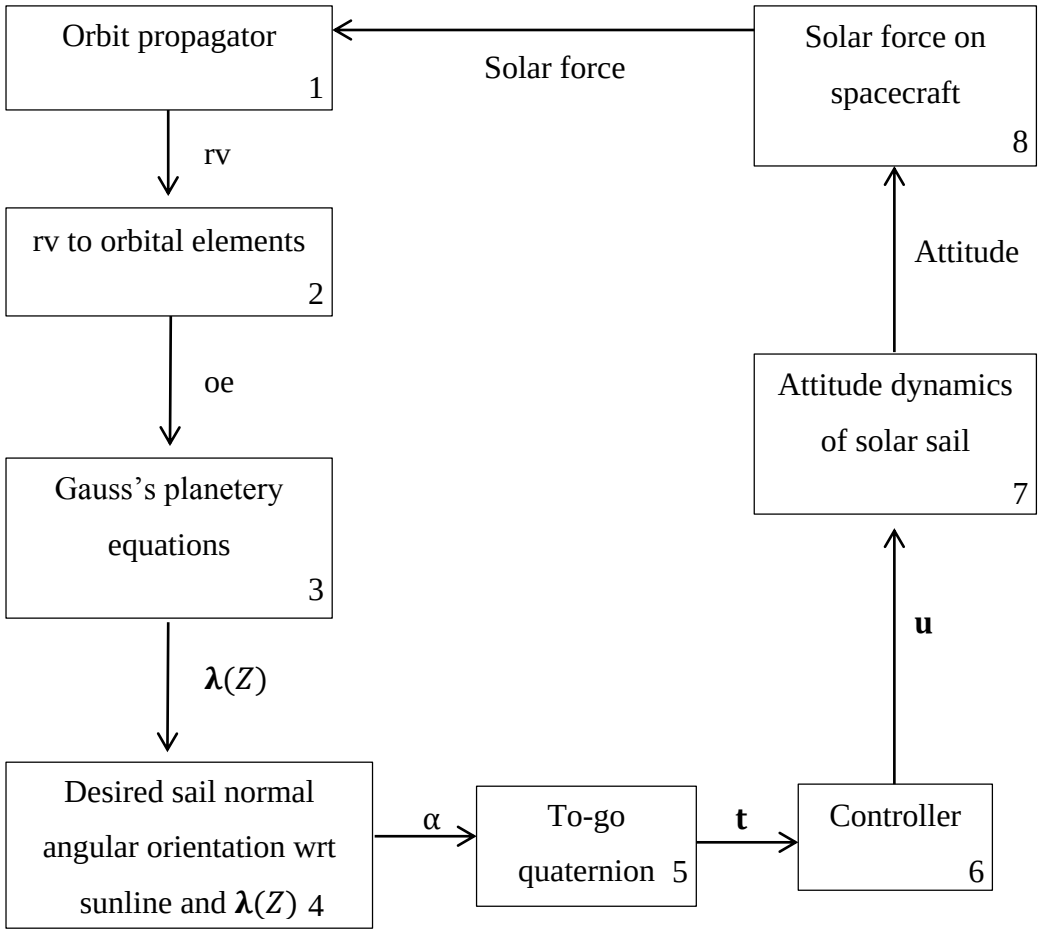

Figure 4.1 Simulation schematics

Since the purpose of this work is to show the instantaneous maximization of decay or rise in orbital elements, and the associated attitude control problem, only a simple gravitational field without the spherical harmonics, is considered in the simulation. The physical properties of the satellite are listed in Table 4.1 together with the controller parameters. A non-diagonal inertia matrix is chosen to include the inertial coupling between the coordinates. The control system parameters on the other hand are chosen for the system to have good damping and acceptable response time. 4^{th} order Runge-Kutta numerical integration is performed for time step $\Delta t = 30$ s.

Table 4.1 Cube sail and control properties

Parameter	**Value**
Mass	6 [kg]
Inertia	[7.1589 -0.03 -0.03;-0.03 3.5794 -0.03;-0.03 -0.03 3.5794] [kgm^2]
Solar sail area	25 [m^2]
Natural Frequency	ω_n=0.01 [rad/s]
Damping Ratio	$\xi = 0.7$

Initial condition for the solar sail orbit is given in the Table 4.2

Table 4.2 Initial orbital parameters

Orbital elements	**Magnitude**
Semi-major axis (α)	42000[km]
Eccentricity (*e*)	0.2
Inclination (*i*)	45[deg]
RAAN (Ω)	90[deg]
Argument of periapse (w)	90[deg]
True anomaly(*v*)	270[deg]

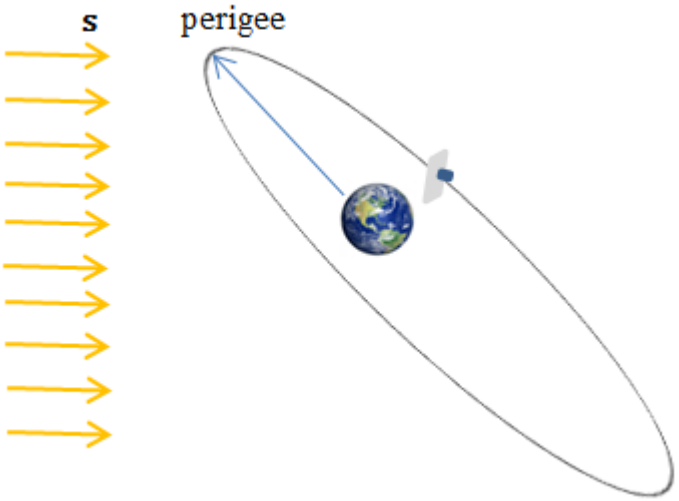

Figure 4.2 Initial orbital conditions

Body fixed coordinate system of the solar sail is initially aligned with Earth centered inertial coordinate system. Simulations will be run for 5 orbits and orbit period will be assumed to be constant during the simulations. During the simulation it is assumed that sunline vector direction is constant because daily change of sunline direction is about 0.986 [deg/day].

4.1 Two Body Simulation without Radiation Pressure

The simulation will be run without any perturbation or solar radiation force. To show the numerical errors. The initial conditions are given in Table 4.2

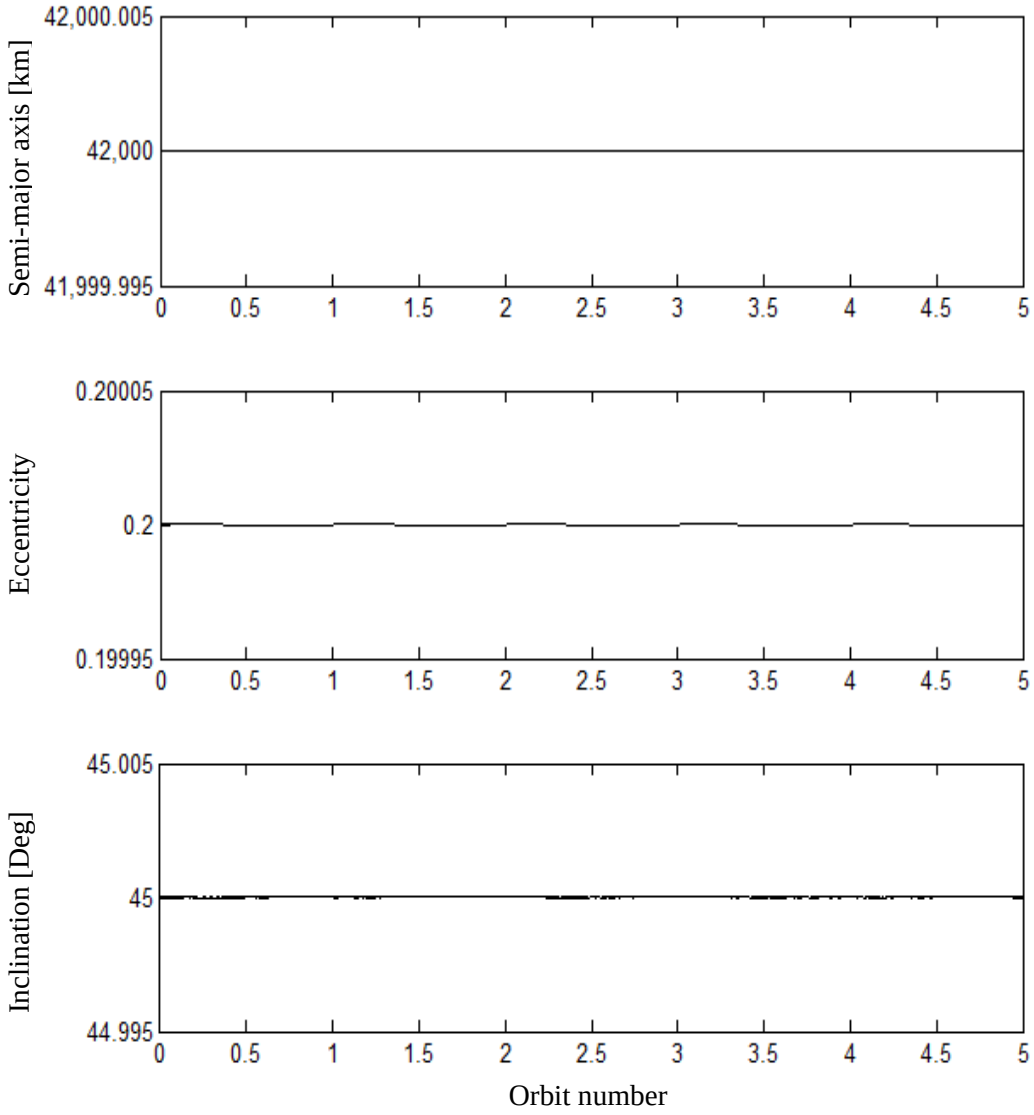

Figure 4.3 Orbital elements change only for two body

Because of the restricted number of integers the numerical errors accumulated.

That's why there can be slight change in the simulation even there is no perturbations

4.2 Two Body Simulation with Radiation Pressure and Constant Attitude

In this section the simulation will be run including the solar radiation force on the spacecraft with constant attitude.

During the simulation the reflective side of solar sail is kept normal to the sunline. In other words solar sail normal is aligned with sunline direction vector.

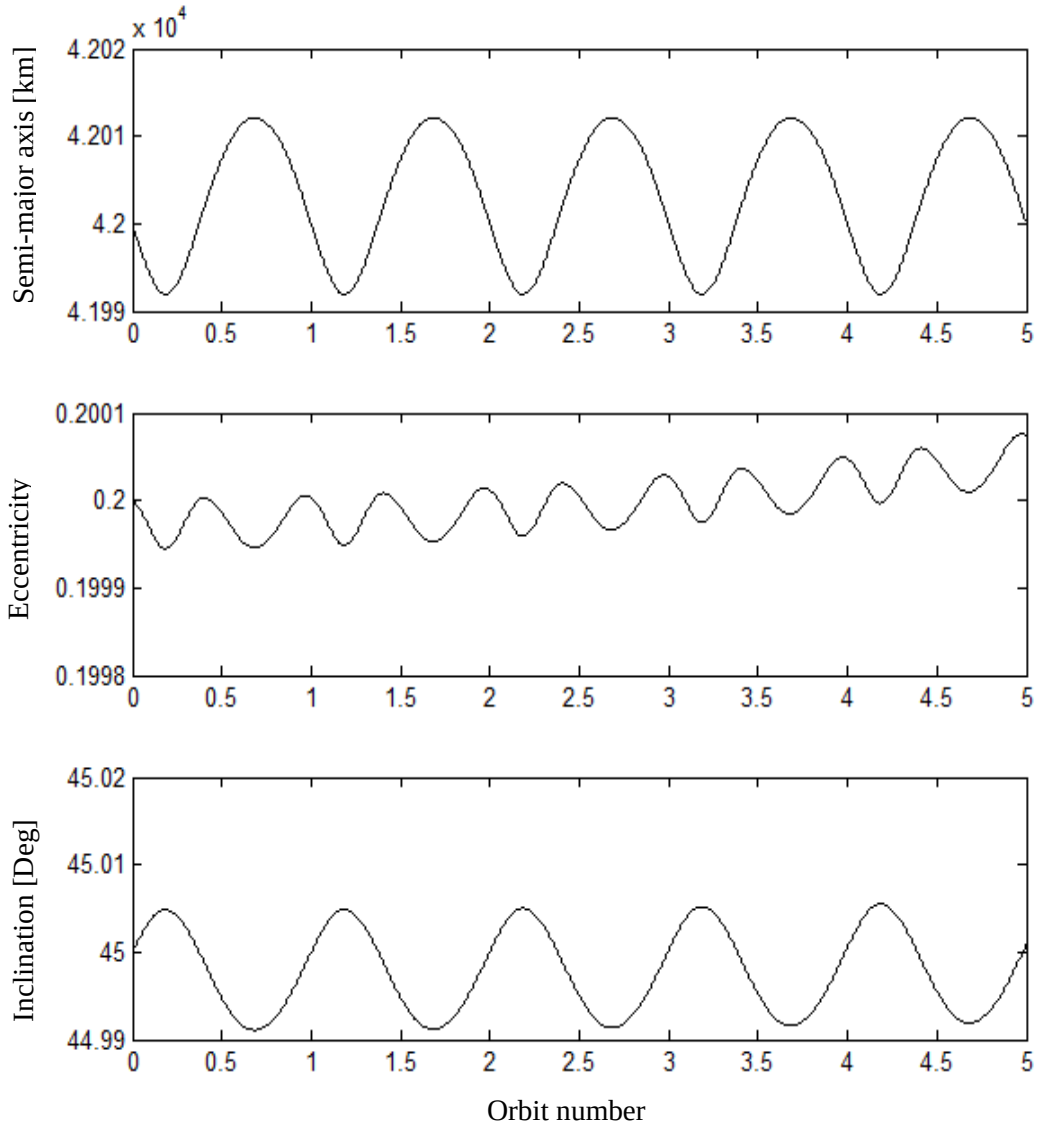

Figure 4.4 Orbital elements change with radiation pressure

Figure 4.4 shows the effect of solar radiation pressure on the satellite orbital elements. From the figure, a slow progress in the orbital elements is evident.

4.3 Increasing Semi-major Axis by Energy Method

As it is explained in section 3.4.1 the semi-major axis can be changed by considering the orbital energy of the solar sail. In this section semi-major axis will be changed by increasing the orbital energy. Initial orbital configuration for the simulation of increasing the semi-major axis by energy method is shown in Figure 4.5, and it has zero eccentricity with zero inclination and 42000 km semi-major axis.

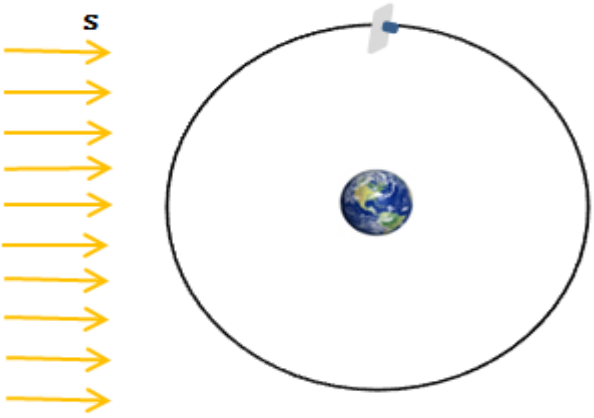

Figure 4.5 Initial orbital conditions for zero inclination

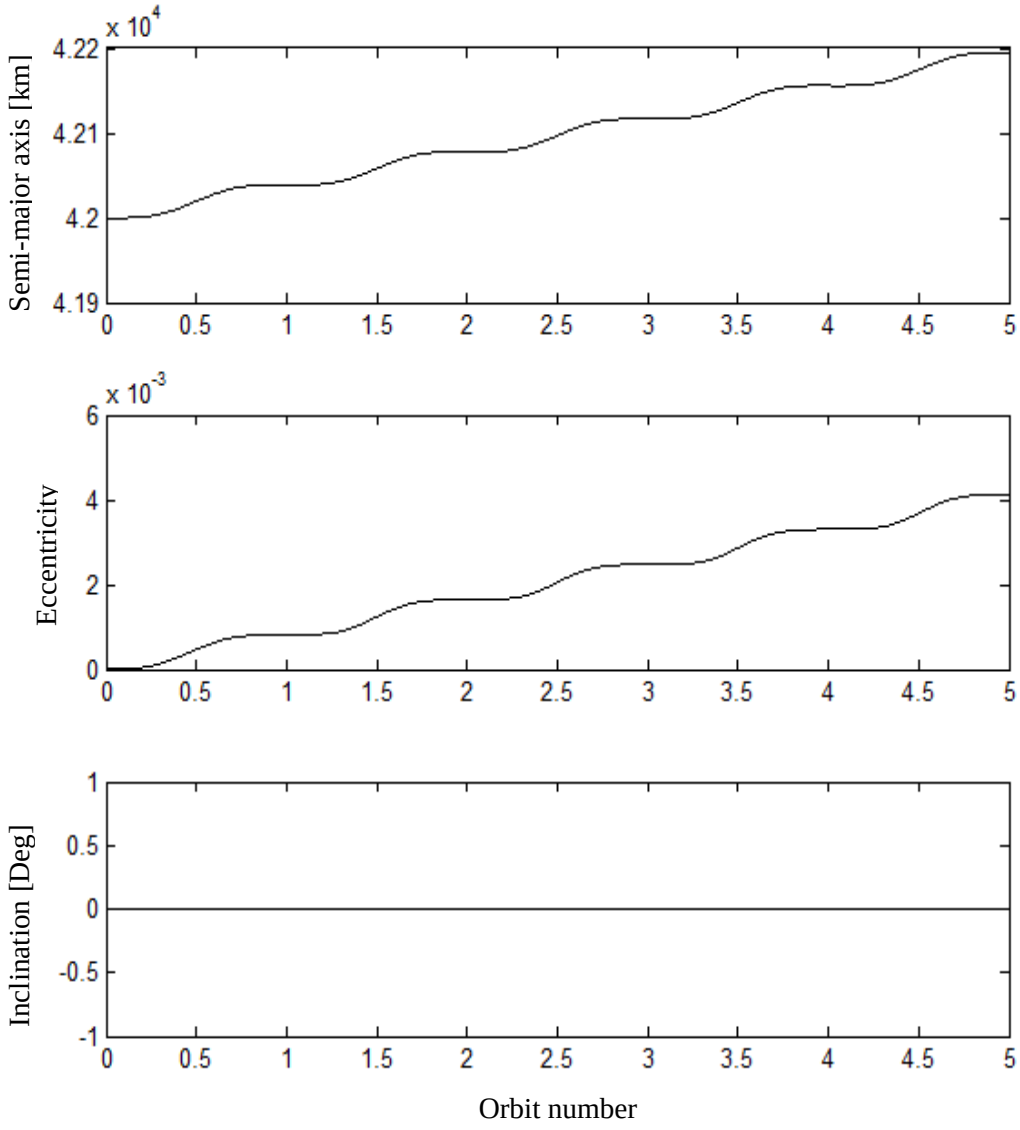

Figure 4.6 Orbital elements change by increasing orbital energy

Since the sunline is parallel to the orbital plane there is no out of plane component of solar radiation force. Consequently the inclination remains constant. It may be observed from the simulation results presented in Figure 4.6 that there is a continuous increase in semi-major axis.

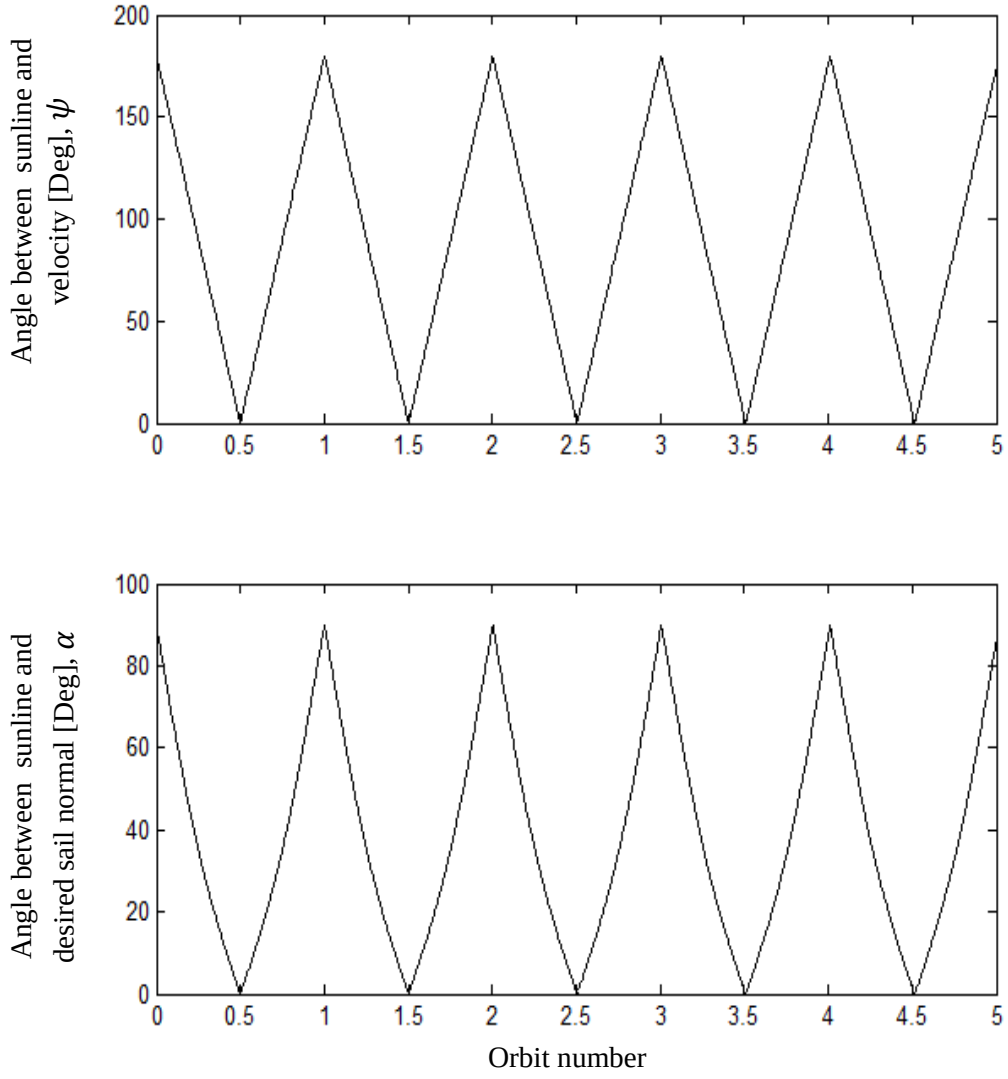

Figure 4.7 Angular position of velocity and desired sail normal with respect to sunline for increasing semi-major axis by energy method

The angles between sunline and velocity ψ and sunline and sail normal α are plotted in Figure 4.7. The figure shows that the angle between sunline and velocity vector changes between 0 and 180 [deg] and corresponding angular orientation of desired sail normal and sunline changes between 90 and 0 [deg].

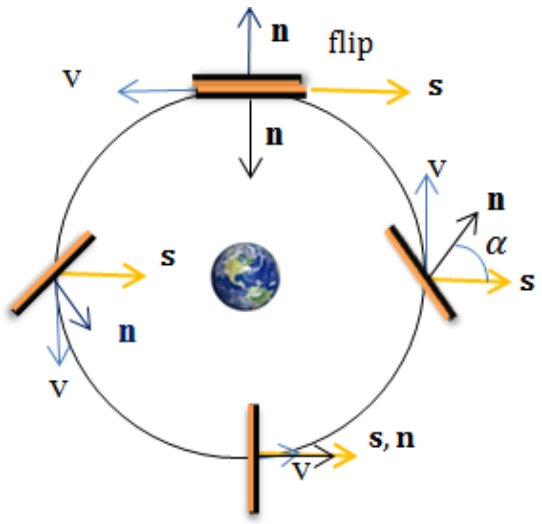

Figure 4.8 Solar sail flips

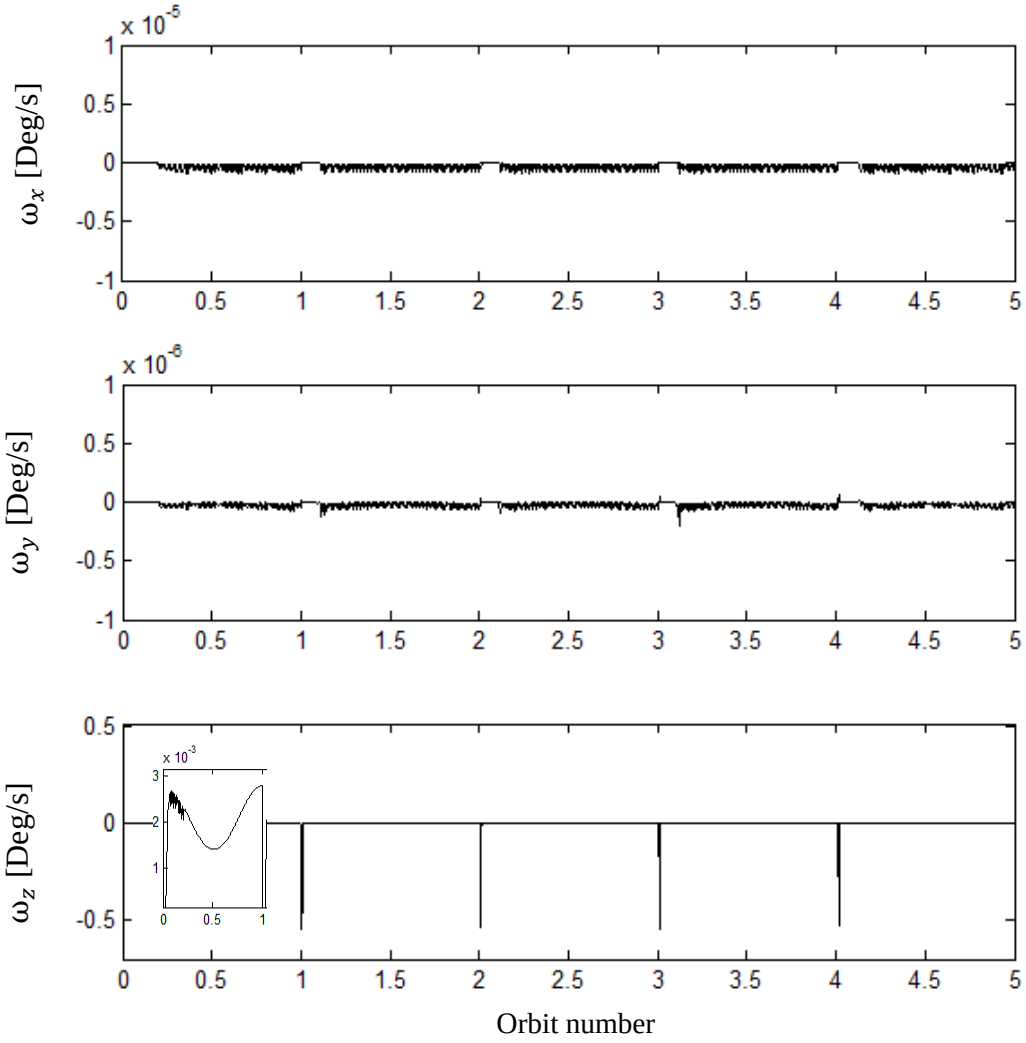

Figure 4.9 Body fixed frame angular rates

The above figure shows the angular rates in the body fixed frame. Actually there are no rotation about roll and pitch axis but vibrations about zero. These vibration are due to non- zero terms in the inertia matrix. As it can be seen in Figure 4.8 for each full orbital rotation sail makes a flip that's why there is peaks Figure 4.9 about yaw axis, which is initially along orbit normal direction.

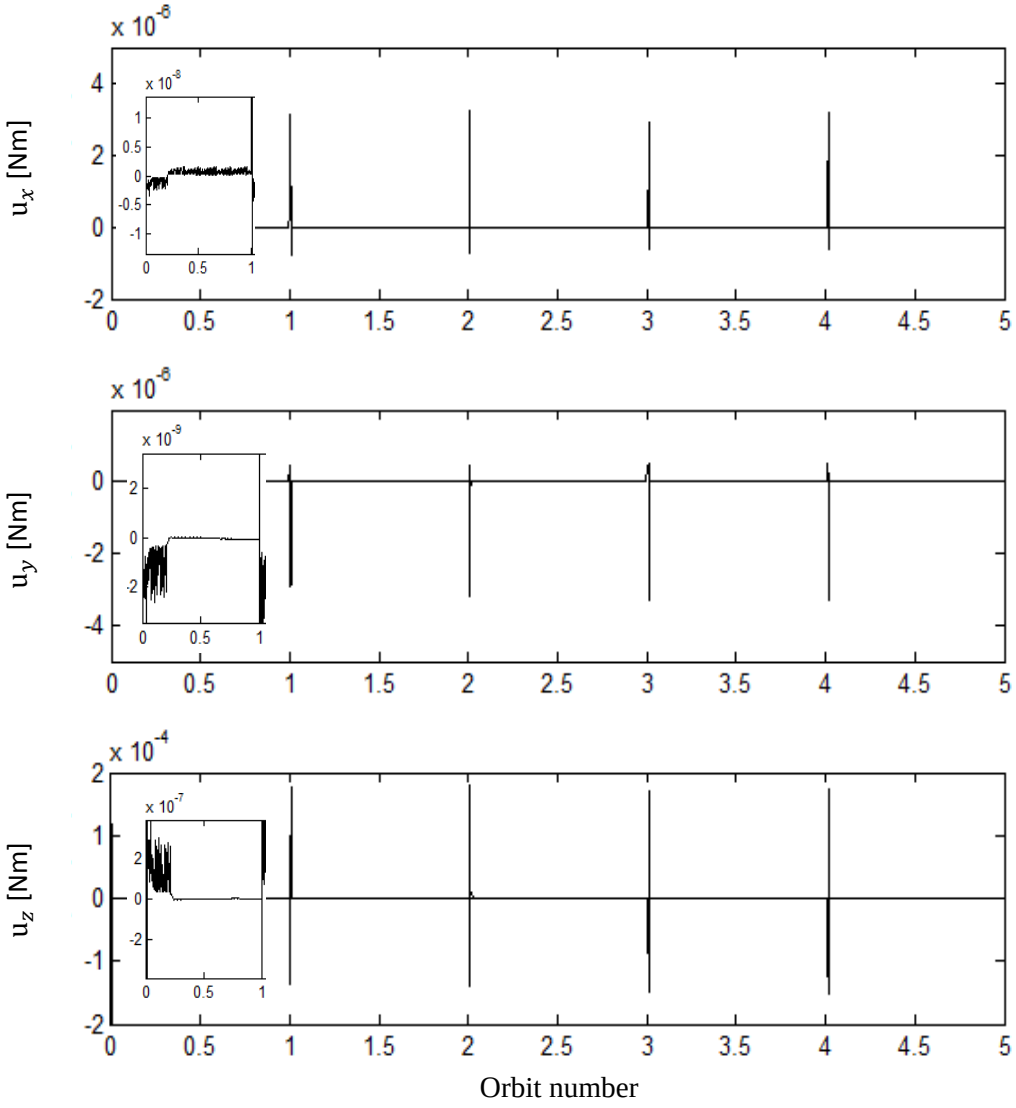

Figure 4.10 Controller torques about body axes

In between flips the rotation of the satellite is continuous and it completes its full rotation approximately in one day that's why controller torques are very small.

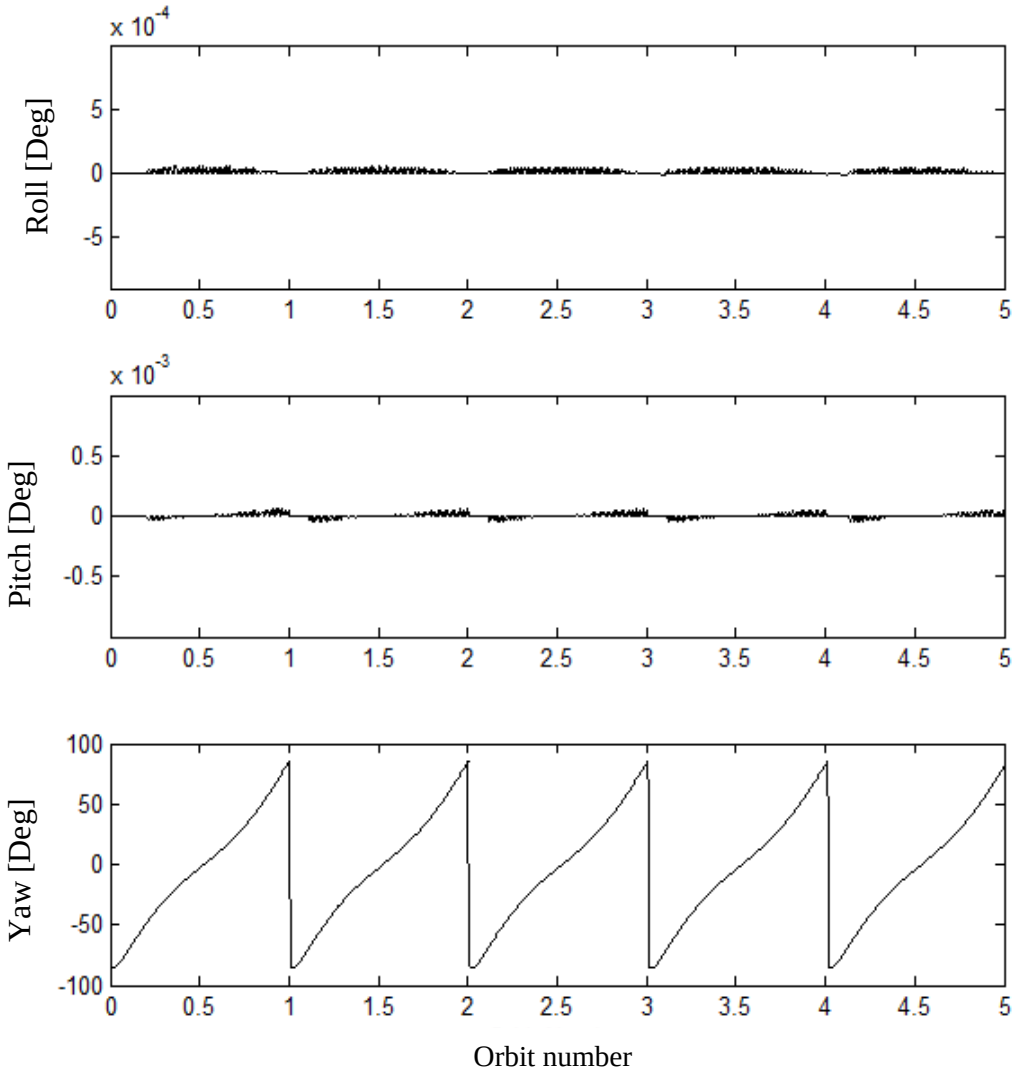

Figure 4.11 Orientation of solar sail with respect to inertial frame

The rotation sequence of Euler angles are 1 ← 2 ← 3. Axis 3 is the Z- axis ,axis 2 is the Y –axis and axis1 is the X-axis. Initially the body frame axes are aligned with the inertial frame axes and yaw axis is normal to the orbital plane of the spacecraft. So only one axis of rotation is required to reorient the solar sail.

In this section semi-major axis changed by changing the orbital energy. For this simulation a very simple initial orbit is chosen to understand the behavior of the solar force on the spacecraft.

4.4 Raising Semi-major Axis

As it is stated in the previous sections the control aim is to maximize the instantaneous rate of change of a particular orbital element. In this section by using the equations in section 3.3. Proper solar sail steering law will be generated to maximize the rate of change of semi-major axis. From equation (3.2) we have the following vector function for semi-major axis.

$$\boldsymbol{\lambda}(a) = [esinv \quad \frac{p}{r} \quad 0] \tag{4.1}$$

This vector is transformed to the Earth centered inertial frame using the following transformation [27].

$$\begin{bmatrix}\lambda_{aX}\\ \lambda_{aY}\\ \lambda_{aZ}\end{bmatrix} = \begin{bmatrix}cos\Omega & -sin\Omega & 0\\ sin\Omega & cos\Omega & 0\\ 0 & 0 & 1\end{bmatrix}\begin{bmatrix}1 & 0 & 0\\ 0 & cosi & -sini\\ 0 & sini & cosi\end{bmatrix} \times \begin{bmatrix}\cos(v+w) & -sin(v+w) & 0\\ sin(v+w) & cos(v+w) & 0\\ 0 & 0 & 1\end{bmatrix}\begin{bmatrix}\lambda_{aR}\\ \lambda_{aT}\\ \lambda_{aN}\end{bmatrix} \tag{4.2}$$

By using $\boldsymbol{\lambda}(a_{XYZ})$ and the procedure described in section 3.4, required angle between sunline and $\boldsymbol{\lambda}(a_{XYZ})$ is calculated. Then the desired attitude is found and finally by using the procedure described in section 3.7 required control torques can be found to achieve attitude maneuver.

In this section simulation is run for an inclined orbit with initial orbital configuration given in Table 4.2 to show the effectiveness of proper attitude determination and going to desired attitude mechanization.

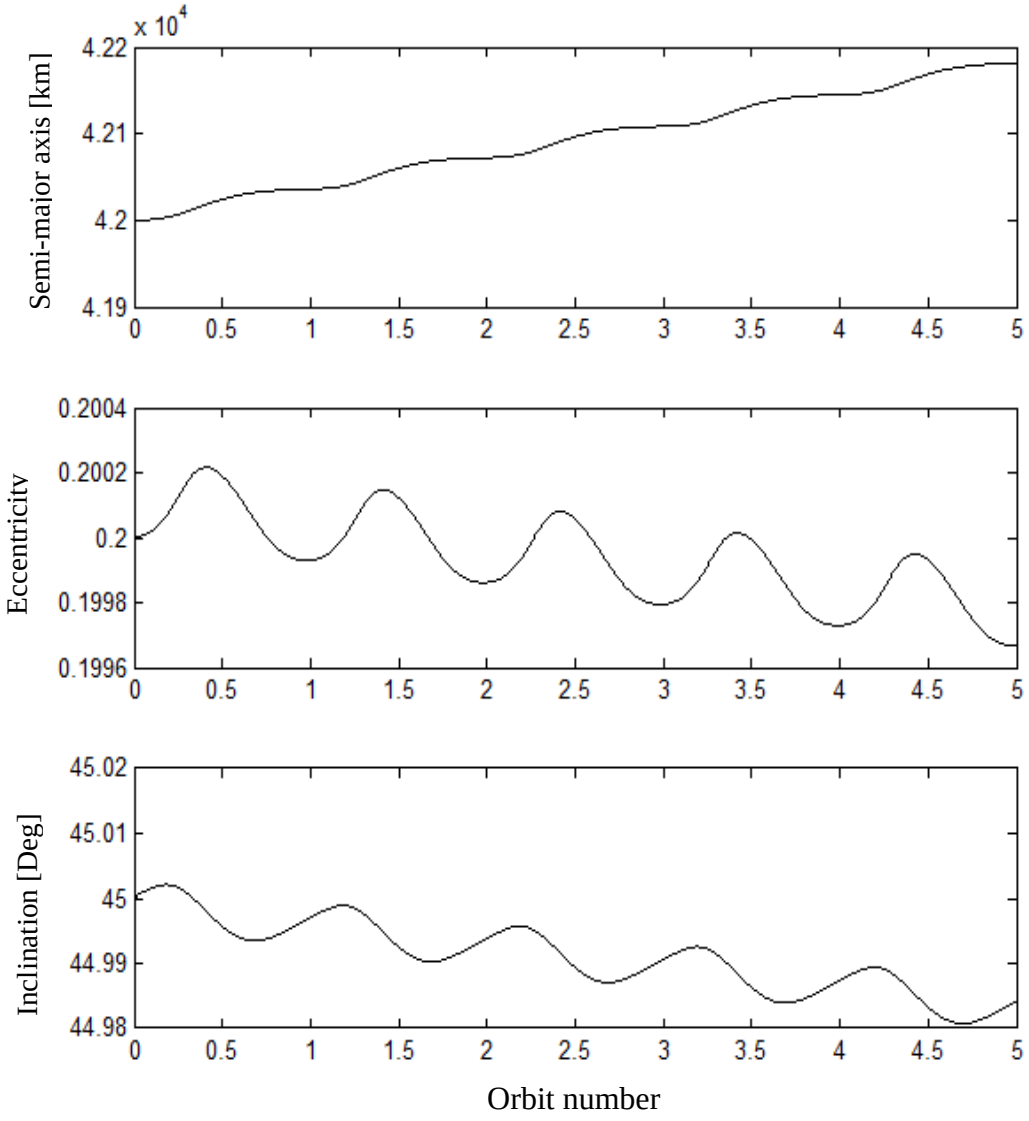

Figure 4.12 Orbital elements change when maximizing change in semi-major axis

Increase in the semi-major axis for this initial orbit and for the solar sail properties is shown in Figure 4.12. This increase in semi-major axis results in decrease in eccentricity and inclination. This behavior of eccentricity can be explained by the orientation of the perigee and by solar sail performance. The inclination changes due to out of plane component of radiation force.

By increasing semi-major axis geostationary (GEO) satellites can be moved to graveyard orbits. Graveyard orbit is an orbit just above the GEO altitude, roughly 300 km above. The simulation shows that, by carrying a light weight solar sail to orbit, and deploy it at the end of life, it is feasible to move the satellite to the graveyard orbit.

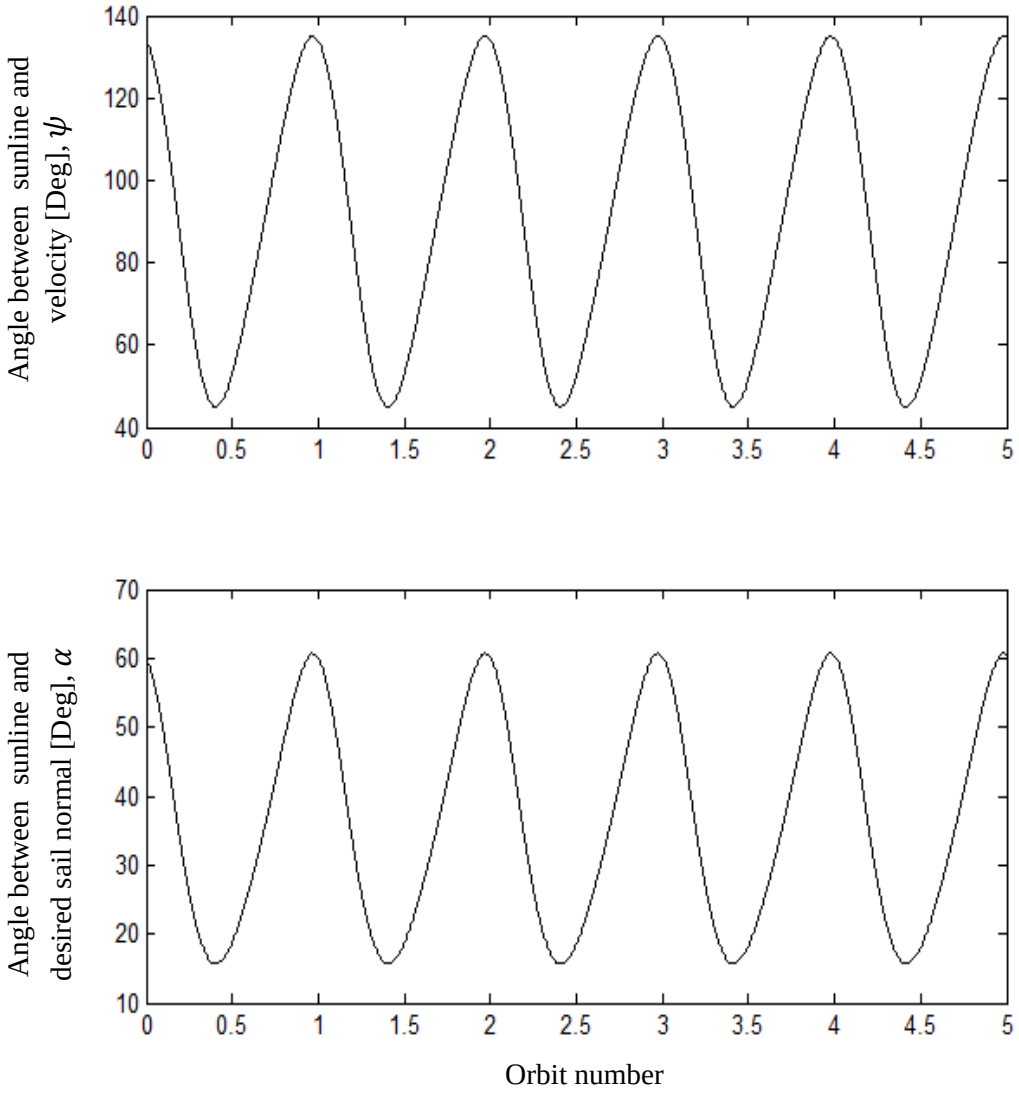

Figure 4.13 Angular positions of semi-major axis function and desired sail normal with respect to sunline for increasing semi-major axis

As it seen, in the Figure 4.13 angle between sunline and vector function of semi-major axis changes between 45 and 135 degree. This interval depends on the inclination angle.

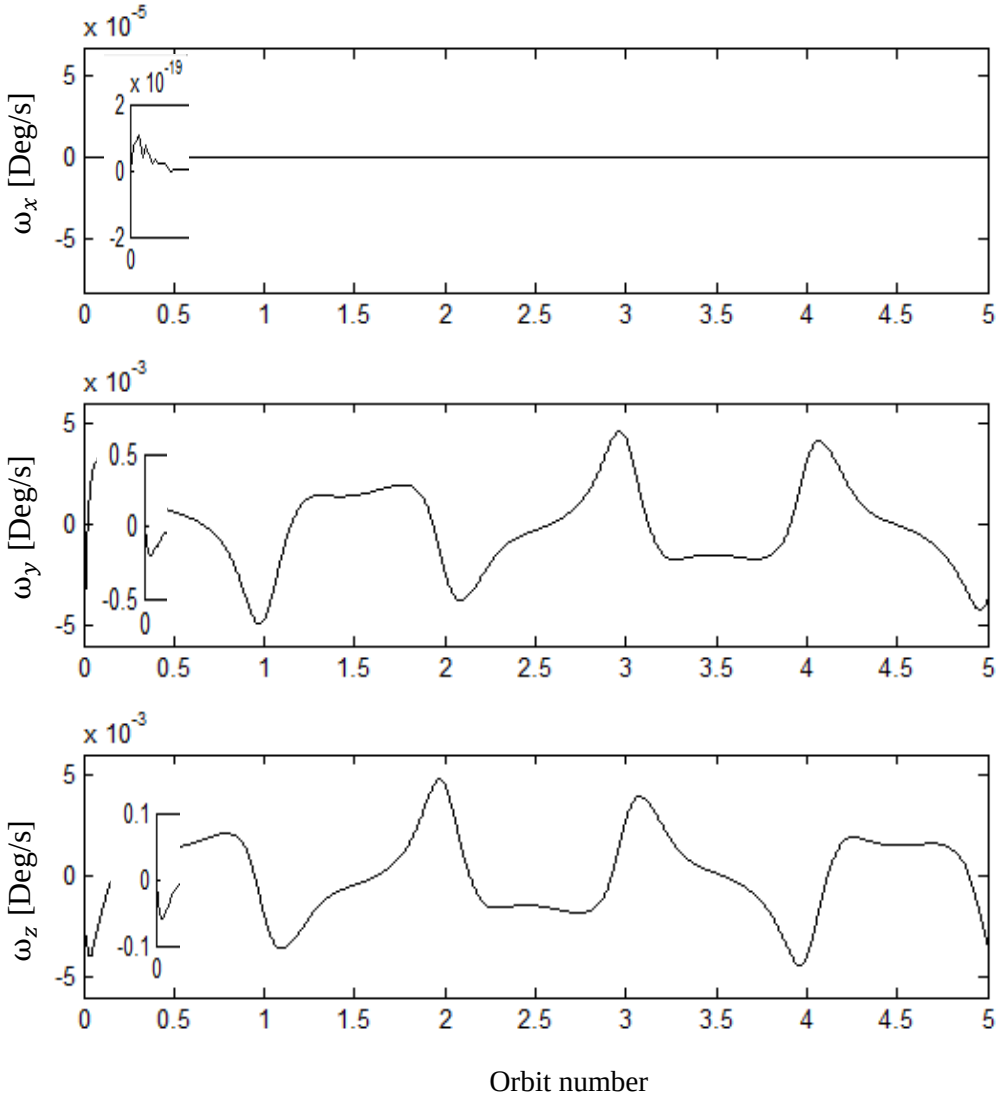

Figure 4.14 Body fixed frame angular rates for increasing semi-major axis

As it can be seen in the Figure 4.14 solar sail rotates about its 2 axes to orient its normal with respect to sunline vector. The error in the roll axis is due to non- diagonal terms in the inertia tensor of the satellite.

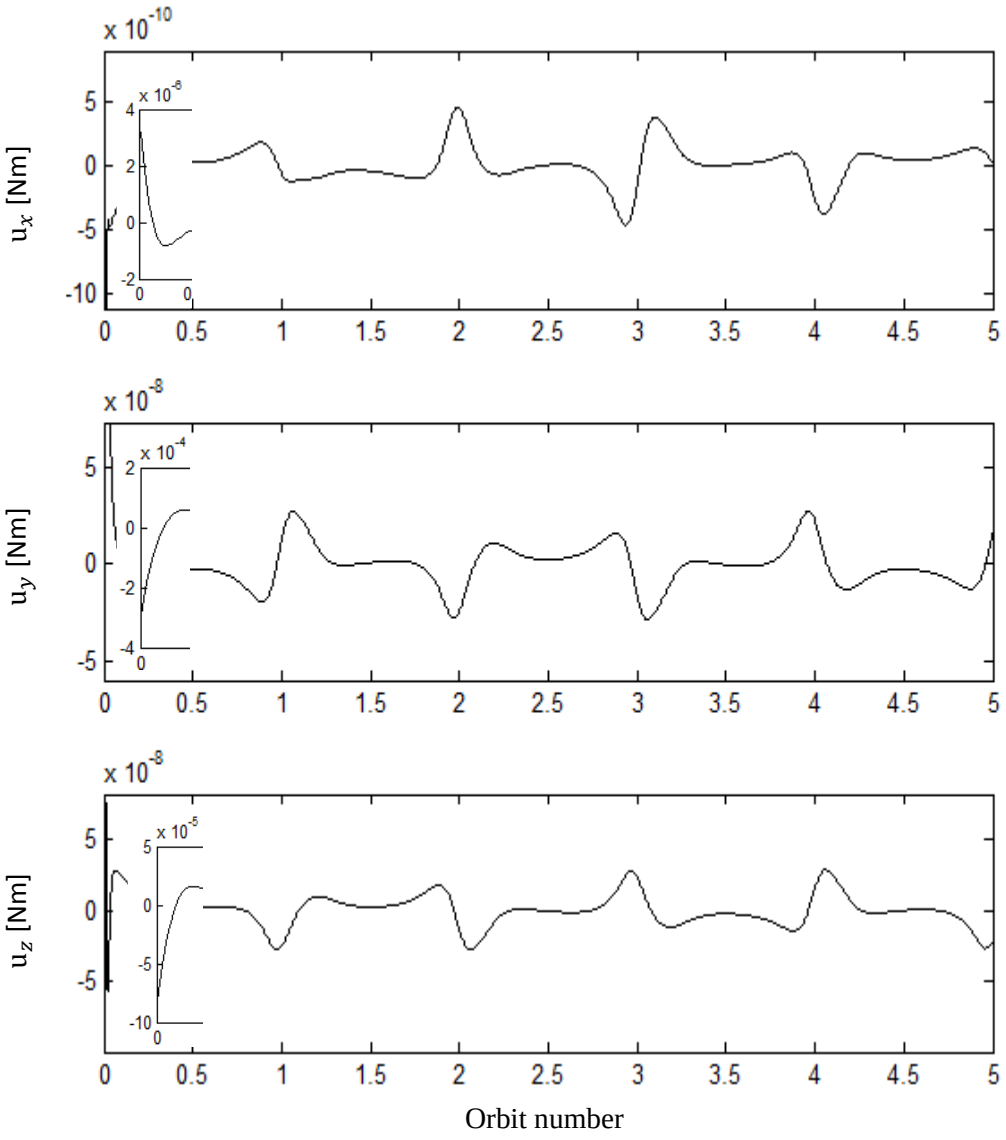

Figure 4.15 Controller torques about body axes for increasing semi-major axis

Initially the solar sail makes a rapid rotation to go to a proper orientation from its initial orientation afterwards, its rotations becomes smooth and consequently control torques are quite small.

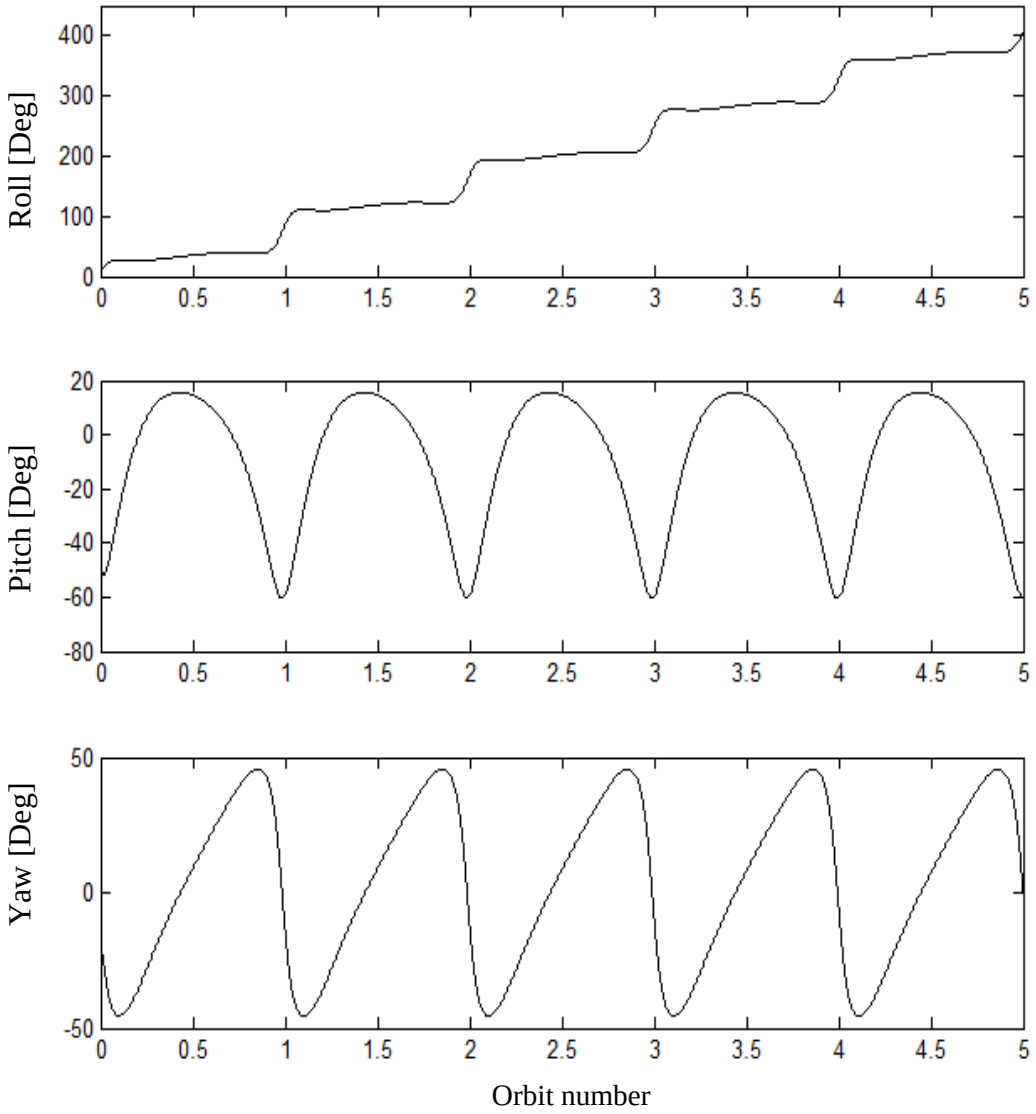

Figure 4.16 Orientation of solar sail with respect to inertial frame to increase the semi-major axis

Rotations about axis 3 and 2 brings the solar sail normal into correct orientation but one more rotation is required to completely align the frames so third rotation appears about axis 1

4.5 Increasing Eccentricity

To increase the eccentricity the following vector is used:

$$\boldsymbol{\lambda}(e) = [psinv \quad [(p+r)cosv + re] \quad 0] \tag{4.3}$$

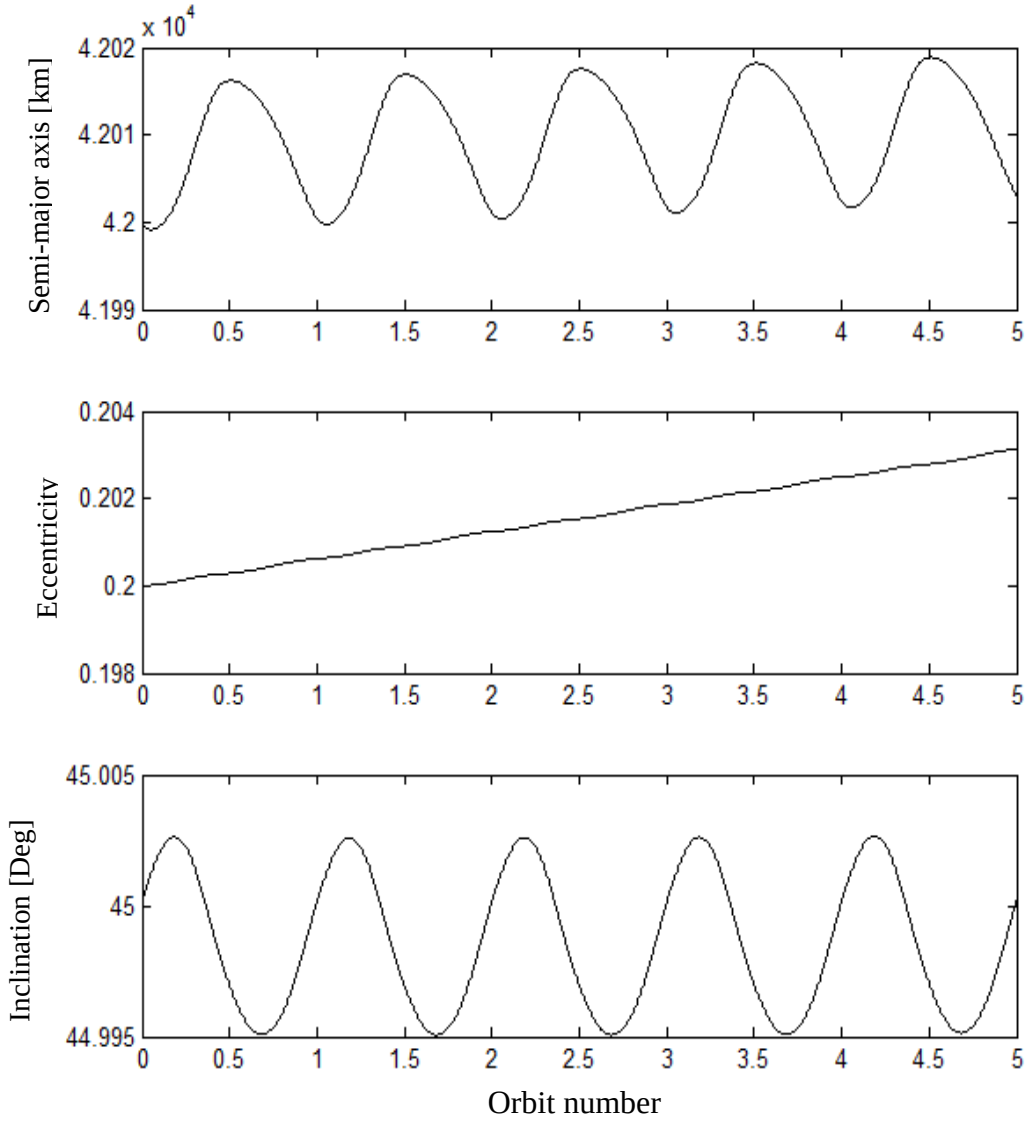

Figure 4.17 Orbital elements change when maximizing change in eccentricity

Figure 4.17 shows that eccentricity is steadily increasing. Since eccentricity is related to both shape and size of the orbit. In order to increase the eccentricity periapsis decreases and apoapsis increases. That's why increasing eccentricity causes oscillations of semi-major axis. The inclination is also oscillatory due to orbit normal forces.

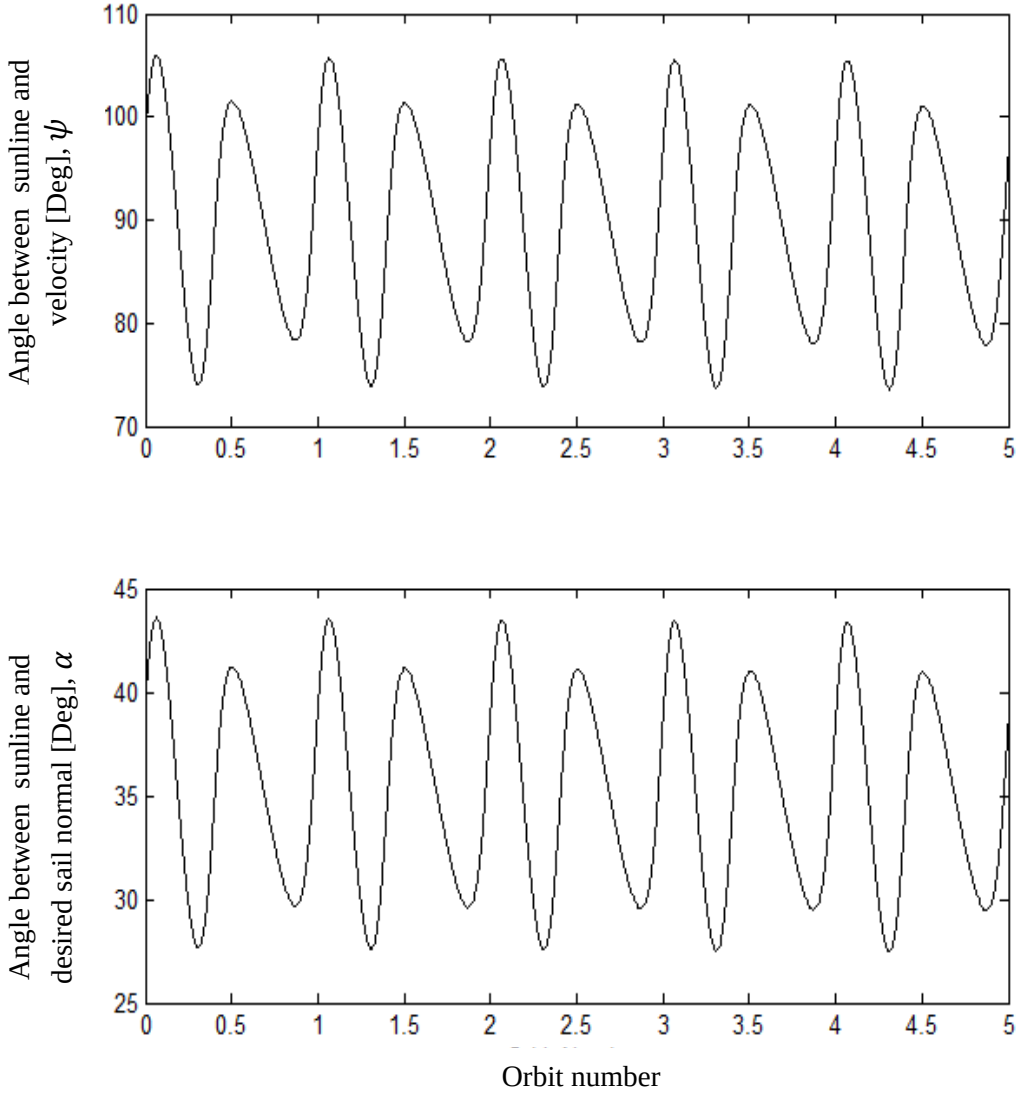

Figure 4.18 Angular positions of semi-major axis function and desired sail normal for increasing eccentricity

Angular orientation of vector function of inclination and desired solar sail normal is given in Figure 4.18

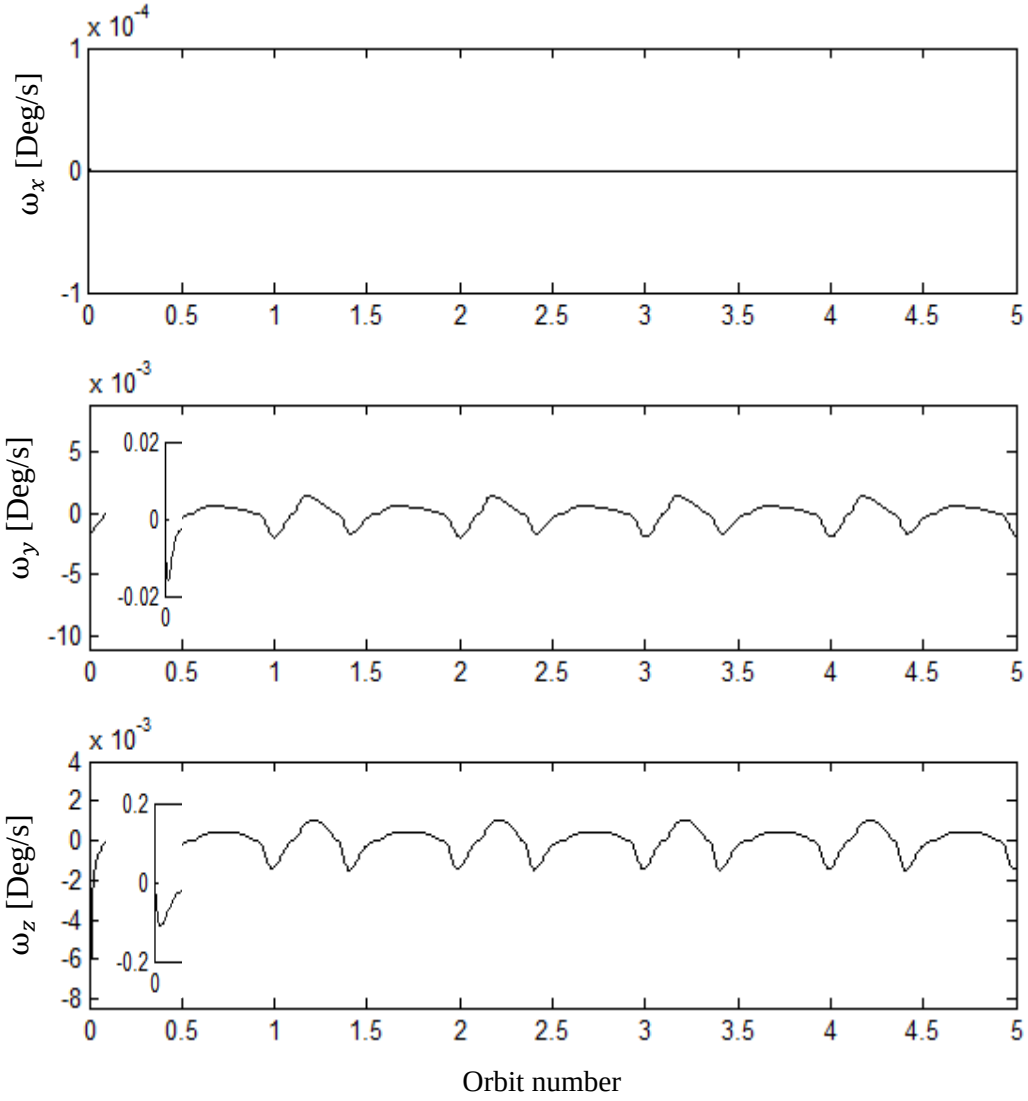

Figure 4.19 Body fixed frame angular rates for increasing eccentricity

Rotation about sail normal does not change the orientation of it with respect to sunline. Since the aim of the attitude maneuver is to orient the sail normal there is no rotation about roll but vibration due to non-diagonal term in the inertia matrix.

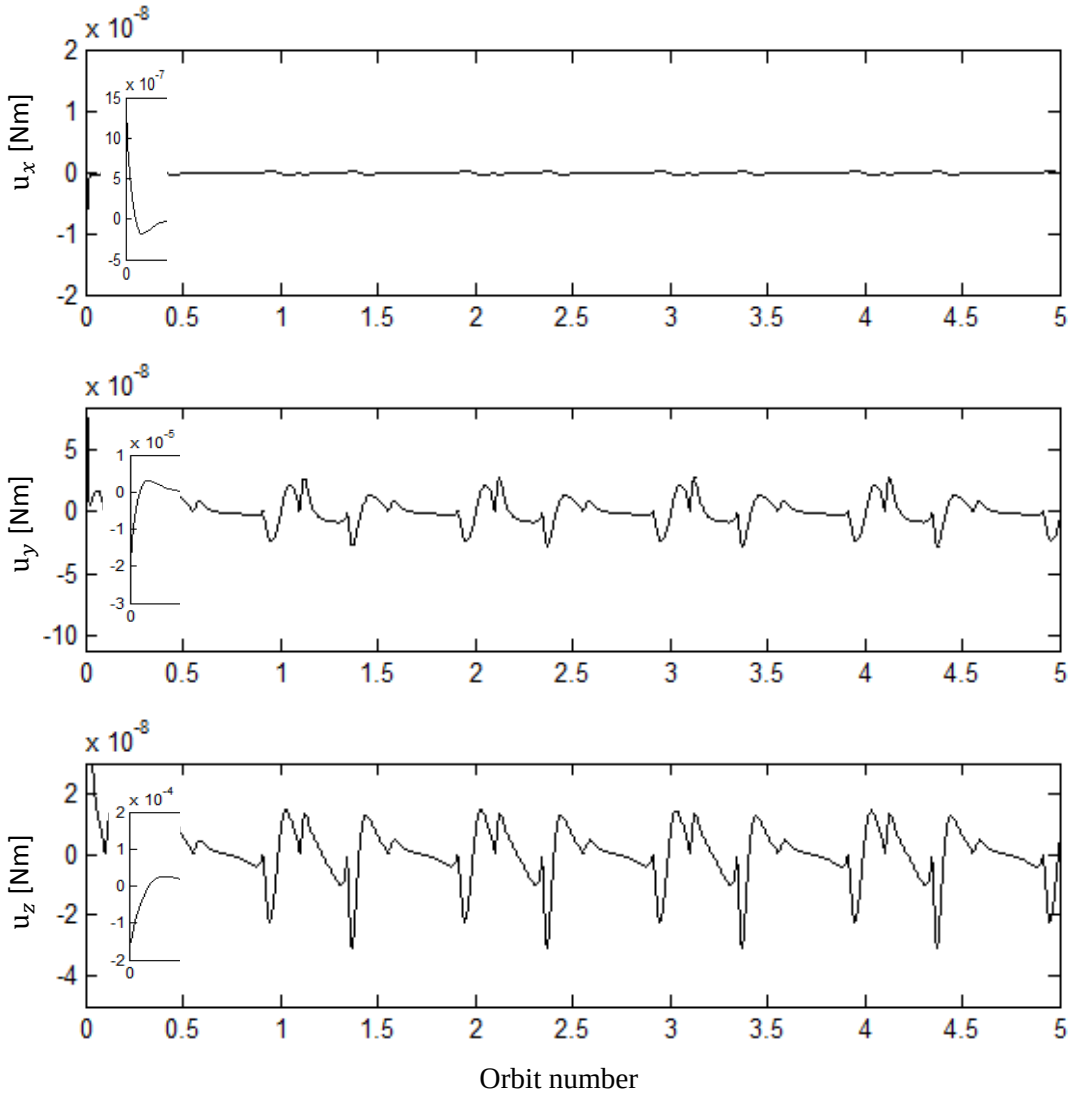

Figure 4.20 Controller torques about body axes for increasing eccentricity

Reorienting the spacecraft from initial condition to desired orientation requires large rotation. So at the beginning controller torque is very big compare to the other times.

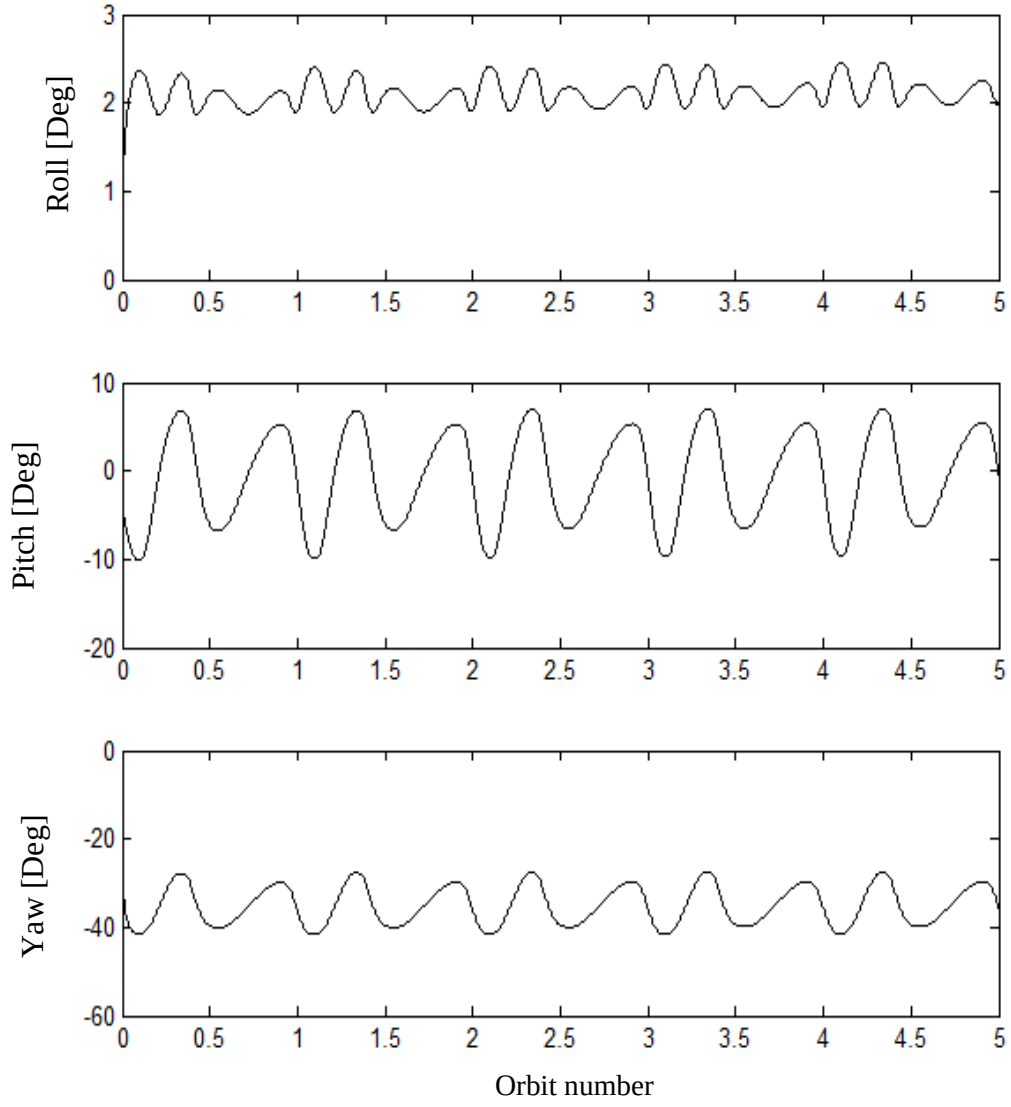

Figure 4.21 Orientation of solar sail with respect to inertial frame to increase the eccentricity

Figure 4.21 shows the orientation of the solar sail

4.6 Increasing Inclination

The following vector direction is used for increasing the inclination.

$$\boldsymbol{\lambda}(i) = \begin{bmatrix} 0 & 0 & \frac{r\cos\theta}{h} \end{bmatrix} \tag{4.4}$$

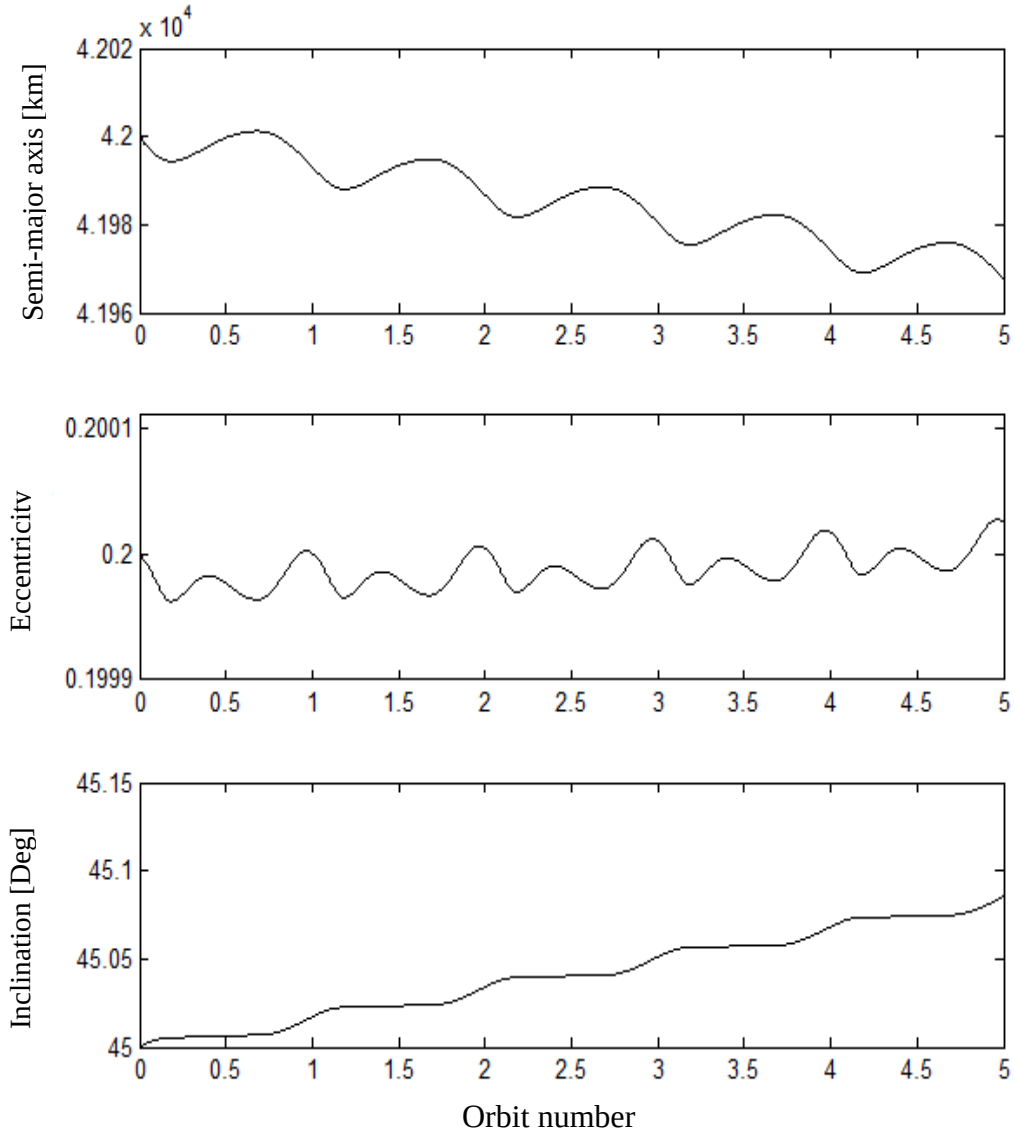

Figure 4.22 Orbital elements change when maximizing increase in inclination

İn order to change the inclination of the orbit the force component in the direction of orbit normal must be maximized. This means that the force component in the orbital plane will be minimized automatically.

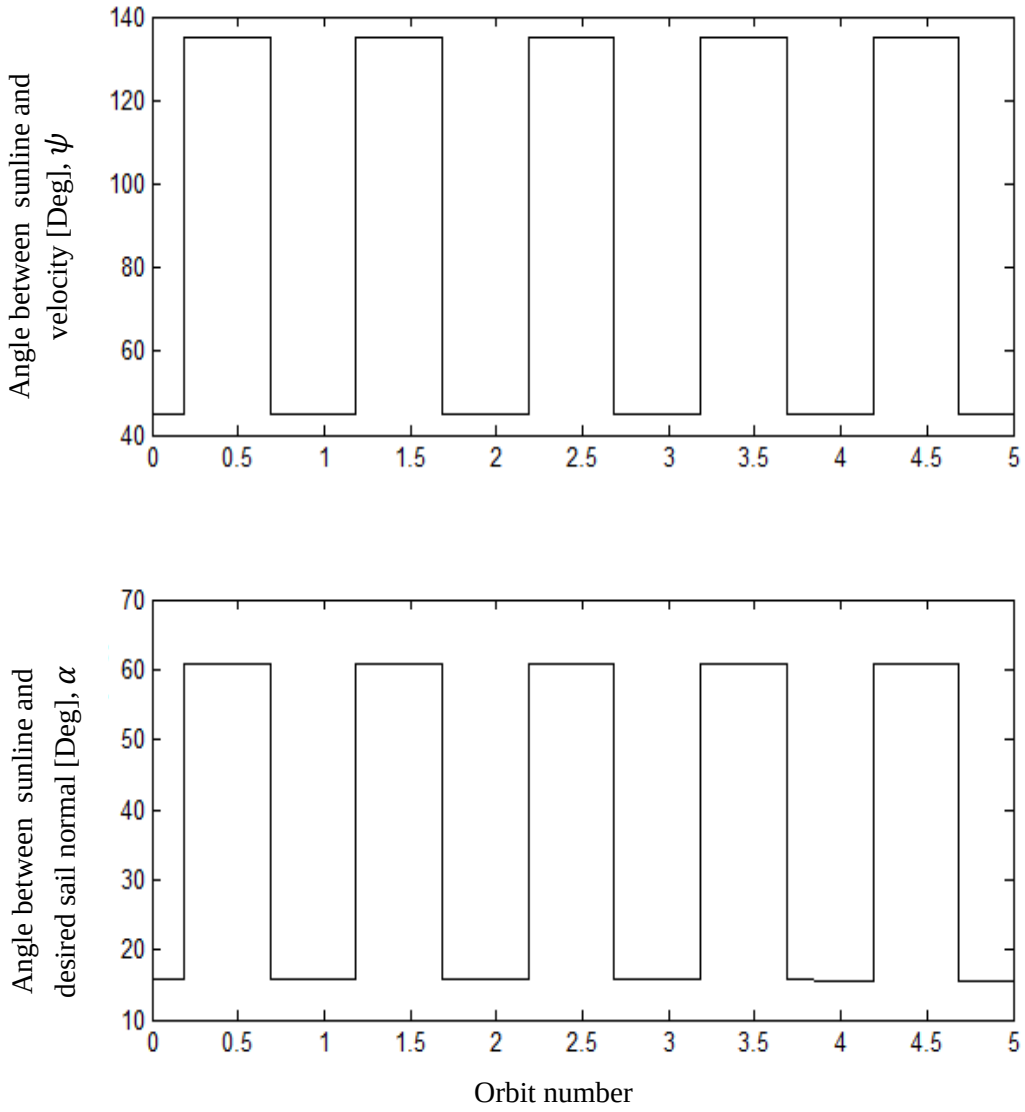

Figure 4.23 Angular position of inclination vector function and desired sail normal for increasing inclination

As it can be seen in Figure 4.23 in order to change the inclination of the orbit the direction of the thrust must be perpendicular to the orbital plane that's why the angular change between inclination vector function and sail normal are stepwise

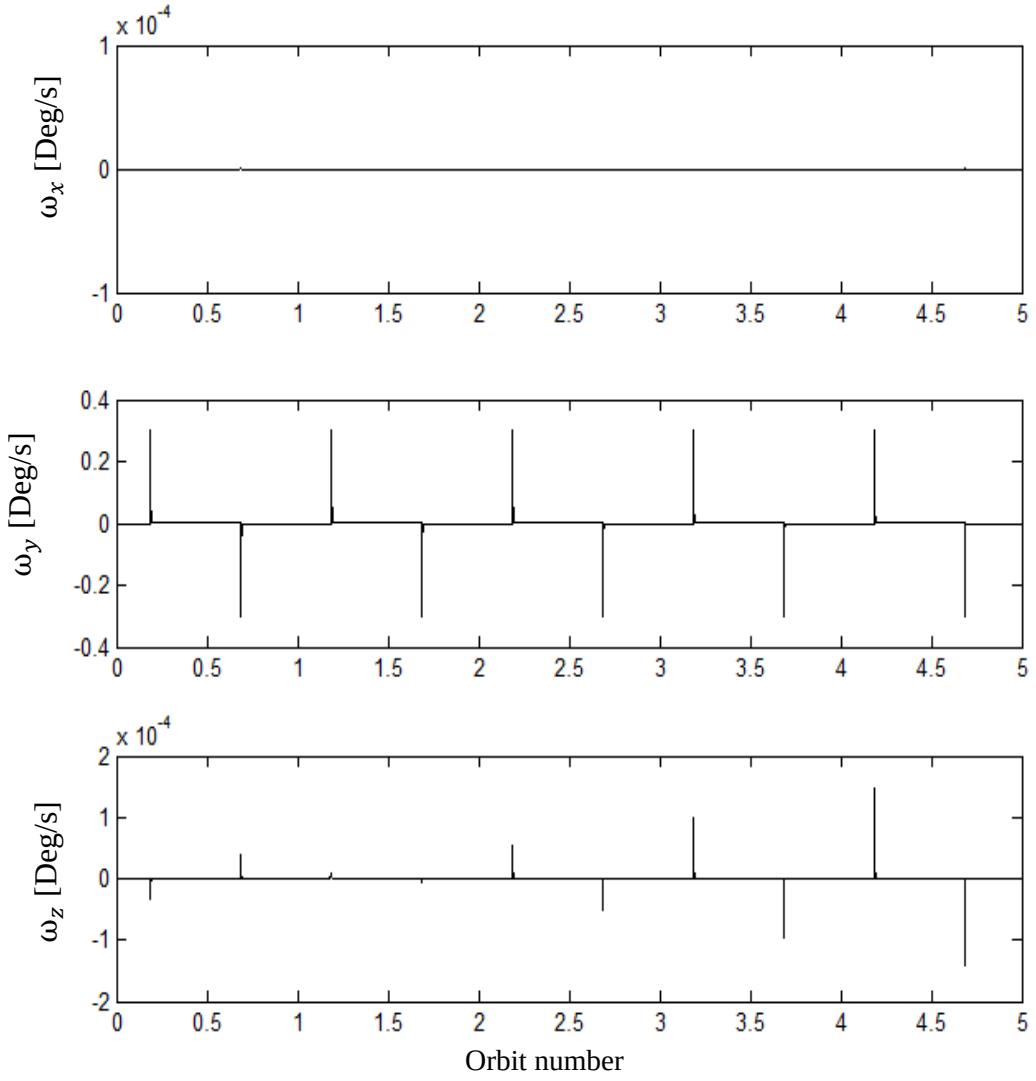

Figure 4.24 Body fixed frame angular rates for increasing inclination

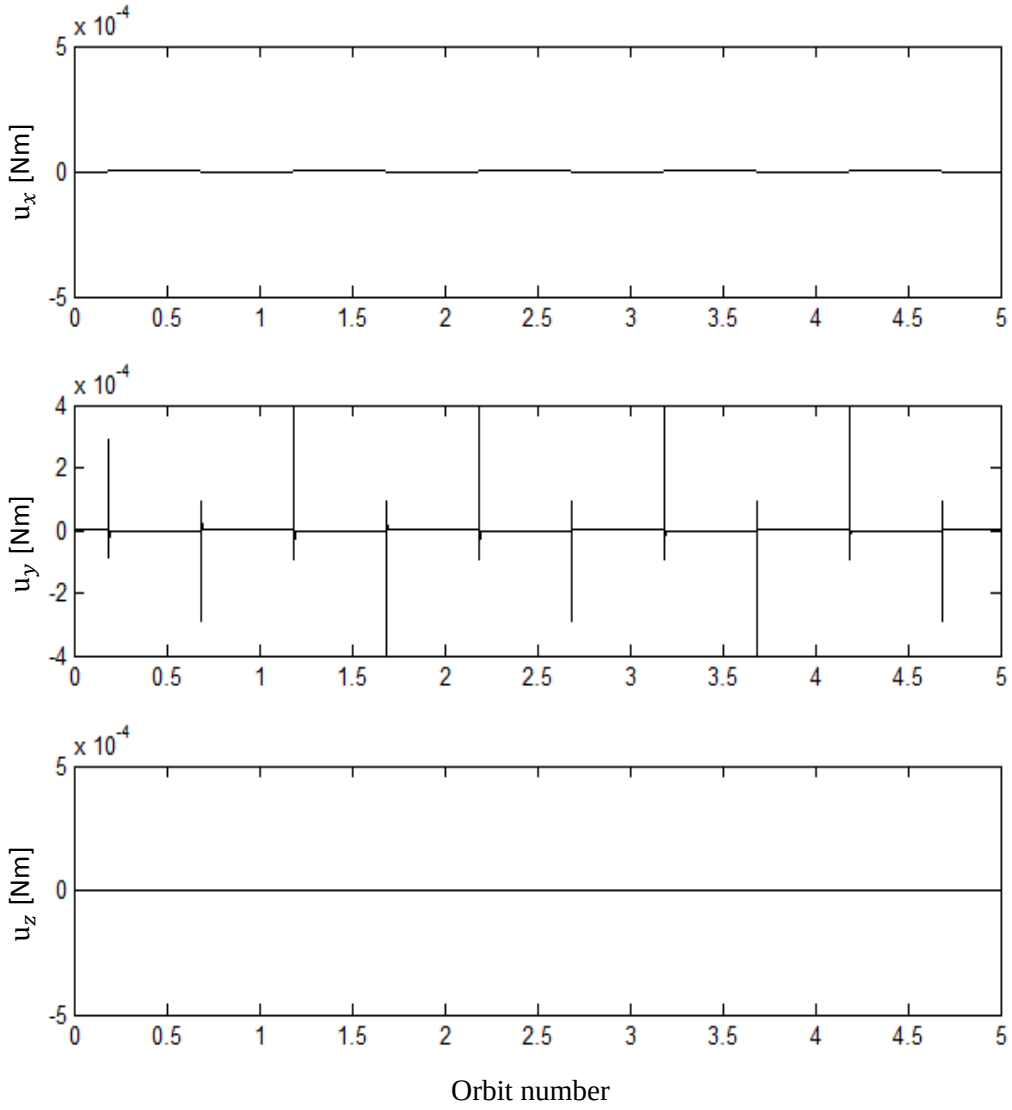

Figure 4.25 Controller torques about body axes for increasing inclination

Due to rapid flip motion of the satellite the pulses of control toques are needed, as shown in Figure 4.25

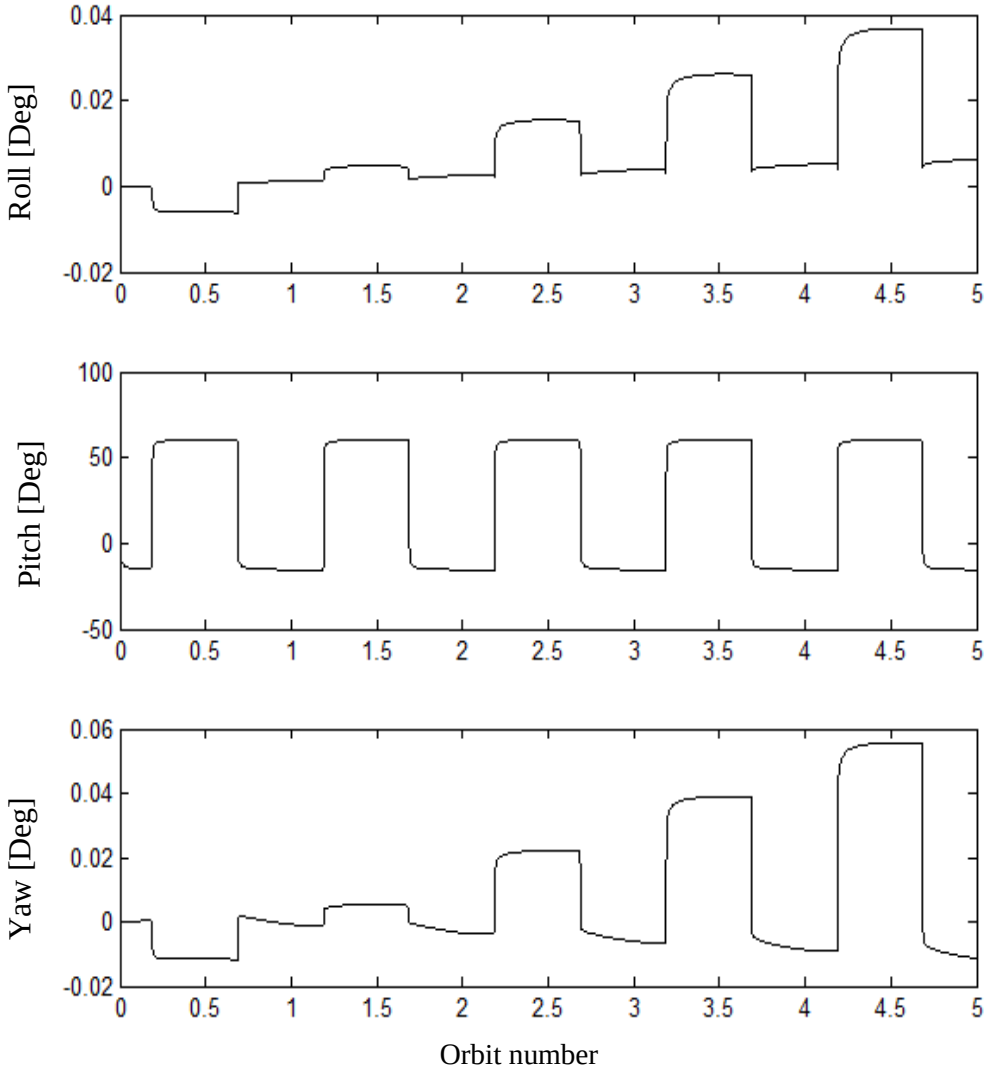

Figure 4.26 Orientation of solar sail with respect to inertial frame to increase the inclination

Figure 4.26 shows the Euler angles. From the figure it may be observed that the main activity is in the pitch axis.

CHAPTER 5

CONCLUSION AND FUTURE WORK

5.1 Conclusion

In this thesis, an attitude control mechanization is developed for steering the solar sail spacecraft. For this purpose locally optimal steering laws are employed for an Earth orbiting solar sail spacecraft.

The steering angles are obtained for progressively changing semi-major axis, eccentricity and inclination.

The mechanization developed effectively calculates the necessary to-go quaternions to be used for Lyapunov based nonlinear control.

Trough the simulations, it is shown that both the locally optimal steering approach and attitude control mechanization developed is quite effective.

5.2 Future Work

In this thesis particular orbital element's rate of change is maximized without considering the change of other orbital elements. In the future proper attitude control algorithms and methods will be investigated to make a desired orbital maneuver by considering coupling in orbital elements

REFERENCES

[1] G. Gupta, "Solar Sails," *The Journal of Department of Applied Sciences & Humanities*, vol. 6, pp. 65-71, 2006.

[2] M. Travis, "Lunar Sail," RocketTheme, [Online]. Available: http://www.lunarsail.com/project-background/. [Accessed 08 01 2013].

[3] C. R. McInnes, "Solar sailing: mission applications and engineering challenges," *The Royal Society*, vol. 361 , pp. 2989-3008, 2003.

[4] C. R. McInnes, Solar Sailing Technology, Dynamiics and Mission Applications, Londan: Springer, 1999.

[5] P. Lebedew, "The pressure of Light on Gases," *Astrophysical Journal*, vol. 31, p. 385, 1910.

[6] X. C. M. Cubillos and L. C. G. Souza, "Solar Sails – The Future of Exolorationnof the Space," in *2º Workshop em Engenharia e Tecnologia Espaciais*, Maio, 2011.

[7] A. C. Clarke, Project Solar Sail, New York: Penguin Books, 1990.

[8] W. A. Hollerman, "The Physics of Solar Sails," NASA, 2002.

[9] B. Wie, "Thrust Vector Control of Solar Sail Spacecraft," in *AIAA Guidance, Navigation, and Control Conference and Exhibit*, California, 2005.

[10] B. L. Diedrich, "Attitude Control and Dynamics of Solar Sails," in *University of Washington*, 2001.

[11] J.-Y. Prado, A. Perret and I. Dandouras, "Using a Solar Sail for a Plasma Storm Early Warning System," in *Environment Modelling for Space-based Applications, Symposium Proceedings (ESA SP-392)*, Noordwijk, 1996.

[12] A. Farres and A. Jorba, "Station keeping of a solar sail around a Halo orbit," *Acta Astronautica,* vol. 94, pp. 527-539, 2014.

[13] C. Lucking, C. Colombo and C. R. McInnes, "A passive satellite deorbiting strategy for medium earth orbit using solar radiation pressure and the J2 effect," *Acta Astronautica,* vol. 77, pp. 197-206, 2012.

[14] L. Johnson, M. Whorton, A. Heaton, R. Pinson, G. Laue and C. Adams, "NanoSail-D: A solar sail demonstration mission," *Acta Astronautica,* vol. 68, pp. 571-575, 2011.

[15] NASA, "NonoSail-D Home page," NASA, 13 01 2012. [Online]. Available: http://www.nasa.gov/mission_pages/smallsats/nanosald.html.. [Accessed 25 12 2013].

[16] Y. Tsuda, O. Mori, R. Funase, H. Sawada, T. Yamamoto, T. Saiki, T. Endo and J. Kawaguchi, "Flight status of IKAROS deep space demonstrator," *Acta Astronautica,* vol. 69, pp. 833-840, 2011.

[17] U. Geppert, B. Biering, F. Lura, J. Block, M. Straubel and R. Reinhard, "The 3-step DLR-ESA Gossamer road to solar sailing," *Advances in Space Research*, vol. 48, pp. 1695-1701, 2011.

[18] M. Straubel, J. Block, M. Sinapius and C. Hühne, "Deployable composite booms for various gossamer space structures," in *52th AIAA/ASME/ASCE/AHS/ASC Structures, Structural Dynamics, and Materials Conference*, Denver, 2011.

[19] L. Friedman, K. Pichkhadze, V. Kudryashov, G. Rogovsky, V. Linkin, V. Gotlib, A. Lipatov, J. Cantrell and J. Garvey, "Cosmos1- The attempt to fly the first solar sail mission," in *34th COSPAR Scientific Assembly, The Second World Space Congress*, Houston, 2002.

[20] J. K. Laystrom-Woodard, "Design and testing of the CubeSail payload," in *7th Annual CubeSat Developers' Workshop*, San Luis Obispo, CA, 2010.

[21] R. L. Burton, J. K. Laystrom-Woodard, G. F. Benavides, D. L. Carroll, V. L. Coverstone, G. R. Swenson, A. Pukniel, A. Ghosh and A. D. Moctezuma, "Initial development of the CubeSail/UltraSail spacecraft," CU Aerospace / Marshall Space Flight Center, Illinois, 2010.

[22] V. Lappas, N. Adeli, L. Visagie, J. F. V. Fernandez, T. Theodorou, W. Steyn and M. Perren, "CubeSail: A low cost CubeSat based solar sail demonstration mission," *Advances in Space Research*, vol. 48, no. 11, p. 1890–1901, 2011.

[23] J. M. Fernandez, V. J. Lappas and A. J. Daton-Lovett, "Completely stripped solar sail concept using bi-stable reeled composite booms," *Acta Astronautica*, vol. 69, pp. 78-85, 2011.

[24] L. Visagie, "Mission Requirement," 2012.

[25] M. H. B. R. Olive Stohlman, "Sail System Testing Report," DeOrbitSail Project, 2012.

[26] R. H. Battin, An Introduction to the Mathematics and Methods of Astrodynamics, New York: AIAA, 1987.

[27] B. Wie, Space Vehicle Dynamics and Control (2nd Edition), American Institute of Aeronautics and Astronautics., 2008.

APPENDIX A

DECREASING ORBITAL ELEMENTS

In this chapter simulations will be given for decreasing orbital elements, particularly for semi-major axis, eccentricity and inclination. Cube sail and controller properties are given in Table 4.1 and initial orbit given in Table 4.2

A.1 Decreasing Semi-major Axis

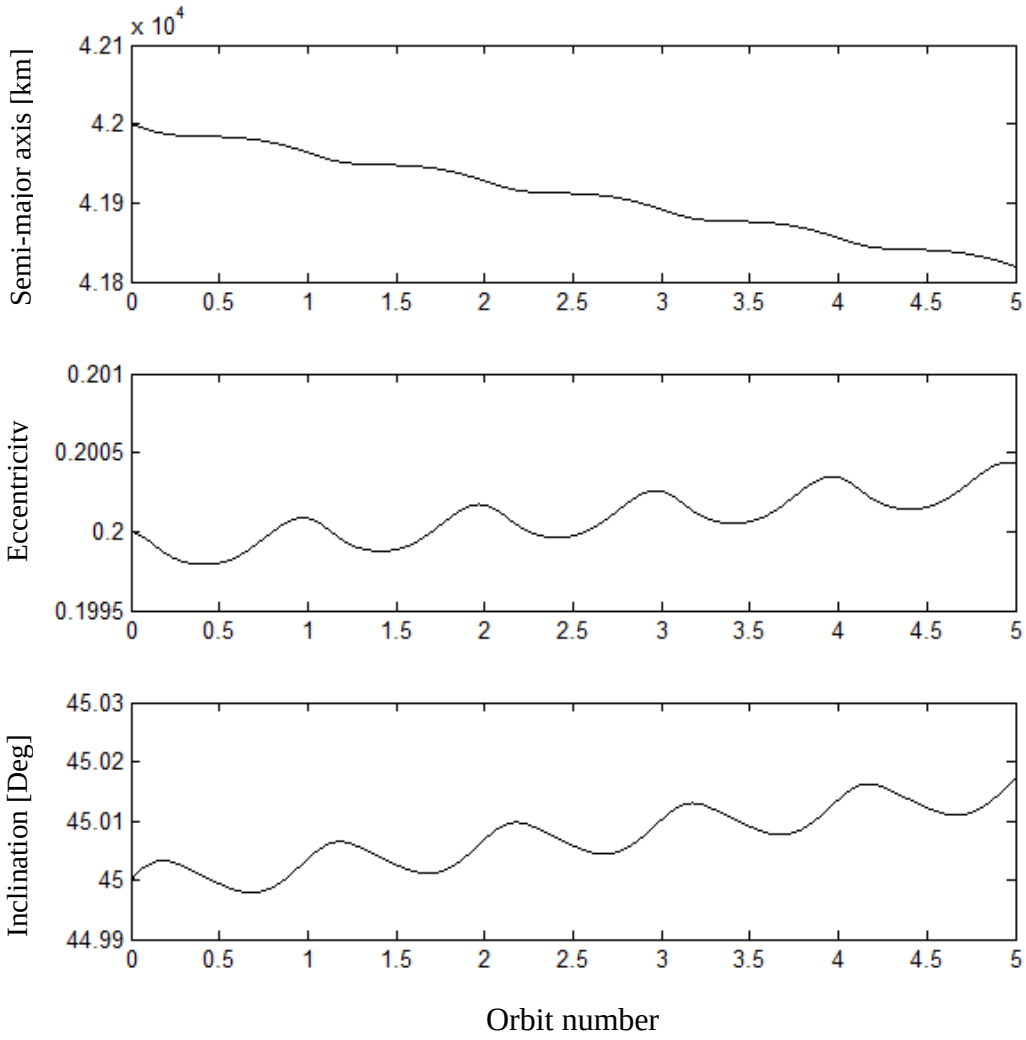

Figure A.1 Orbital elements change when decreasing semi-major axis

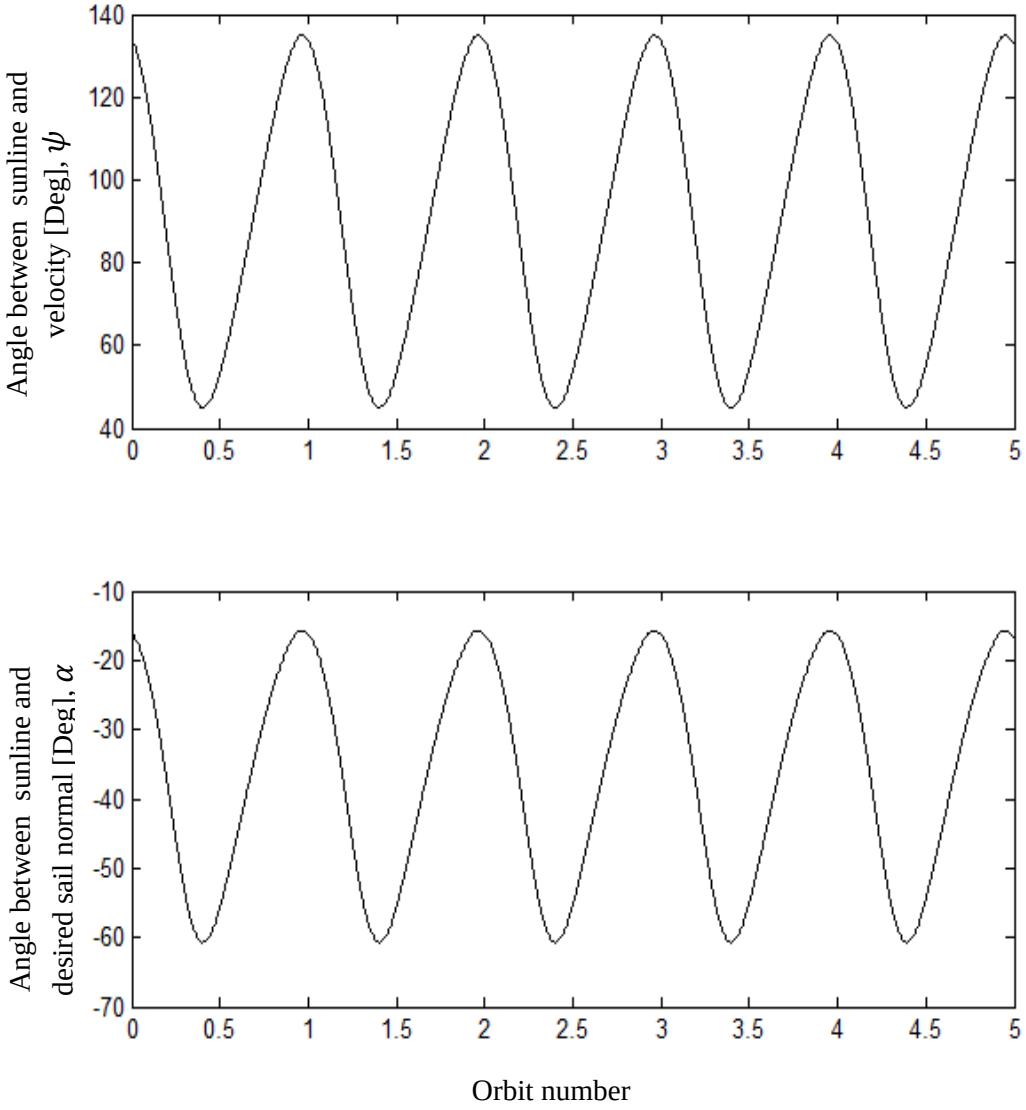

Figure A.2 Angular position of semi-major vector function and desired sail normal for decreasing semi-major axis

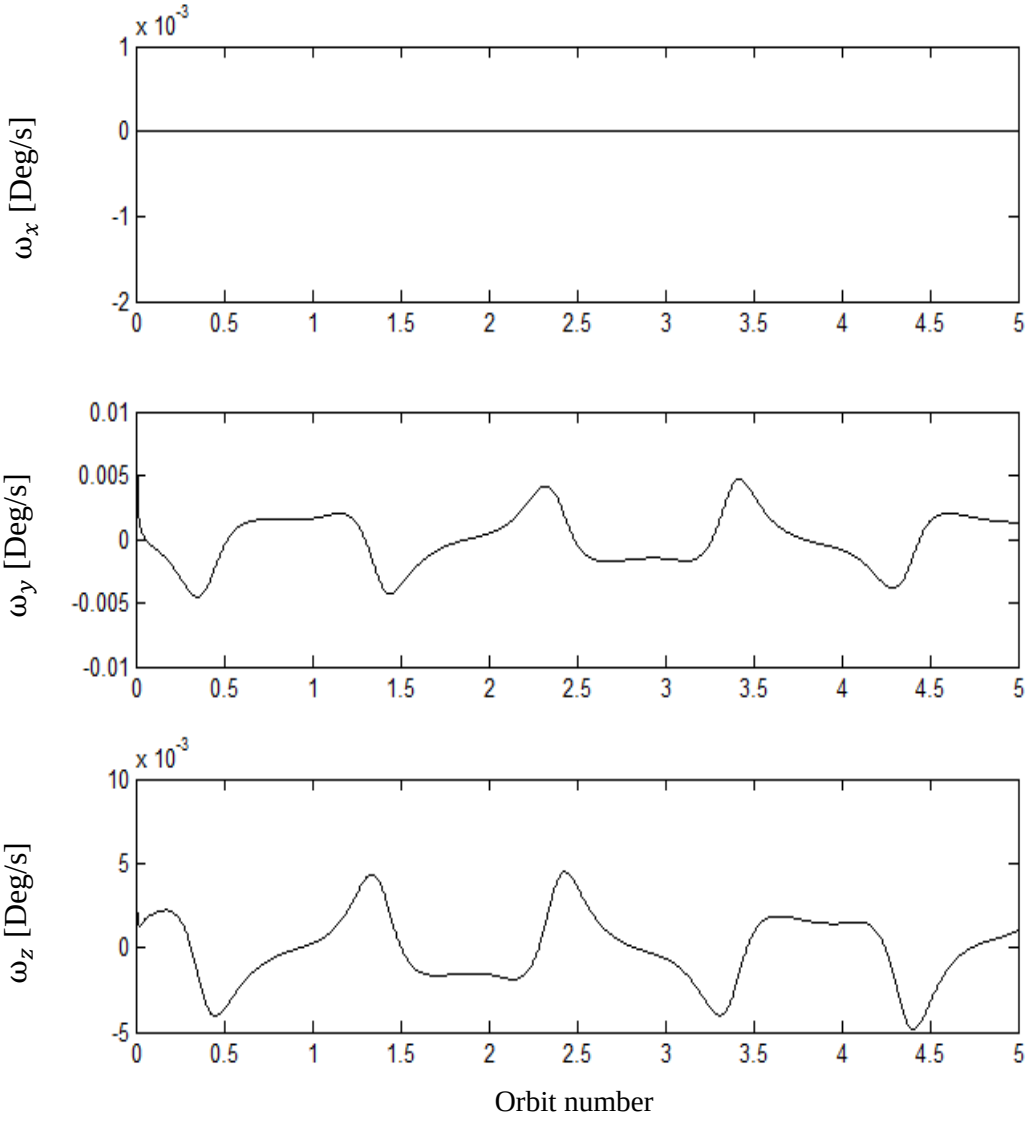

Figure A.3 Body fixed frame angular rates for decreasing semi-major axis

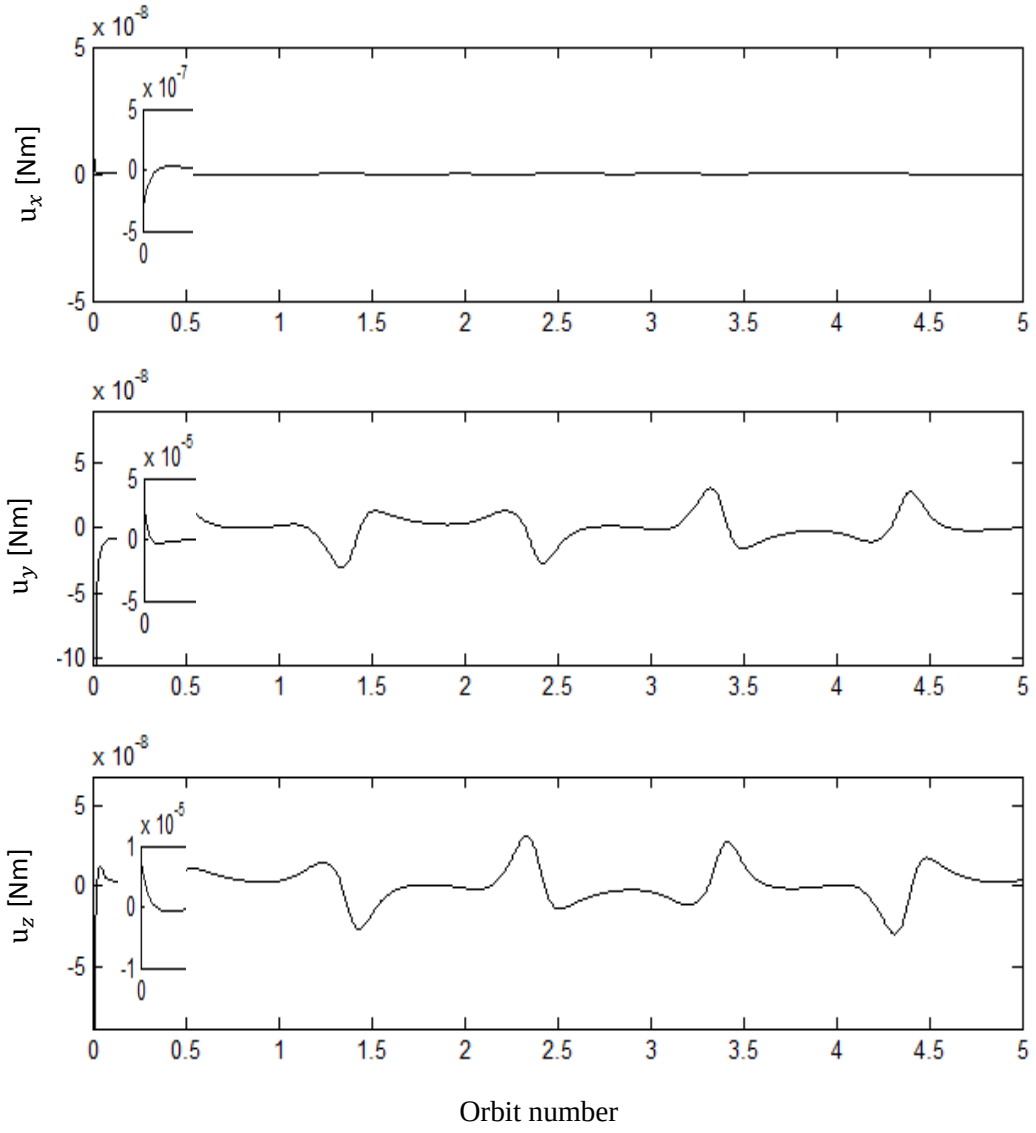

Figure A.4 Controller torques about body axes for decreasing semi-major axis

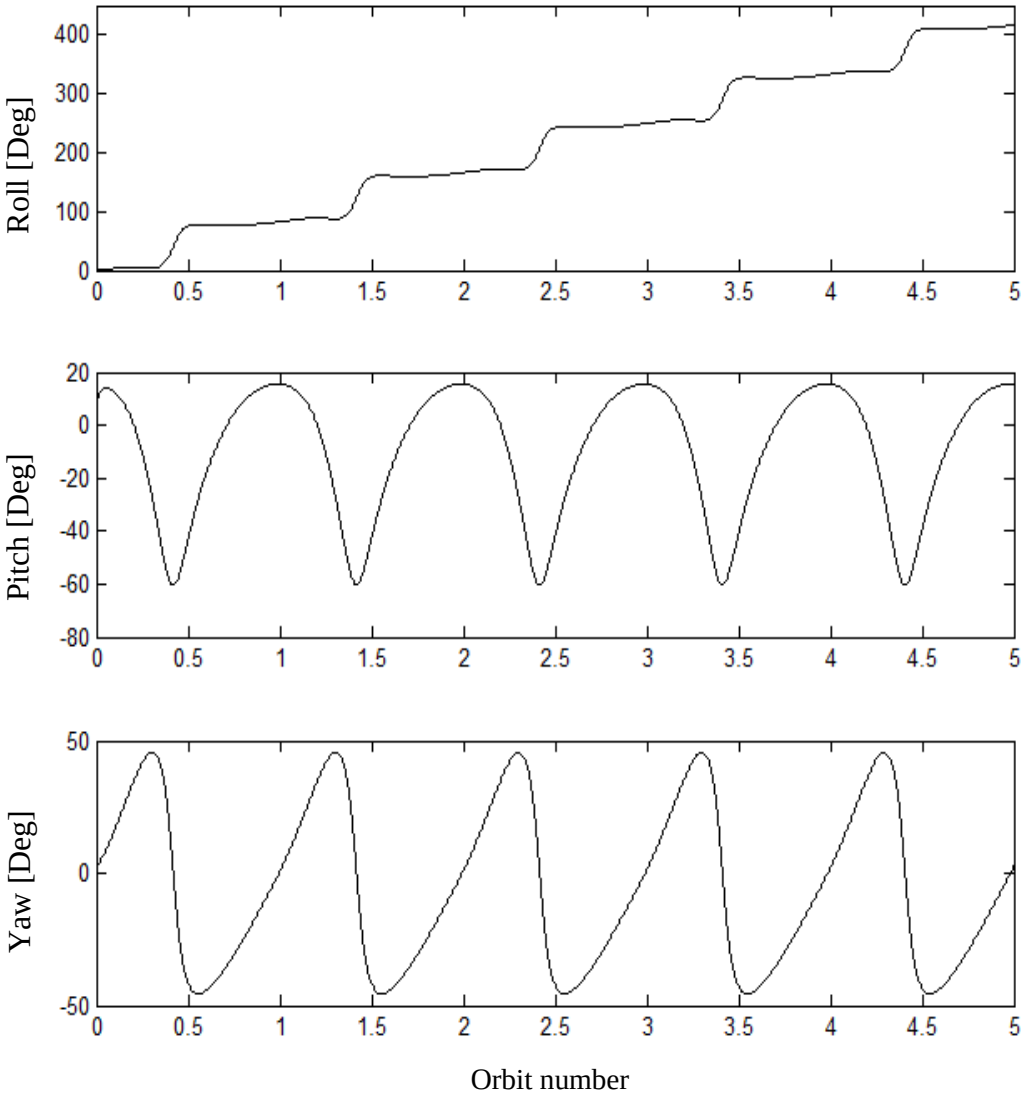

Figure A.5 Orientation of solar sail with respect to inertial frame to decreasing semi-major axis

A.2 Decreasing Eccentricity

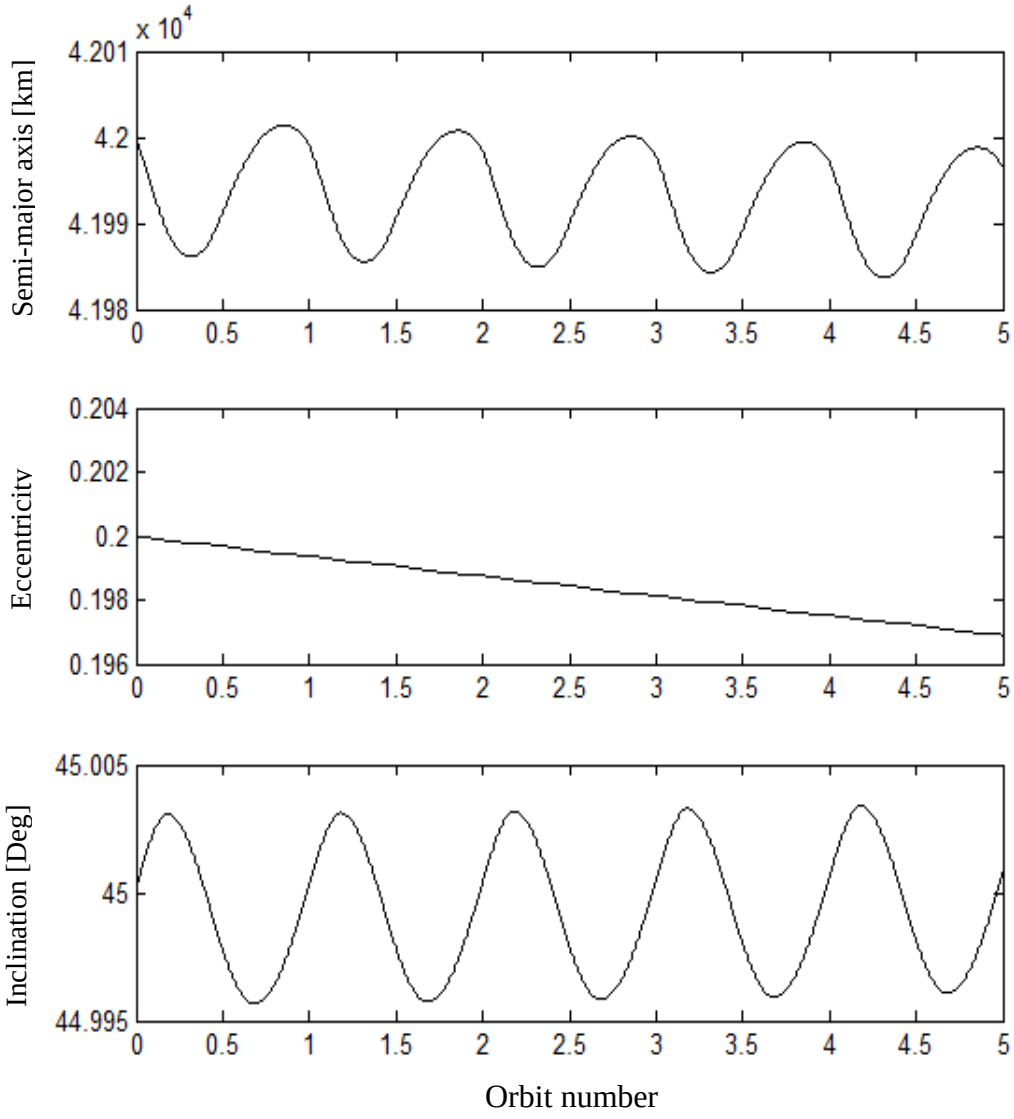

Figure A.6 Orbital elements change when decreasing eccentricity

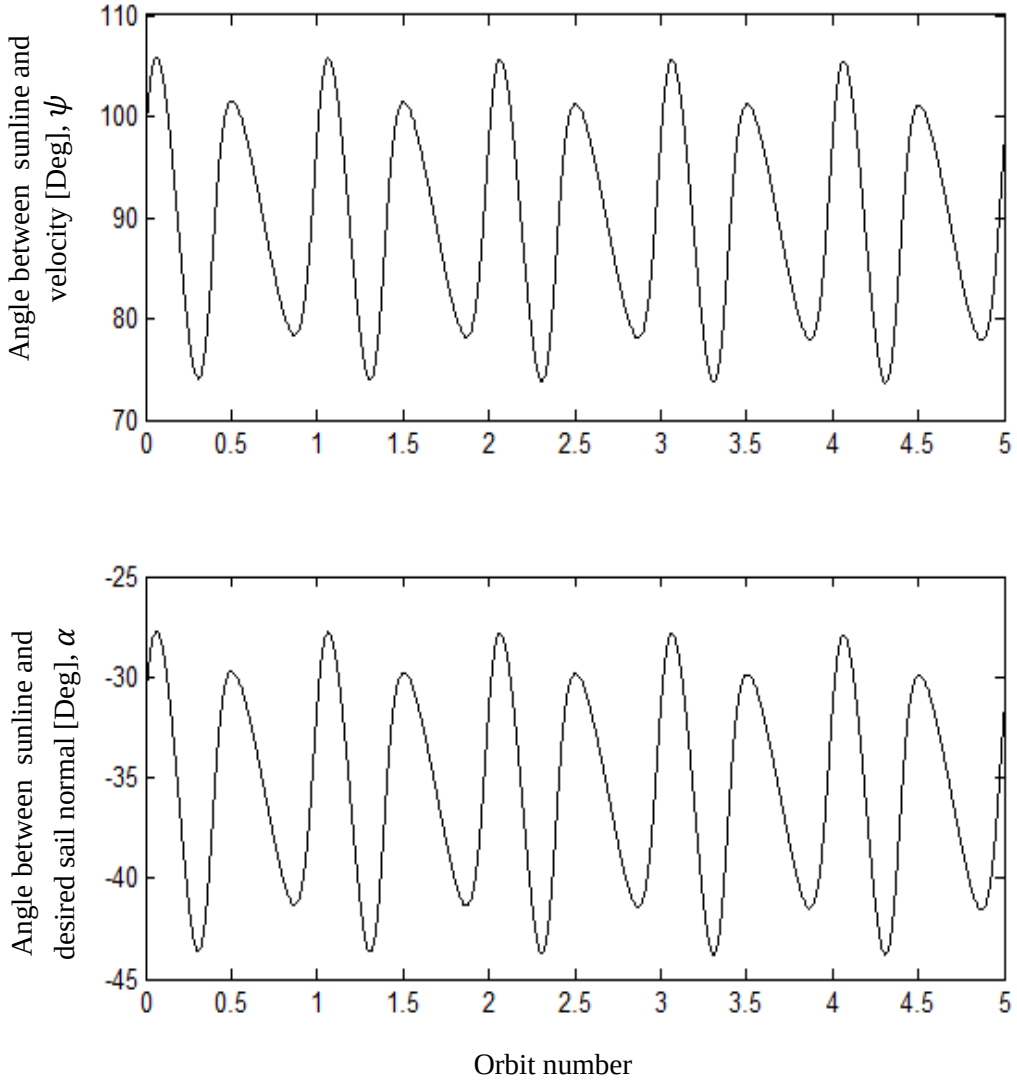

Figure A.7 Angular position of eccentricity vector function and desired sail normal for decreasing eccentricity

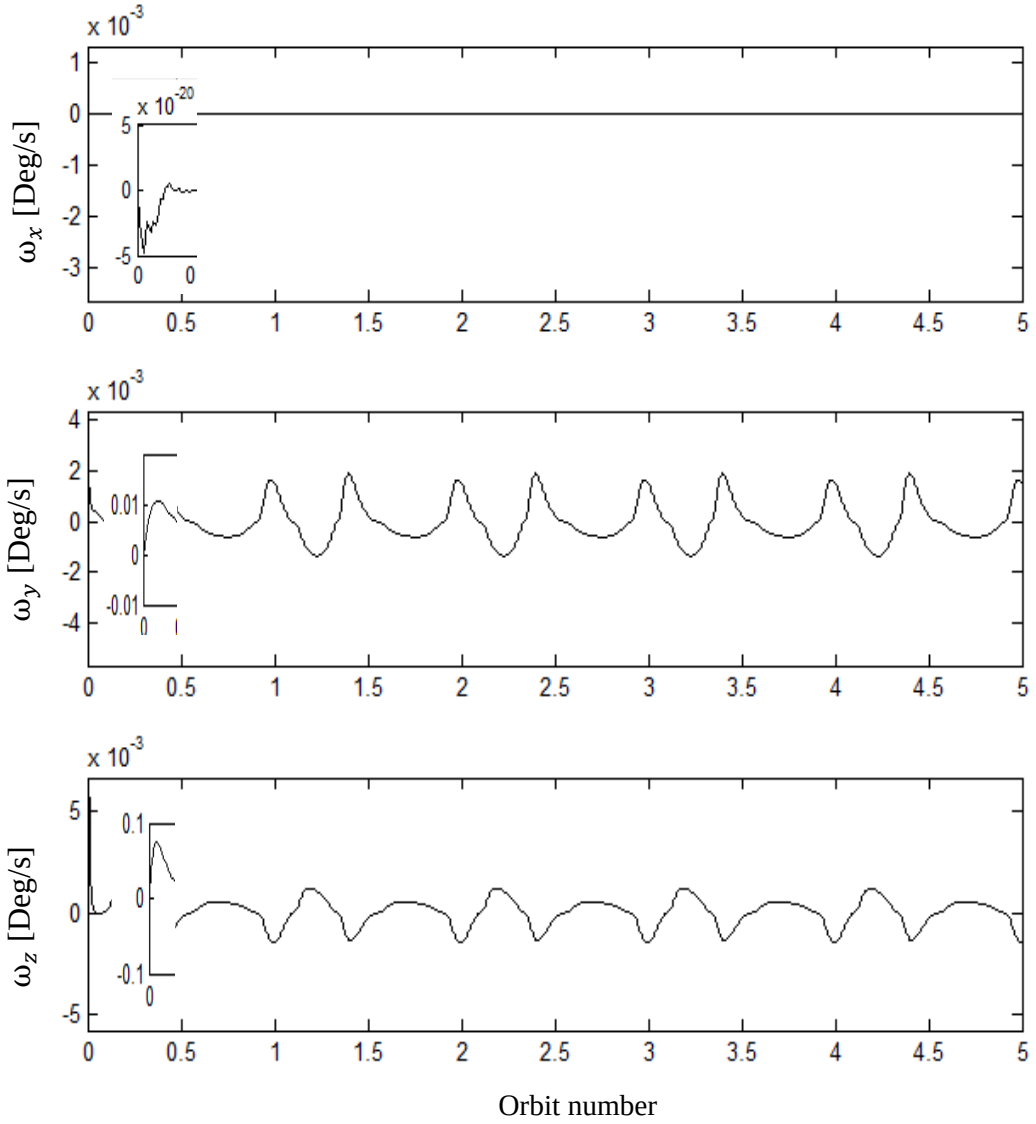

Figure A.8 Body fixed frame angular rates for decreasing eccentricity

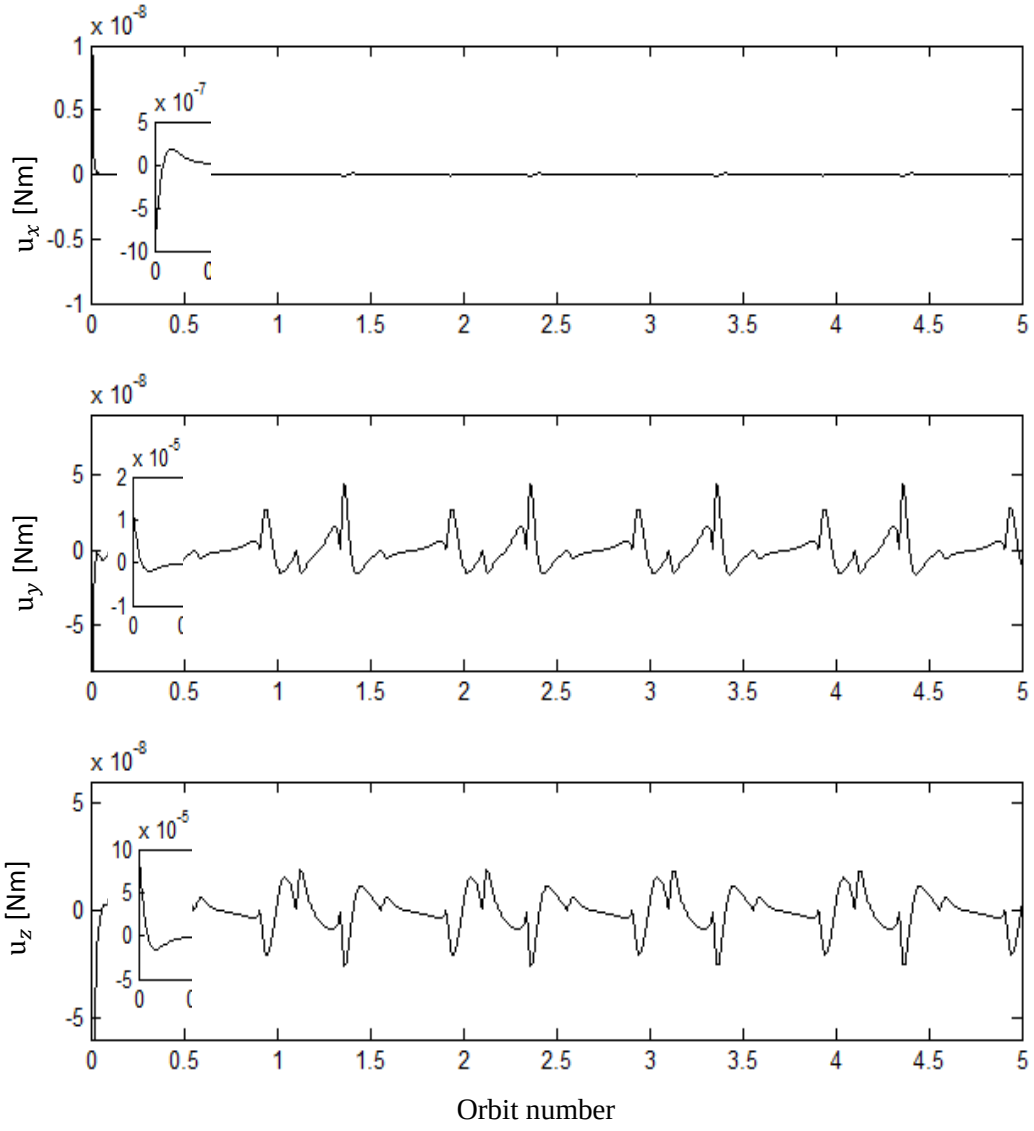

Figure A.9 Controller torques about body axes for decreasing eccentricity

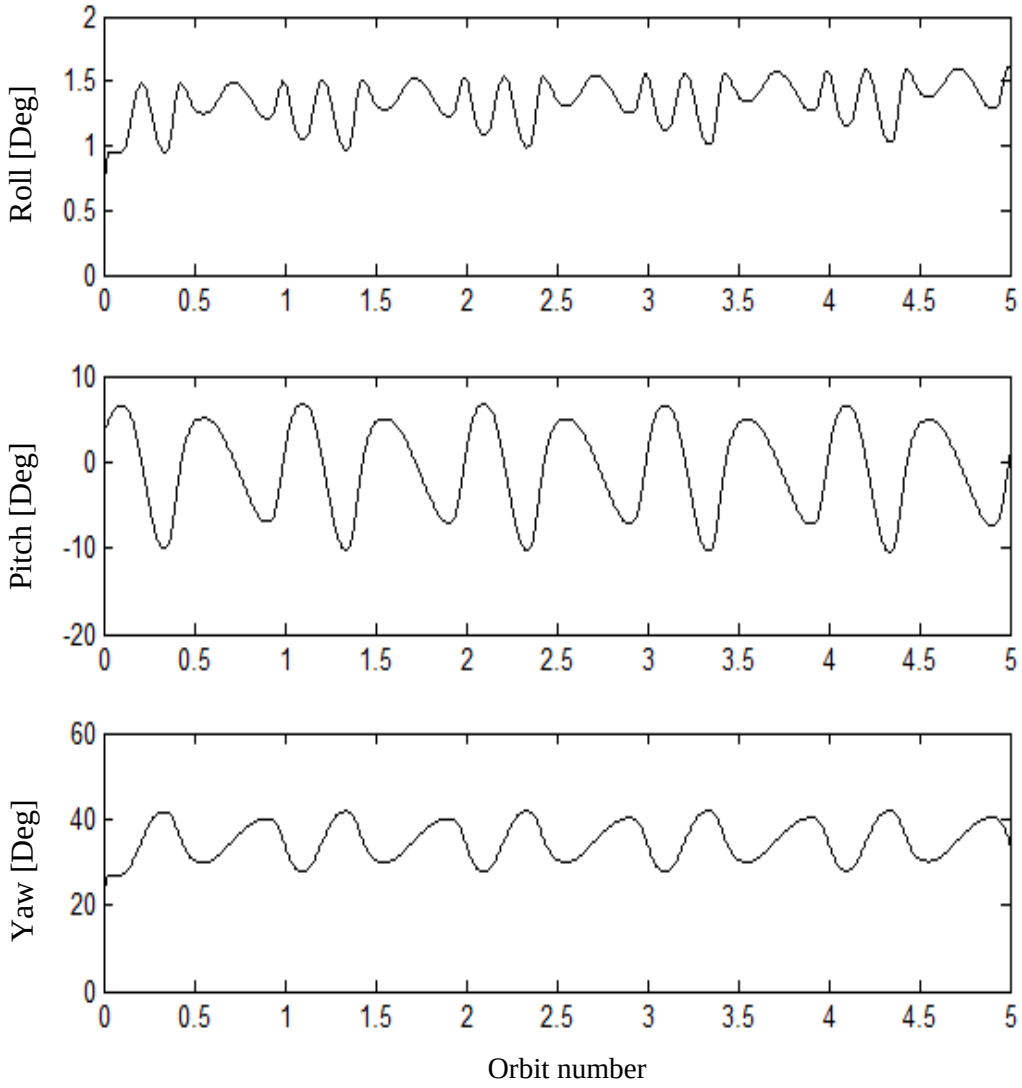

Figure A.10 Orientation of solar sail with respect to inertial frame to decreasing eccentricity

A.3 Decreasing Inclination

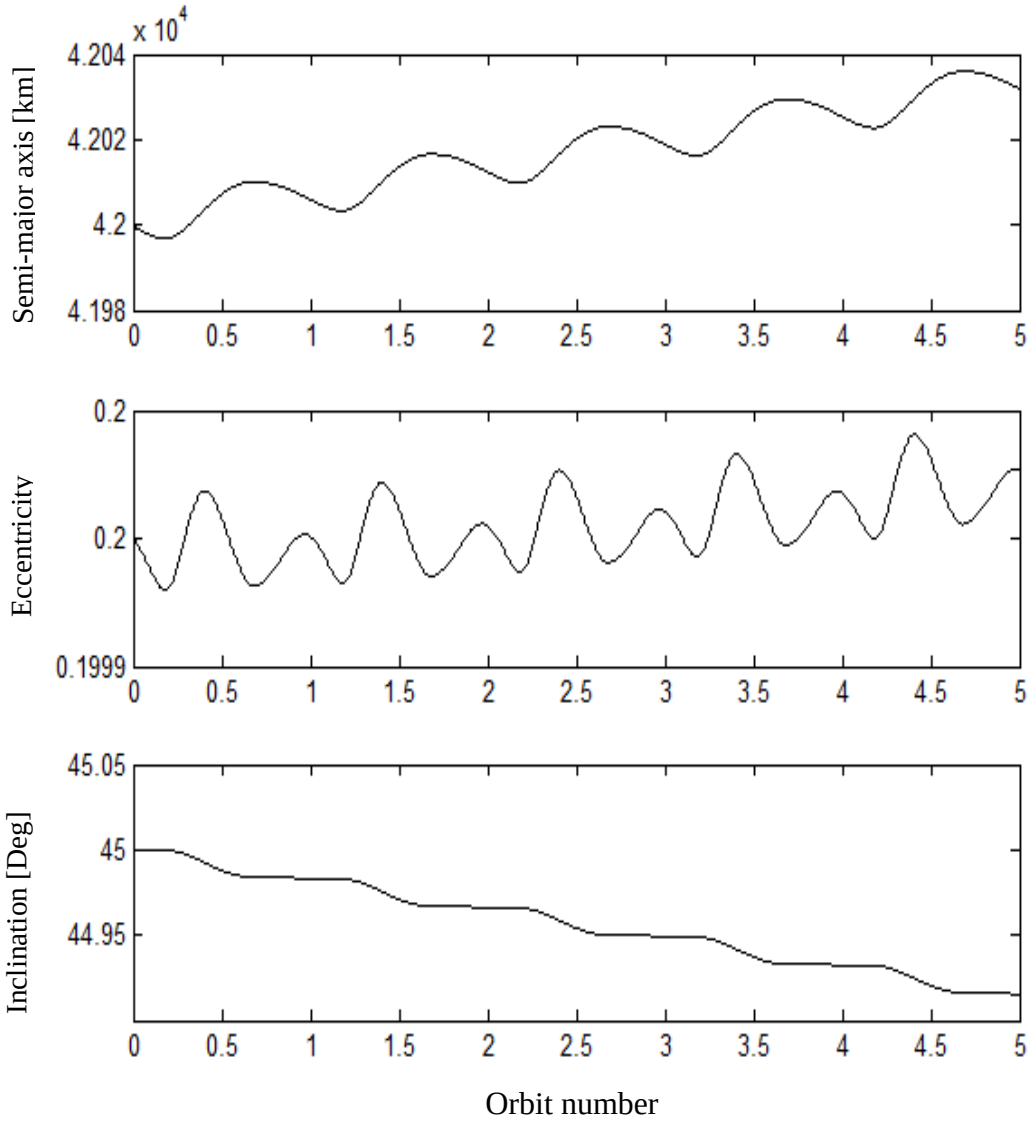

Figure A.11 Orbital elements change when decreasing inclination

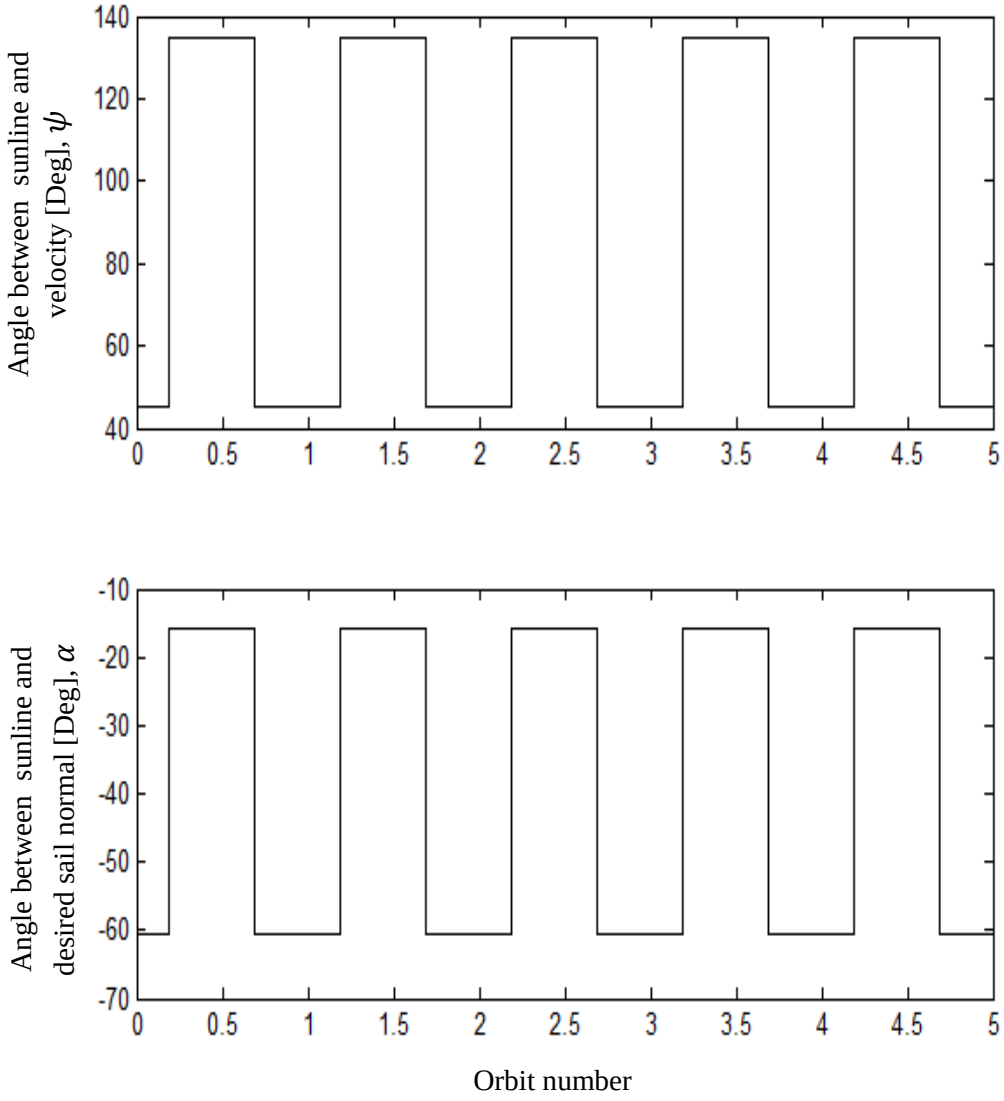

Figure A.12 Angular position of inclination vector function and desired sail normal for decreasing inclination

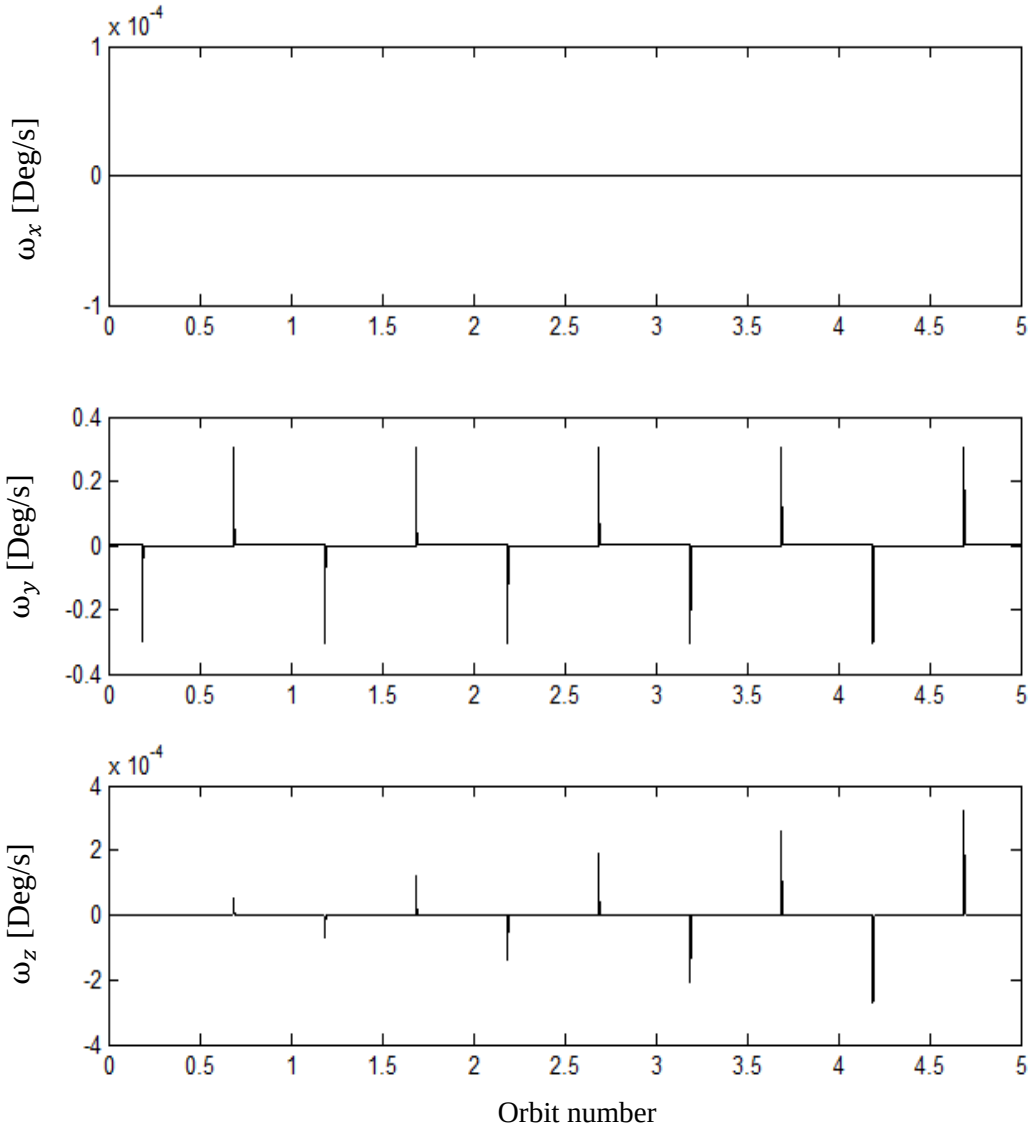

Figure A.13 Body fixed frame angular rates for decreasing inclination

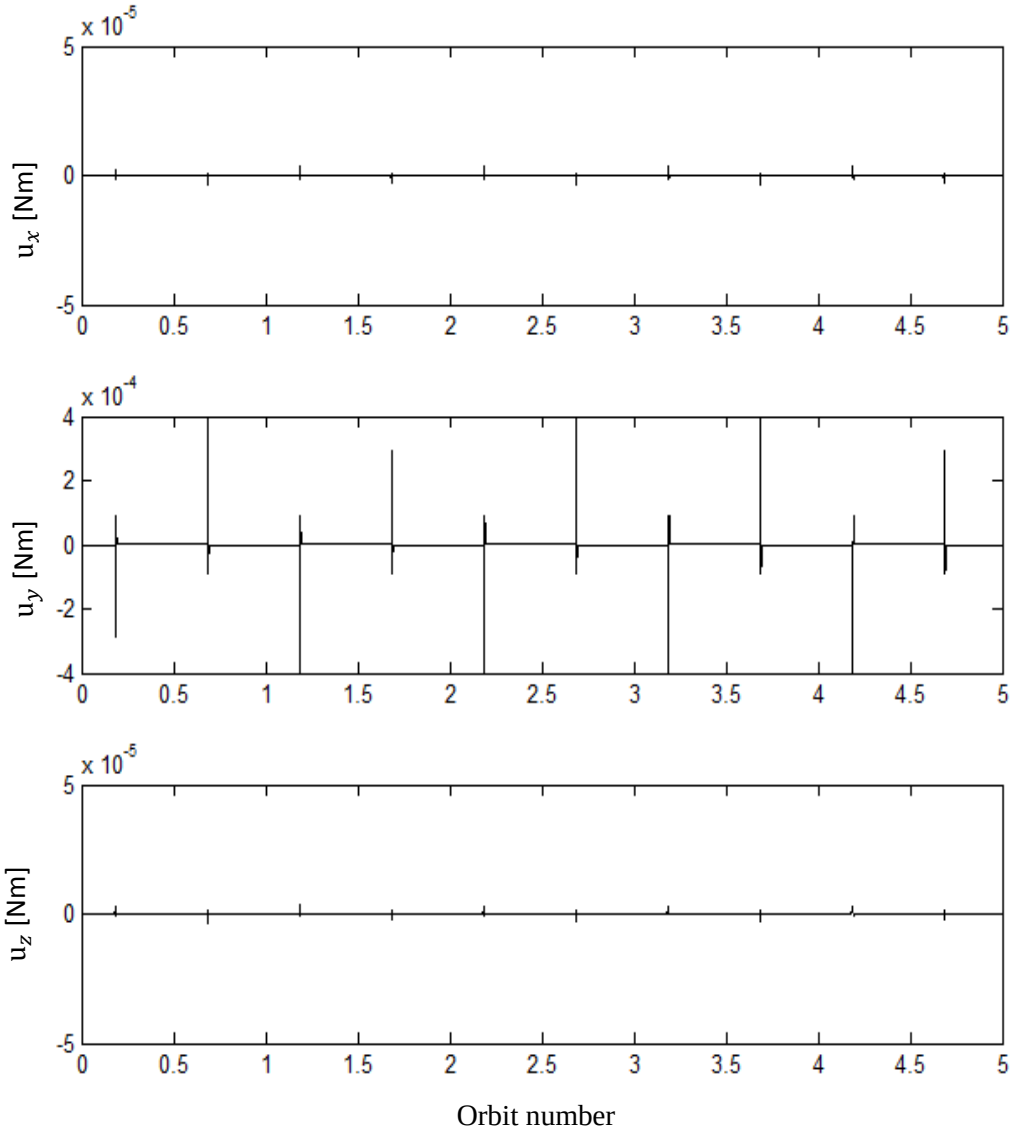

Figure A.14 Controller torques about body axes for decreasing inclination

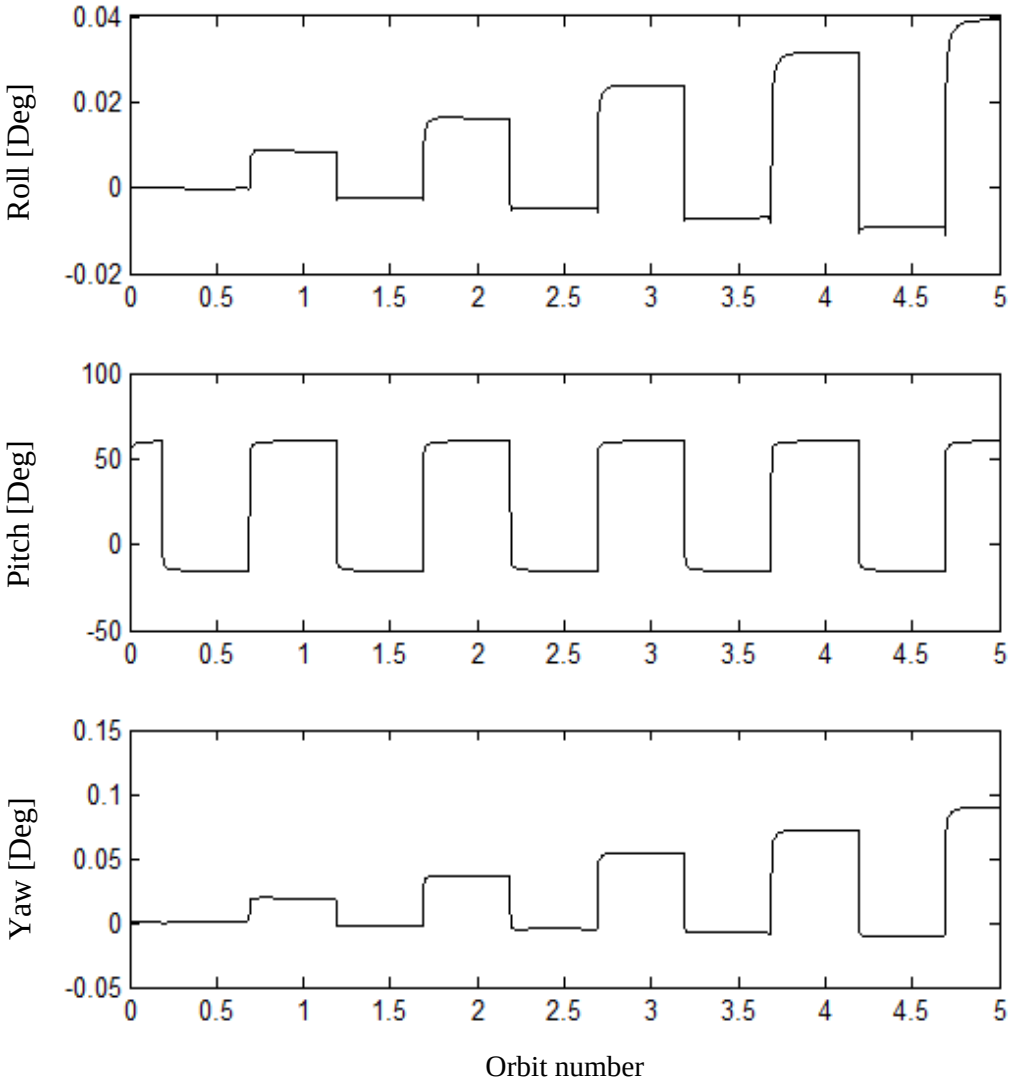

Figure A.15 Orientation of solar sail with respect to inertial frame to decrease inclination